

Massive stars

D. Vanbeveren^{1,2}, C. De Loore¹, and W. Van Rensbergen¹

¹ Astrophysical Institute, Vrije Universiteit Brussel, Pleinlaan 2, B-1050 Brussels, Belgium
(e-mail: dvbevere@vub.ac.be; wvanrens@vub.ac.be; cdeloore@nets.ruca.ua.ac.be)

² Institute of Technology Louvain, Campus Vesalius, Vesaliusstraat 12, B-3000 Louvain, Belgium
(e-mail: dvb@groept.be)

Received 17 July 1998

Abstract. We describe the present state of massive star research seen from the viewpoint of stellar evolution, with special emphasis on close binaries. Statistics of massive close binaries are reasonably complete for the Solar neighbourhood. We defend the thesis that within our knowledge, many scientific results where the effects of binaries are not included, have an academic value, but may be far from reality. In chapter I, we summarize general observations of massive stars where we focus on the HR diagram, stellar wind mass loss rates, the stellar surface chemistry, rotation, circumstellar environments, supernovae. Close binaries can not be studied separately from single stars and vice versa. First, the evolution of single stars is discussed (chapter I). We refer to new calculations with updated stellar wind mass loss rate formalisms and conclusions are proposed resulting from a comparison with representative observations. Massive binaries are considered in chapter II. Basic processes are briefly described, i.e. the Roche lobe overflow and mass transfer, the common envelope process, the spiral-in process in binaries with extreme mass ratio, the effects of mass accretion and the merging process, the implications of the (asymmetric) supernova explosion of one of the components on the orbital parameters of the binary. Evolutionary computations of interacting close binaries are discussed and general conclusions are drawn. The enormous amount of observational data of massive binaries is summarized. We separately consider the non-evolved and evolved systems. The latter class includes the semi-detached and contact binaries, the WR binaries, the X-ray binaries, the runaways, the single and binary pulsars. A general comparison between theoretical evolution and observations is combined with a discussion of specially interesting binaries: the evolved binaries HD 163181, HD 12323, HD 14633, HD 193516, HD 25638, HD 209481, ϕ Per and ν Sgr; the WR+OB binary V444 Cyg; the high mass X-ray binaries Vela X-1, Wray 977, Cyg X-1; the low mass X-ray binaries Her X-1 and those with a black hole candidate; the runaway ζ Pup, the WR+compact companion candidates Cyg X-3, HD 50896 and HD 197406. We finally propose an overall evolutionary model of massive close binaries as a function of primary mass, mass ratio and orbital period. Chapter III deals with massive star population synthesis with a realistic population of binaries. We discuss the massive close binary frequency, mass ratio and period distribution, the observations that allow to constrain possible asymmetries during the supernova explosion of a massive star. We focus on the comparison between observed star

numbers (as a function of metallicity) and theoretically predicted numbers of stellar populations in regions of continuous star formation and in starburst regions. Special attention is given to the O-type star/WR star/red supergiant star population, the pulsar and binary pulsar population, the supernova rates.

Keywords: massive singlet stars – massive close binaries – massive star population synthesis

Contents

I. Single stars	67
1. Observations of massive single stars	67
1.1. The HR-diagram of massive stars	67
1.2. Stellar winds of massive stars	69
1.2.1. The CHB phase	70
1.2.2. The RSG phase	70
1.2.3. The WR phase	71
1.2.4. The dependence of \dot{M} on the metallicity Z	71
1.3. Chemistry	72
1.4. Stellar rotation	72
1.5. Circumstellar shells	73
1.6. The space velocity of massive stars	73
1.7. Single pulsars	74
1.7.1. The rotation periods and magnetic fields of pulsars	75
1.7.2. The space velocity of pulsars	75
2. The evolution of massive single stars: present state	77
2.1. Opacities	77
2.2. Convective core overshooting	77
2.3. Semi-convection	79
2.4. The effect of stellar wind mass loss	79
2.4.1. The solar neighbourhood	81
2.4.2. The magellanic clouds	83
2.5. Post-CHeB evolution	84
2.6. The effect of rotation on massive single star evolution	84
2.7. Comparison to observations	85
2.7.1. The HR diagram	85
2.7.2. The position of RSGs and WR stars	87
2.7.3. The BHG	87
2.7.4. The effects of rotation compared to observations	88
2.7.5. The runaway ζ Pup as massive single star	89
II. Massive close binaries	91
3. General	91
4. Binary evolutionary processes	94
4.1. The RLOF process in case A/case B _r MCBs with initial $q > 0.2$	94
4.1.1. The mass loser	94
4.1.2. Mass transfer	95
4.1.3. The mass gainer	95
4.1.4. The formation and the evolution of contact binaries	97
4.1.5. The effect of an LBV type stellar wind	98

4.2.	The evolution of case A/case B _r MCBs where the mass ratio ≤ 0.2	98
4.3.	The RLOF process in case B _c /case C MCBs	99
4.4.	The variation of the binary period due to mass loss	99
4.4.1.	Spherical symmetric stellar wind mass loss	99
4.4.2.	The RLOF in case A/case B _r binaries with initial mass ratio $q > 0.2$	100
4.4.3.	The CE phase in case B _c /C binaries	101
4.4.4.	The SpI process in case A/case B _r binaries with mass ratio ≤ 0.2	102
4.5.	The effect of the supernova explosion of one of the compo- nents of a MCB on the system parameters	103
5.	MCB evolutionary computations	103
5.1.	The mass loser	104
5.2.	The mass gainer	105
5.2.1.	Accretion case 1a	105
5.2.2.	Accretion case 1b	107
5.2.3.	Accretion case 2	107
5.2.4.	The variation of the chemical abundance at the surface of a mass gainer	107
5.3.	The binary after the RLOF/CE/SpI process: a CHeB+OB binary or a merger?	108
5.3.1.	The evolution of mergers	108
5.3.2.	The evolution of a CHeB+OB binary	108
5.4.	The final fate of primaries of MCBs	110
5.5.	The evolution of a MCB after the collapse of the core of the primary	110
5.6.	The effect of rotation on the evolution of a MCB	111
5.6.1.	The primary	111
5.6.2.	The secondary	112
6.	Observations of MCBs	112
6.1.	Massive OBA+OBA binaries	113
6.1.1.	The OBA+OBA mass ratio distribution	113
6.1.2.	The OBA+OBA period distribution	114
6.1.3.	The OBA+OBA binary frequency	115
6.1.4.	Special cases	117
6.2.	WR+OB binaries	120
6.3.	The X-ray binaries	124
6.3.1.	The OB-type high mass X-ray binaries (HMXB)	124
6.3.2.	The low mass X-ray binaries (LMXB)	126
6.4.	The O type runaway ζ Pup as a binary component	127
6.5.	Critical remarks	129
6.6.	The descendants of OB+cc binaries: the CHeB (WR)+cc candidates	130
III.	Massive star population synthesis	136
7.	General	136
8.	The X-ray binaries	138
9.	The WR-O-RSG population	141
9.1.	Continuous star formation regions	142
9.1.1.	The population of O-Type stars	142

9.1.2.	The WR population	143
9.1.3.	Why the number of Galactic X-ray binaries with a WR type optical component is so small? . . .	144
9.2.	Starburst regions	144
9.2.1.	The population of O-type stars and WR stars . . .	144
9.2.2.	The population of RSGs and WR type stars in starbursts	147
10.	The pulsar population and the fraction of binary pulsars	147
11.	The SN rates	147

Introduction

The numerical solution of the time dependent stellar structure equations and the full scheme of thermo-nuclear processes allow to propose a minimum mass a star must have initially so that it was able to form a non-degenerate iron-nickel core at the end of its life. This minimum value depends only slightly on the initial chemical composition of the star but may differ significantly for single stars and for components of a binary. The present state of stellar evolution promotes $\sim 8M_{\odot}$ for single stars (chapter I) and $\sim 10M_{\odot}$ for close binary components (Chapter II). If the stellar mass exceeds these minima, the star is classified as a massive star.

The solution also predicts the evolution of a star in the HR-diagram. By comparing the observed properties of stars with this theoretical prediction, it is possible to identify the following subclasses as massive stars:

- stars with luminosity class V or IV and spectral type earlier than B3
- stars with luminosity class III and spectral type earlier than B4
- stars with luminosity class II and spectral type earlier than B5
- the OBA stars with luminosity class Ib, Iab, Ia and IaO
- the Luminous Blue Variables (LBVs)

There are two types of LBVs (Humphreys and Davidson, 1994): those brighter than $M_{\text{bol}} \approx -9.5$ (a.o. η Car, P Cyg) and the fainter ones (a.o. R71, R101). The latter have lower mass loss rates and are presumably in a post-RSG phase of stellar evolution.

- the Yellow Supergiants (YSGs), Red Supergiants (RSGs) and the Hypergiants
- the Wolf-Rayet (WR) stars

Massive stars are by definition, the progenitors of supernova (SN) explosions whereas they are at the origin of the chemical evolution of the cosmos and thus at the origin of life.

Massive stars have been the topic of numerous research projects that resulted in a countless number of papers. The present review summarizes the present state. Chapter I (respectively chapter II) focuses on the single stars (resp. the binaries). Chapter III then deals with population synthesis and the effect of binary evolution.

More information can be found in the extended review of Van den Heuvel (1993) and in the monograph ‘The Brightest Binaries’ (Vanbeveren et al. 1998a).

Frequently used abbreviations

BH:	Black Hole
BHG:	Blue Hertzsprung Gap
BSC:	Bright Star Catalogue
cc:	compact companion
CE:	Common Envelope
CHB:	Core Hydrogen Burning
CHeB:	Core Helium Burning
HMXB:	High Mass X-ray Binary
HRD:	Hertzsprung-Russell Diagram
HSB:	Hydrogen Shell Burning
LBV:	Luminous Blue Variable
LMC:	Large Magellanic Cloud
LMXB:	Low Mass X-ray Binary
MB:	Massive Binary
MC:	Magellanic Cloud
MCB:	Massive Close Binary
NLTE:	Non Local Thermodynamic Equilibrium
NS:	Neutron Star
PNS:	Population Number Synthesis
RLOF:	Roche lobe overflow
RSG:	Red Supergiant
SMC:	Small Magellanic Cloud
SN:	Supernova
SpI:	Spiral-in
SW:	Stellar Wind
TZO:	Thorne-Zytkow Object
VMCB:	Very Massive Close Binary (primary mass $> 40M_{\odot}$)
WC:	WR of the Carbon sequence
WN(E):	WR of the (early) WN sequence
WN(L):	WR of the (late) WN sequence
WR:	Wolf-Rayet star
YSG:	Yellow Supergiant
ZAMS:	Zero age main sequence

I. Single stars

1. Observations of massive single stars

First, let us recall that for massive stars, it is very hard to observe a small mass companion and/or a companion orbiting with a large period. Therefore, absence of binary evidence for a particular massive star is not necessarily evidence of absence.

1.1. The HR-diagram of massive stars

Humphreys & McElroy (1984) proposed a $M_{\text{bol}} - T_{\text{eff}}$ calibration for O-M type stars. They then collected data for a large number of galactic stars within 3 kpc from the Sun, for the LMC and for the SMC. Figure 1 illustrates the HR-diagrams (HRD). In

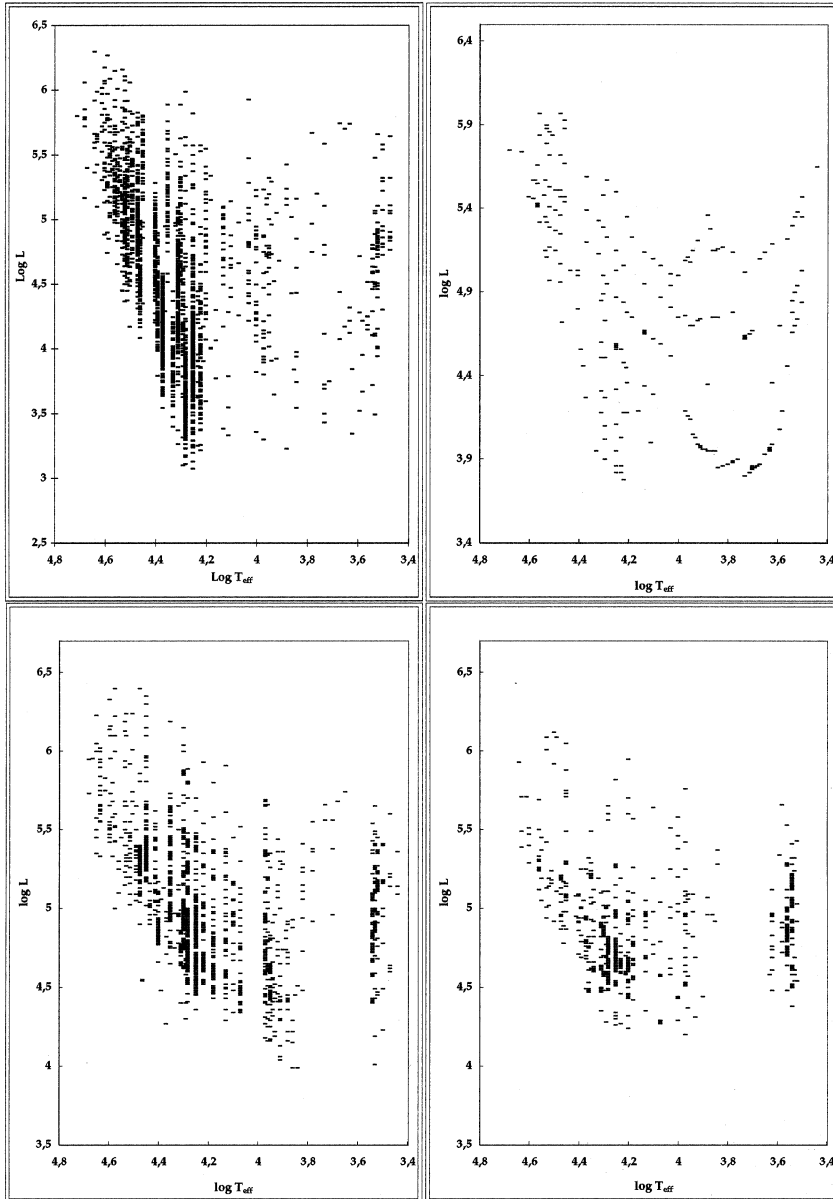


Fig. 1. The HR diagram of 2400 stars belonging to stellar aggregates in the solar neighbourhood (upper-left), of ~ 2700 massive galactic field stars in the solar neighbourhood (upper-right; since a $[M_{\text{bol}} - T_{\text{eff}}]$ -spectral type-luminosity class calibration is used, one point in the diagram may represent many stars), of ~ 1300 LMC stars (lower-left), of ~ 500 SMC stars (lower-right)

the case of the Galaxy, we consider separately the stellar aggregate members and the field stars.

A word of caution is appropriate here. The T_{eff} of most stars follows from the B-V index and a small error in the latter may result into a significant error in T_{eff} . This is especially true for supergiants. Furthermore, aggregate membership of O-type stars and early B-type supergiants sometimes relies on faith rather than on strong kinematics arguments. To illustrate this, two O-type stars HD 73882 and HD 75759 have been listed by Humphreys and McElroy as Vela OB1 members at 1.8 kpc from the Sun. However, using the Hipparcos data, both stars appear to be at a distance of ~ 500 pc.

In Fig. 2 we show an overall HR diagram including the LBVs and the WR stars. The data of the LBVs have been reviewed by Humphreys & Davidson (1994) whereas the WR area corresponds to the NLTE results of Hamann et al. (1995), Koesterke & Hamann (1995), Koesterke et al. (1992), Crowther et al. (1995).

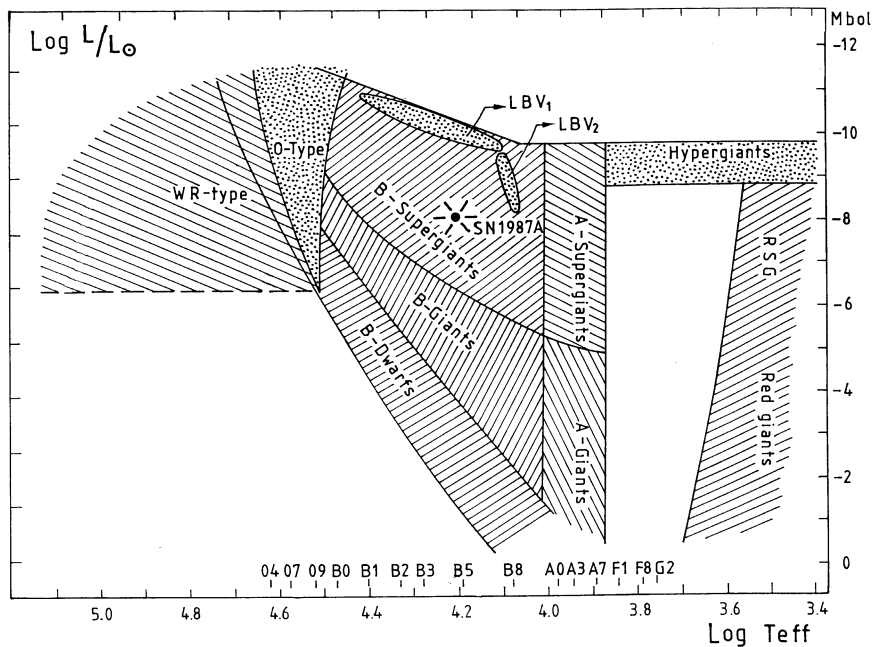


Fig. 2. The overall HRD of the massive stars in the Galaxy together with the probable position of the progenitor of SN 1987A; LBV₁ (resp. LBV₂) is the area occupied by the more violent (resp. less violent) LBVs

1.2. Stellar winds of massive stars

The evolution of a massive star depends critically on the adopted stellar wind mass loss rate formalisms during the core hydrogen burning (CHB) phase, the hydrogen shell burning (HSB) phase and the core helium burning (CHeB) phase. The evolutionary calculations of massive stars allow us to conclude that CHB corresponds to O and early B-type stars, the end of CHB and HSB of the most massive stars ($\geq 40M_{\odot}$) to

the LBV phase, the red part of CHeB to RSGs, the hydrogen deficient blue part of CHeB to WR stars. In the following, \dot{M} is expressed in M_{\odot}/yr and the luminosity L in L_{\odot} .

1.2.1. The CHB phase

From the compilation of De Jager et al. (1988), we selected the OB-type stars and updated the \dot{M} values of the 24 stars studied by Puls et al. (1996). The following relation (with coefficient of correlation = 0.9) between \dot{M} , L and T_{eff} can be deduced

$$\log(-\dot{M}) = 1.67 \log L - 1.55 \log T_{\text{eff}} - 8.29 \quad (1.1)$$

The latter equation can be used in an evolutionary code for massive CHB stars prior to the LBV phase.

When the star becomes an LBV with $M_{\text{bol}} \leq -9.5$, the SW mass loss becomes very large although the exact rate is poorly known. Due to the fact that no RSGs are observed brighter than $M_{\text{bol}} = -9.5$ (Fig. 2), we use as a working hypothesis for evolution

‘the \dot{M} during the LBV phase of a star with $M_{\text{bol}} \leq -9.5$ must be sufficiently large to suppress a large expansion, hence to prohibit the redward evolution in the HRD’

or relaxing somewhat the foregoing criterion

‘the \dot{M} during the LBV and RSG phase of a star with $M_{\text{bol}} \leq -9.5$ must be sufficiently large to assure a RSG phase which is short enough to explain the lack of observed RSGs with $M_{\text{bol}} < -9.5$ ’.

The limit $M_{\text{bol}} = 9.5$ corresponds to stars with initial mass $\sim 40M_{\odot}$, i.e. the working hypothesis is applied for all stars with initial mass larger than $40M_{\odot}$.

1.2.2. The RSG phase

Jura (1987) proposed a mass loss rate formula for RSGs using infrared data. With IRAS data, Reid et al. (1990) determined the stellar wind mass loss rate applying Jura’s formalism for 16 RSGs in the LMC with $M_{\text{bol}} \leq -7$. The following equation gives a surprisingly well defined relation (correlation coefficient = 0.96) between the mass loss rate and the luminosity of these RSGs, i.e.,

$$\log(-\dot{M}) = 0.8 \log L - 8.7 \quad (1.2)$$

Equation (1.2) is valid for the LMC. If the metallicity dependence of the stellar wind mass loss expressed by Equation (1.4) also applies for RSGs, using $Z = 0.008$ for the LMC and $Z = 0.02$ for the Galaxy, the mass loss rates for Galactic YSGs/RSGs may be 1.6 times larger than predicted by Equation (1.2).

In our evolutionary code, once the star becomes a RSG, Equation (1.2) is used to calculate the mass loss.

1.2.3. The WR phase

A stellar wind mass loss rate formalism for WR stars can be deduced as follows:

- Using a NLTE atmosphere code where the stellar wind is assumed to be homogeneous, Hamann et al. (1995) determined values for a large number of WR stars. However, the assumption of homogeneity overestimates these values, typically by a factor of two (Hillier, 1996; Moffat, 1996; Schmutz, 1996; Hamann & Koesterke, 1998). To illustrate this: a detailed wind model of the WN5 star HD 50896 including clumping has been established by Schmutz (1997). The model yields a luminosity of $\log L/L_{\odot} = 5.6\text{--}5.7$ and a SW mass loss rate $\approx (4 \pm 1) \cdot 10^{-5} M_{\odot}/\text{yr}$.
- The mass loss rate of the WNE component of the binary V444 Cyg resulting from the observed orbital period variation is $\sim 1.1 \pm 0.5 \cdot 10^{-5} M_{\odot}/\text{yr}$ (Khaliullin et al., 1984; Underhill et al., 1990). The orbital mass of the WR star is very well known and equals $\sim 9 M_{\odot}$ implying a luminosity $\log L/L_{\odot} \approx 5$ (Sect. 5.3.2).
- The discovery of very massive BHs in X-ray binaries (e.g. Cyg X-1, Sect. 6.3) indicates that stars with initial mass $> 40 M_{\odot}$ should end their life with a mass larger than $10 M_{\odot}$ (= the mass of the star at the end of CHeB, Sect. 6.3.1),
- the observed star number ratio of WN/WC in the Solar neighbourhood ≈ 1 ; the theoretically predicted value is largely dependent on the adopted \dot{M} ; an \dot{M} that is too large (resp. too small) predicts a too small (resp. too large) WN/WC ratio (Sect. 5.3.2).

Anticipating, a WR relation that meets these constraints (within the errors) is given by

$$\log(-\dot{M}) = \log L - 10 \quad (1.3)$$

In an evolutionary code, once a CHeB star resembles a WR type star, Equation (1.3) can be used to compute the stellar wind mass loss.

However, when does a stellar model (calculated with an evolutionary code) correspond to a WR star?

A star is classified as a WR star when it emits an emission line spectrum that satisfies a number of specific criteria. Since stellar evolution does not depend on the treatment of the outermost layers, the physics of the latter is kept very simple so that the spectrum criteria cannot be used to assign the WR classification to the evolutionary model. However, the interpretation of the spectrum of a WR star with detailed NLTE atmosphere codes allows to conclude that WR stars are massive hydrogen deficient stars with $\log L/L_{\odot} \geq 4.5$ and $T_{\text{eff}} > 30\,000\text{K}$. A possible evolutionary definition is then the following:

a WR star is a hydrogen deficient CHeB star with $\log L/L_{\odot} \geq 4.5$ and $T_{\text{eff}} \geq 30\,000\text{K}$.

Anticipating, stellar evolutionary calculations learn us that the latter definition corresponds to hydrogen deficient CHeB stars with mass larger than $\sim 5 M_{\odot}$.

1.2.4. The dependence of \dot{M} on the metallicity Z

Most of the semi-empirically determined rates are uncertain by at least a factor 2 and it is therefore difficult to deduce any kind of metallicity dependency from observations.

The theory of outflowing atmospheres predicts a relation between the \dot{M} of OB-type stars (prior to the LBV phase) and Z [Castor et al. 1975, Pauldrach et al. 1994, Puls et al. 1996] i.e.

$$\dot{M} \propto Z^\zeta \quad \text{with } 0.5 \leq \zeta \leq 1 \quad (1.4)$$

Whether or not this dependency also applies for LBVs, RSGs and WR stars is unclear at present.

1.3. Chemistry

The determination of the chemical abundances of the elements in the atmosphere of a massive star is not straightforward. First, one needs high quality stellar spectra and, secondly, a stellar atmosphere code capable to reproduce these spectra. The latter depends on the degree of completeness of the physics involved. To illustrate, using the NLTE code of Munich (Gabler et al. 1989), Herrero et al. (1992) concluded that many OB type supergiants have significantly enhanced helium. The version of the code at that time did not account for the effects of micro-turbulence. The latter has been studied by McErlean et al. (1998) and Smith et al. (1998) and it was concluded that the He abundance needed to explain the observations is reduced significantly when micro-turbulence is included.

An increased surface He abundance can only be explained by inventing an efficient mixing process, capable to transport CHB products to the surface. It is important to realize that this will always be accompanied by a very significant increase of the surface nitrogen abundance (at least a factor of two). In stars with a suspected He enrichment, an increased N-abundance has never been reported yet. Walborn (1971, 1976) introduced the OBN/OBC classification for those stars that exhibit strong nitrogen (resp. carbon) lines. He suggested that OBC stars could be the chemically normal stars, the ‘normal’ OB stars those with a moderately enhanced N abundance and the OBN types the stars with a large N overabundance.

We conclude that as far as the surface chemistry is concerned, the situation among the OB-type stars is unclear and therefore the suggestion made by Walborn is still speculative.

1.4. Stellar rotation

Observed $v_e \sin i$ for massive OB type stars have been listed by Howarth & Prinja (1989) and in the current Bright Star Catalogue. Using the method outlined by Lucy (1974), Fig. 3 illustrates the v_e distribution of the early OBe-type stars, of the O-type stars (Oe omitted) and of the early B-type stars (Be omitted). As expected, the OBe types have the largest average velocity. However, there are at least as many rapidly rotating OB-types without the emission type spectrum typical for rotating discs (thus no e-classification), as there are OBe types.

Remark that the v_e values tell us something about the rotation of the outermost layers of a star only. How this is related to the rotation of the stellar interior is uncertain (see also Sect. 2.7.4).

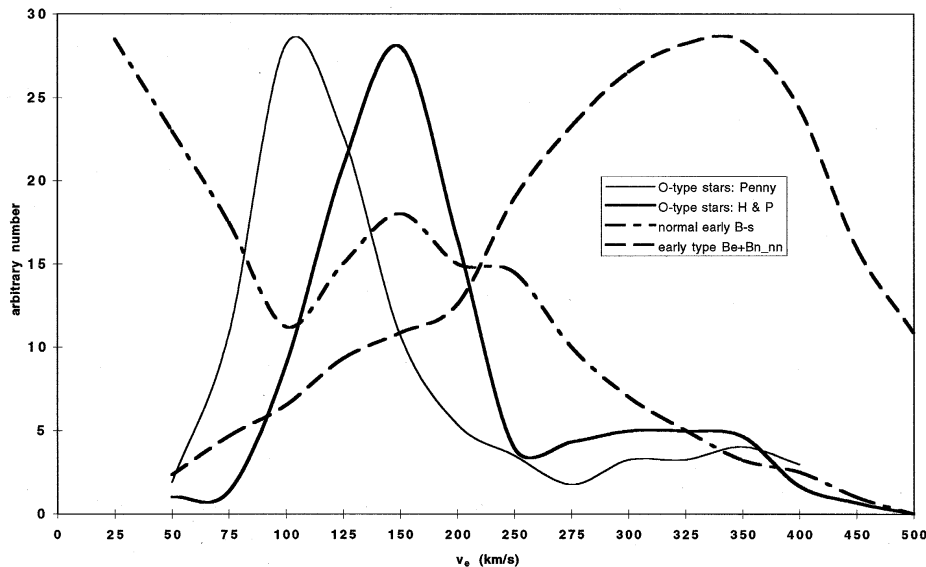


Fig. 3. The statistically expected v_e distribution of O-type stars (using the data set of Howarth & Prinja, 1989, and of Penny, 1996), of the normal early B-type stars and of the early Be stars. All curves are normalized in a way that the maxima are at the same height

1.5. Circumstellar shells

Circumstellar shells have been observed around many LBVs (Nota et al., 1995), RSGs (Stencel et al. 1989) and WR stars (Marston, 1995). Two classes can be distinguished: large cool IRAS shells with a diameter of ~ 10 pc, originating from the previous OB stellar wind phase, and optically observable shells with small diameter, visible around $\sim 31\%$ (resp. $\sim 16\%$) of the galactic single WN stars (resp. WC stars) (Marston et al. 1994). The structures may be indicators that the progenitors of these WR stars went through an LBV and/or RSG phase.

It is interesting to notice that such small scale shells are seldom observed around WR+OB binaries. If confirmed, one may consider this as direct observational proof that the progenitor binaries went through a (quasi)-conservative Roche lobe overflow phase.

1.6. The space velocity of massive stars

After correction for galactic rotation, most of the massive stars have a space velocity of a few km/s. However, some of them have much larger velocities. Blaauw (1961) introduced the term ‘runaway’ when the space velocity exceeds 30 km/s. Using this definition, Gies (1987) concluded that $\sim 10\%$ of the O-type stars are runaways.

We know of two mechanisms that are capable to give a massive star a large space velocity: the cluster ejection mechanism (Leonard & Duncan, 1988, 1990) and the supernova explosion in a binary (Blaauw, 1961).

From the calculations of Leonard & Duncan (1988, 1990), the following conclusion can be formulated:

owing to dynamical interactions between stars, a parsec sized cluster with many (massive) stars and many (massive) close binaries is able to eject a massive star with a velocity larger than 30 km/s.

This conclusion has an important consequence:

if a massive star became runaway due to cluster ejection and if the age of the massive star is at most a few million years, we still have to see the remains of the dense cluster somewhere along the kinematic path of the runaway.

If a massive O-type runaway is close enough to the Sun, the Hipparcos data may give us the answer, at least for this runaway. A famous example and test case may be the O5Ia star ζ Pup. Its distance to the Sun is $\sim 400\text{--}500$ pc whereas, after correction for galactic rotation, the star's space velocity $\sim 60\text{--}80$ km/s. We will return to this star in Sect. 2.7.5.

Other interesting runaways: the WR star HD 50896 with a space velocity $\sim 80\pm 60$ km/s (Sect. 6.6); HD 197406 has been classified as a runaway based on its large distance above the galactic plane (799 pc according to Moffat and Seggewiss, 1980); the WN8 star 209 BAC has been called the 'fastest WR runaway' (Moffat et al., 1982). It has a peculiar radial velocity component of ~ 156 km/s and is located ~ 250 pc above the galactic plane.

Remark. A spherical symmetric SN explosion rarely unbinds a close binary whereas it predicts a runaway velocity for the binary remnant that is larger, the larger the mass of the OBA type optical component (Sutantyo, 1978). The observations reveal just the opposite, i.e. OBA runaways rarely have a neutron star companion whereas the lower mass runaways seem to have the largest velocities (Gies & Bolton, 1986) and this was used as arguments in favor of the cluster ejection mechanism at the origin of runaways.

However, when the new ideas about the asymmetry of the SN explosion in massive stars are confirmed (Sect. 1.7.2), most of the binaries will be disrupted during the SN explosion. Furthermore, a SN explosion that disrupts the binary predicts OBA velocities that are indeed larger, the smaller the mass of the OBA stars.

1.7. Single pulsars

The Fe-Ni core of a massive star finally collapses to form a neutron star or a black hole. When a neutron star is formed, the energy liberated during this collapse is so large (SN explosion) that most of the layers outside the Fe-Ni core are ejected. A pulsar is a highly magnetized, rapidly rotating neutron star. It emits dipole radiation at the magnetic poles. When the Earth lies in the radiation cones, due to the rotation of the neutron star, we observe this dipole radiation as an on-off signal. This explains the term 'pulsar'. In chapter III we will discuss the evidence that the progenitors of many single pulsars were in fact binary components.

A neutron star belonged originally to the core of a massive star and therefore, some properties of neutron stars may tell us something about the properties of convective cores of massive stars. Furthermore, the space velocity of pulsars gives us an indication about the asymmetry of the previous SN explosion and the degree of asymmetry will allow us to determine the post-SN orbital elements of a binary and/or the binary disruption probability due to the SN explosion of one of the components.

1.7.1. The rotation periods and magnetic fields of pulsars

There are presently ~ 900 pulsars known. Most of them have pulse periods (= rotation period) between 0.1 s and 1 s.

As a consequence of the emission of dipole radiation when the neutron star has a magnetic field B , it slows down according to

$$B \propto \sqrt{P\dot{P}} \quad (\text{Pacini, 1967}) \quad (1.5)$$

For many pulsars, the time variation of the period has been measured and thus B can be estimated. The distribution appears to be Gaussian in $\log B$ with average ≈ 12.5 and standard deviation ≈ 0.3 .

It was shown by Bhattacharya et al. (1992) that no significant magnetic field decay occurs in single radio pulsars. It can readily be checked then that the observed periods and the formalism (1.5) is compatible with the statement that most of the neutron stars are born with a spin-period ≥ 0.01 s. Interestingly, all pulsars that are still imbedded in the SN nebula (and which are thus very young), have pulse period larger than 0.01 s, i.e. the Crab pulsar (which is only ~ 1000 yrs old) has a pulse period = 0.033 s, the 50 ms pulsar PSR B0540-69, the 150 ms pulsar PSR B1509-58, and the recently observed Crab-like pulsar in N157B with pulse period = 0.016 s (Marshall et al., 1998).

1.7.2. The space velocity of pulsars

Lorimer et al. (1997) discussed in detail the observed space velocity distribution of pulsars. They concluded that the average value ~ 450 – 500 km/s whereas the distribution contains a high velocity tail (with velocities exceeding 1000 km/s).

An estimate of the distribution function of the space velocity of pulsars at birth, can be obtained as follows:

- To avoid too large distance errors and to avoid significant biases, limit the sample of pulsars with proper motions in distance (< 5 kpc) and age (only pulsars younger than 3 million yrs). From the sample of pulsars with observed transverse velocities, only 27 are left that satisfy both restrictions.
- Account for the effect of the Galactic potential which may slow down the young pulsar.

The distribution of velocities calculated in this way can then very well be described by a χ^2 -like distribution, i.e.

$$f(v_p) = 1.96 \cdot 10^{-6} v_p^{3/2} e^{-3v_p/514} \quad (1.6)$$

which predicts an average of 500 km/s.

A single star pulsar either had a single star past or its progenitor was a binary component where the SN explosion disrupted the system. In the latter case, the space velocity of the pulsar is a complicated function of the kick velocity the neutron star receives at birth and of the orbital parameters of the binary where the explosion takes place (Tauris & Takens, 1998). How the kick-velocity distribution is related to the space velocity distribution of pulsars has been investigated by De Donder & Vanbeveren (1998b). With a population number synthesis code with a realistic binary

frequency (chapter III), starting from a kick velocity distribution, the expected space distribution was determined of single pulsars, i.e. pulsars originating from real single stars and pulsars that became single due to the disruption of the binary during the SN explosion. Two interesting properties:

- Large kicks may explain pulsars with small space velocity. The reason is simple: when the kick is directed opposite to the pre-SN orbital velocity, the space velocity of the pulsar after disruption may be quite small.
- The kick velocity distribution that reproduces the observed space velocity distribution of single pulsars hardly differs from the latter.

In addition to the direct observations of space velocities, Fryer et al. (1998) propose four observational facts which may further constrain the kick-velocity distribution: the number of low mass X-ray binaries (LMXB), the number of high mass X-ray binaries (HMXB), the formation rate of double NS binaries and the number of NSs in globular clusters. The authors conclude that these four constraints point towards a double-peaked kick velocity distribution, i.e. $\sim 30\%$ of the pulsars are expected to receive a kick smaller than 50 km/s, $\sim 70\%$ receive a kick between 600–700 km/s.

A few criticisms are appropriate. Calculating the lifetime that a binary will be visible as an X-ray binary is very uncertain. The existence of systems like Cyg X-3 (Sect. 6.6) complicates the definition of a HMXB. Furthermore, it is not clear to us whether or not the authors accounted for the formation of OBe-X-ray binaries where X-rays are powered by the disk matter around the OBe star, and whether or not the authors accounted for the formation of X-ray binaries with BH components, where a SN explosion has not occurred. The BH binaries may (at least partly) account for the need of small kicks when all X-ray binaries are considered as NS binaries.

The third method is based on the ‘observed’ number of NS+NS binaries. As shown by De Donder & Vanbeveren (1998a), the kick velocity distribution described by Equation (1.6) in combination with a population number synthesis code (chapter III) reproduces the latter number and, again, there is no need for a double peaked distribution.

The large number of NSs observed in globular clusters requires that more than 1% of the NSs remains bound to the cluster (Bhattacharya & Van den Heuvel, 1991). This is a fourth constraint which requires the existence of small kicks. First notice that the χ^2 -distribution proposed above predicts the existence of a small (but non-zero) fraction of low velocity kicks. Furthermore, the population number synthesis model including binaries where the effect of the SN explosion on binary parameters is followed in detail, predicts that at least a few percent of all NSs will either be kicked directly into the OB companion due to the SN explosion, or it will spiral-in into their OB companion during the post-SN evolution of the binary and form a Thorne-Zytkow object (TZO) (Thorne & Zytkow, 1977). These objects have a space velocity of a few 10 km/s (acquired during the SN explosion). Their evolution has been studied by Biehle (1991) and Cannon et al. (1992). It follows that TZOs have the structure of a RSG. Most probably these RSGs will lose all their mass by stellar wind and the cc may become visible again, with a velocity of a few km/s. Whether or not the cc reappears as a pulsar is unclear at present, but if so, they will significantly contribute to the pulsar population in globular clusters making small kicks superfluous.

Nevertheless, although we feel that Equation (1.6) describes in a satisfactory way the present observations of pulsar velocities, large errors in observations of distances and transverse velocities can not entirely be excluded. At present, it seems therefore advisable to study the consequences of asymmetric SN explosions on massive star

evolution in particular, on population number synthesis in general, by adopting a comparable distribution as (1.6) but with a smaller average value, i.e.

$$f(v_p) = 2.70 \cdot 10^{-5} v_p^{3/2} e^{-v_p/60} \quad (1.7)$$

which predicts an average of 150 km/s.

2. The evolution of massive single stars: present state

The equations of stellar structure have been discussed in detail by Chandrasekhar (1957), Schwarzschild (1958), Cox & Giuli (1968), Clayton (1968), Kippenhahn & Weigert (1989), De Loore & Doom (1992).

The evolution of massive single stars has been the subject of many studies, reviewed by Maeder & Conti (1994). Probably the most extended set of computations was published by Schaller et al. (1992) and by Meynet et al. (1994).

Two important points to remember:

- after CHB, during hydrogen shell burning, the evolutionary tracks cross the HR diagram very rapidly, i.e. from theoretical point of view, very few stars are expected to be observed there (the blue Hertzsprung gap = BHG),
- when helium starts burning in the core, the evolution of a star with initial mass smaller than $\sim 15 M_{\odot}$ may be characterized by the presence of blue loops, i.e. the star spends part of its CHeB phase in the red, part in the blue.

Let us discuss the present state of a few parameters affecting single star evolution.

2.1. Opacities

In the larger part of the stellar interior, the opacity is due to electron scattering. Only in the outermost layers, where the plasma temperature becomes smaller than $\sim 500\,000$ K and where the heavier elements are only partially ionized, does bound-free opacity become important. For these layers it is required to use the most sophisticated opacity tables. But, since these outer layers constitute only a small amount of the total mass of the star, it is obvious that the overall stellar interior evolution of a massive star is hardly affected by these outermost layers. This explains why evolutionary computations with the older LAOS (Cox & Tabor, 1976) opacities, are very similar to those calculated with the newer OPAL tables (Iglesias et al. 1992). The main difference between both sets are the T_{eff} values of the models: OPAL opacities are larger, hence the resulting radiation pressure is larger in the outer layers causing the star to be larger. Since the nuclear energy production (and thus the luminosity) depends very little on the opacity in the outer layers, OPAL opacities imply lower T_{eff} values.

2.2. Convective core overshooting

A plasma is convectively unstable when the adiabatic gradient is smaller than the radiative one. It is tempting to define the boundary of the convective region there where both gradients are equal. However, convective motions do not necessarily vanish at this boundary and they may ‘overshoot’ it: convective overshooting.

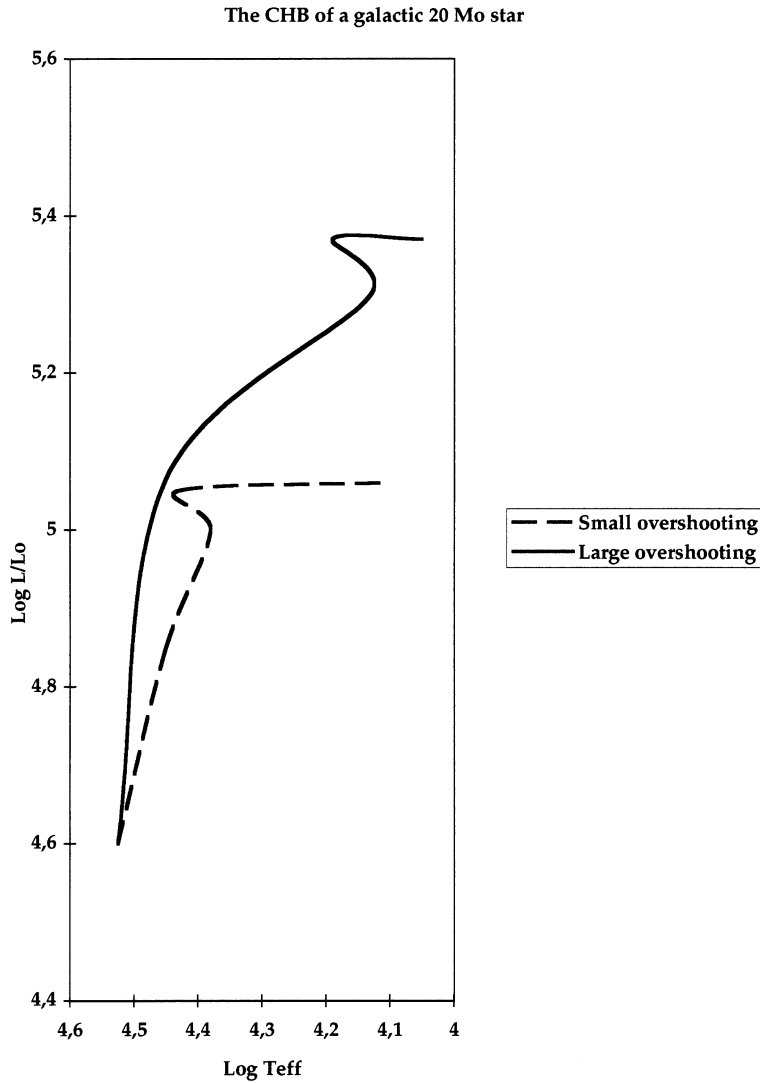


Fig. 4. The effect of convective core overshooting on the evolution of a 20 M_{\odot} star

A description of the problem has been given by e.g. by Roxburgh (1978, 1989, 1992), who proposed an integral condition for the radius r_c of the convective core. However, the latter seems to be incorrect (Eggleton, 1983).

For evolutionary computations it is advisable to parameterize overshooting and to study its effect. The best way to do so is to use the radius r_s of the Schwarzschild core (i.e. the radius of the layer where the adiabatic and the radiative gradients are equal) and to use a fraction αr_s as the overshooting distance. Compared to other parameterizations which appeared in literature this has the advantage that overshooting only occurs there where a convective region is present, which is obviously a condition sine

qua non to have overshooting. Detailed comparison with observations will hopefully restrict the possible values of the parameter α .

Figure 4 illustrates the evolutionary effect of convective core overshooting during core hydrogen burning of a $20 M_{\odot}$ star. We compare a small and a large overshooting case. During the CHB phase, we notice three important effects:

- the CHB time scale increases with increasing convective core overshooting distance,
- the evolutionary models have larger luminosities when convective core overshooting is larger,
- the CHB band extends to lower T_{eff} values when convective core overshooting is larger.

An important consequence of large convective core overshooting during CHB is the suppression of blue loops during the CHeB of a star with initial mass $\leq 15 M_{\odot}$. As a consequence, the stellar population of regions where most of the stars were born simultaneously may give some hints concerning the amount of convective core overshooting. Meynet et al. (1993) collected data of a large sample of clusters and found a few where blue and red supergiants are simultaneously present. The authors consider this as evidence that blue loops are not suppressed and thus that convective core overshooting during CHB must be quite small.

2.3. Semi-convection

The central part of a star where nuclear burning occurs, is always convective (= convective core). It is a general property that as hydrogen burning proceeds, the mass extent of the convective core decreases. In this way a composition gradient is left behind in the stellar interior. Especially in massive stars this zone with varying molecular weight gradient may be dynamically stable but vibrationally unstable (Kato, 1966). This may initiate ‘slow’ mixing, a process commonly known as ‘semi-convection’.

The effect of semi-convection on the evolution of massive single stars has been reviewed by Langer & Maeder (1995). When semi-convection is treated as a very fast diffusion process (the Schwarzschild criterion), evolutionary computations for low metallicity ($Z < 0.004$) regions predict the existence of only few RSGs. However, in the SMC a large population of RSGs is present. This can be used as observational evidence that semi-convection (if present) is a slow diffusion process (the Ledoux criterion). However, Langer and Maeder notice that in this case, only few blue supergiants should be observed in the BHG and this is not the case. This means that the existence of a significant number of stars in the BHG and of a large number of RSGs is somewhat contradictory as far as the effect of semi-convection on single star evolution is concerned. As will be discussed in Sects. 5.2.2 and 5.3.1, the stars in the BHG may not be related to single stars so that we retain the RSG argument to conclude that semi-convection is a slow diffusion process.

2.4. The effect of stellar wind mass loss

Figure 5 illustrates the evolution of massive single stars assuming a small amount of convective core overshooting, assuming that semi-convection is a slow diffusion process (Ledoux criterion, Ledoux, 1947) and using OPAL opacities, for the Solar

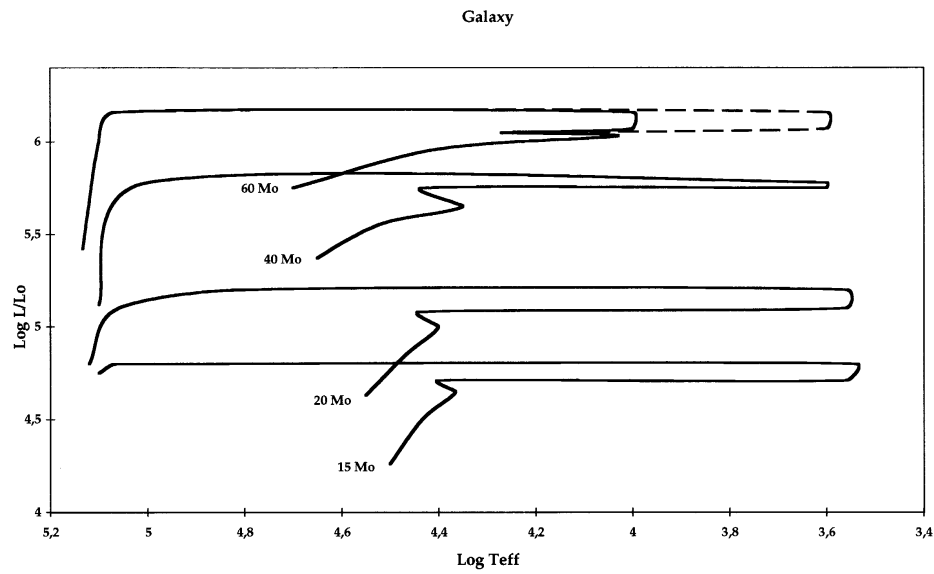


Fig. 5a. Evolutionary tracks of galactic massive single stars. The evolution of the 60 M_{\odot} star is first computed by assuming that the LBV stellar wind is large enough to prohibit redward evolution (full track); the dashed evolutionary track corresponds to the case where the LBV mass loss is smaller, the star becomes a RSG and loses its remaining hydrogen rich layers there.

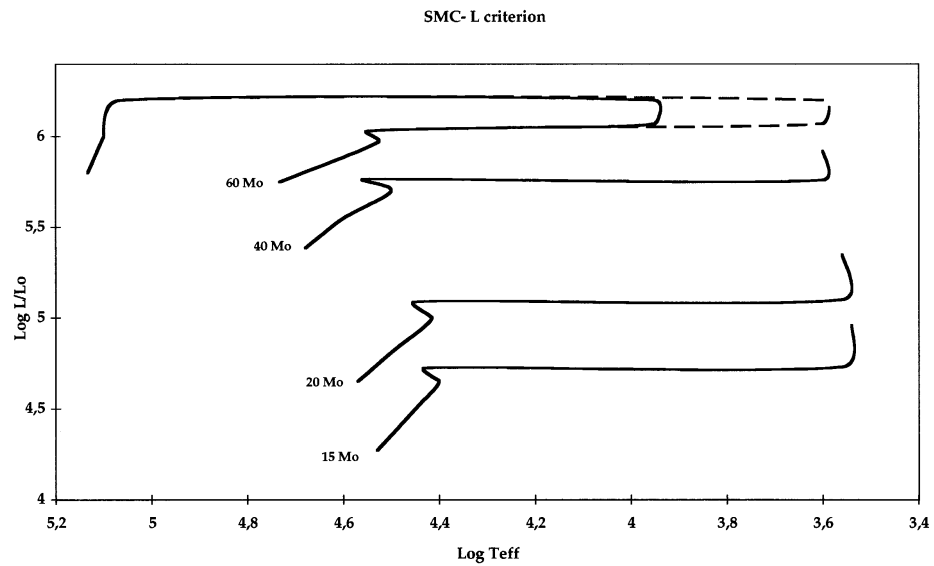


Fig. 5b. Evolutionary tracks of massive single stars with initial abundances holding for the SMC ($X = 0.76$, $Z = 0.002$), semi-convection is treated as a very inefficient mixing mechanism (Ledoux criterion), the stellar wind mass loss rates during the RSG and LBV phase are assumed to depend on the metallicity as predicted by the radiatively driven wind theory (Equation 1.4 with $\zeta = 0.5$).

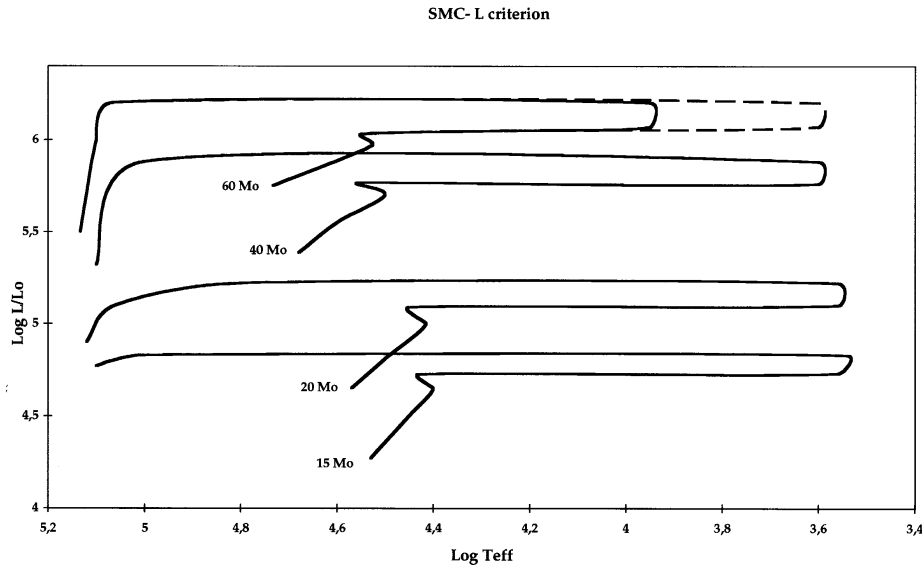


Fig. 5c. Similar as Fig. 5b but the RSG and LBV stellar wind mass loss rates are assumed to be independent from the metallicity and the same values apply as for the Galaxy

neighbourhood and for the SMC. The effect of stellar wind mass loss has been calculated by adopting the formalisms discussed in Sect. 1.2. Table 1 summarizes the results. It is interesting to compare them with evolutionary computations of Schaller et al. (1992) who used very different stellar wind mass loss rates during the RSG and WR phases.

We notice a few important points:

2.4.1. The solar neighbourhood

- Stellar wind mass loss during CHB has only a small effect on the general evolution of a star with initial mass up to $\sim 40 M_{\odot}$. After CHB, hydrogen burning continues in a shell just outside the He core. The star expands on the thermal time scale, and crosses the HR diagram very rapidly. At the beginning of CHeB the star becomes a RSG. So far, our evolutionary results differ only marginally from those of Schaller et al. (1992).
- Stellar wind mass loss during the RSG phase is of primary importance; when Equation (1.2) is applied during the whole RSG phase,

all stars with initial mass between $\sim 15 M_{\odot}$ and $40 M_{\odot}$ lose most of their hydrogen rich layers during the RSG phase.

Even if we account for the uncertainty of RSG mass loss rates and we use a 2 times lower rate, it follows that all stars with initial mass between $20 M_{\odot}$ and $40 M_{\odot}$ lose all their hydrogen. Here we encounter the first main difference with the Schaller et al. tracks.

- Table 1 gives the time of the CHeB star spent as a RSG (the remaining lifetime then obviously equals the fraction spent as a blue hydrogen stripped CHeB star).

Table 1. The time (in millions of years) spent by a star as a CHB star, a RSG, a WR, the total CHeB lifetime, the mass M_{eCHB} at the end of CHB, the mass M_{bWR} at the beginning of the WR phase, the mass M_{bWC} at the beginning of the WC phase and the final mass M_{final} at the end of CHeB, for two formalisms of the stellar wind mass loss rate during the RSG phase

Galaxy								
$\log(-\dot{M}) = 0.8 \log L - 8.7$								
M_{ZAMS}	T_{CHB}	T_{RSG}	T_{WR}	T_{He}	M_{eCHB}	M_{bWR}	M_{bWC}	M_{final}
15	14.8	0.75	0	1.12	15	–	–	4.9
20	10.1	0.59	0.26	0.85	19.5	7.1	–	5
25	8.2	0.46	0.27	0.73	24	9.9	5.2	5
30	6.9	0.32	0.28	0.6	28	12.9	7.8	6
40	5.5	0.18	0.29	0.47	36	19.2	12.3	8
60	3.4	–	0.35	0.35	48	32	23	10.6
$\log(-\dot{M}) = 0.8 \log L - 9.0$								
M_{ZAMS}	T_{CHB}	T_{RSG}	T_{WR}	T_{He}	M_{eCHB}	M_{bWR}	M_{bWC}	M_{final}
15	14.8	1.12	0	1.12	15	–	–	8
20	10.1	0.75	0	0.75	19.5	7.3	–	7.3
25	8.2	0.63	0.02	0.65	24	10	–	8.9
30	6.9	0.52	0.04	0.56	28	13.2	–	11
40	5.5	0.36	0.11	0.47	36	19.8	12.6	12
60	3.4	–	0.35	0.35	48	32.5	23	10.6
SMC ($Z = 0.002$)								
M_{ZAMS}	T_{CHB}	T_{RSG}	T_{WR}	T_{He}	M_{eCHB}	M_{bWR}	M_{bWC}	M_{final}
15	16.1	0.8	0	1.0	15	–	–	5.4
20	11.5	0.64	0.18	0.82	20	7.9	–	5.7
25	9.2	0.49	0.2	0.69	25	11.5	–	6
30	7.9	0.37	0.2	0.57	29.5	16.5	8.1	6.4
40	6.2	0.15	0.29	0.44	39	26.1	13.7	8.7
60	3.9	–	0.32	0.32	53	36	25.1	11.2

The results of the table are computed using Equation (1.3) to determine the stellar wind mass loss rate once the star becomes a WR star. A hydrogen deficient helium burning star is considered as WR when its mass is larger than $5 M_{\odot}$ (Sect. 1.2.3). The star first resembles a WN star with hydrogen (= WNL). Due to SW mass loss, the layers in which still some hydrogen was left, are removed (the star will be observed as a WN star without hydrogen = WNE). If mass loss by stellar wind continues, layers may appear at the surface which have at some time been in the CHeB core and one expects to see a star with atmospheric chemistry corresponding to the 3α -process. This means that ^{14}N has disappeared completely and an overabundance of C and O is expected: the star has turned into a WC type star. Compared to the results of Schaller et al., we notice two differences: single WR stars originate from stars with lower initial progenitor masses and the final mass of the stars at the end of CHeB in our calculations is significantly larger than in the Schaller et al. computations.

- We started with the assumption that the LBV mass loss is large enough to prohibit redward evolution for stars with initial mass larger than 40–50 M_{\odot} (the tracks in full). Whether or not the large value of \dot{M} that is needed corresponds with observations of LBVs is a matter of faith. If in reality the average rates are lower, also stars with initial mass larger than 40 M_{\odot} will evolve to the red part of the HR diagram, similarly as those with lower initial mass. This is illustrated in Fig. 5a. As an example, let us consider the evolution of a 60 M_{\odot} star. The star loses $\sim 12 M_{\odot}$ during CHB as a consequence of a normal O-type SW. At the end of CHB, it still has a $\sim 16 M_{\odot}$ hydrogen rich envelope. To avoid the redward evolution (i.e. to avoid a RSG phase), this whole envelope has to be removed during the LBV phase. However, if we suppose that the real (observed) SW is two times lower than is needed, only 8 M_{\odot} will be lost during the LBV phase and the star becomes a RSG with luminosity $\log L/L_{\odot} \approx 6.1$. Applying Equation (1.2), the RSG will lose mass by SW at a rate $\sim 2 \cdot 10^{-4} M_{\odot}/\text{yr}$. It thus takes $\sim 40\,000$ yrs to remove the 8 M_{\odot} envelope that was left after the LBV phase. This time scale is sufficiently short to explain the lack of observed RSGs with $M_{\text{bol}} < -9.5$.
- During the entire WN phase, the star has atmospheric layers which belonged to the hydrogen burning core during several million years: these layers should have CNO equilibrium abundances. Evolutionary computations of massive stars therefore predict that all (massive) WN stars should have very similar surface chemistry.
- At the beginning of the WR phase when hydrogen is still present, the luminosity of the star is determined by the CHeB reactions and by the hydrogen burning in the shell just outside the helium burning core. As stellar wind strips the star further down until all hydrogen is removed, the hydrogen shell burning is obviously turned off. This is visible in the tracks of Fig. 5 where at a certain moment the luminosity drops considerably.

2.4.2. The magellanic clouds

The LMC evolutionary tracks are very similar to the galactic ones. Evolutionary tracks for SMC single stars are shown in Fig. 5b. Quantitative results are included in Table 1. We conclude:

- All massive stars become RSGs and thus at least some of them could become single WR stars provided that the RSG stellar wind mass loss is large enough. The computations shown in Fig. 5c correspond to the case where Equation (1.2) also applies during the RSG phase of SMC single stars. If the RSG mass loss depends on the metallicity as predicted by the radiation driven wind theory [Equation (1.4)] the SMC value could be a factor 3 smaller than in the Galaxy. In this case the stars remain in the red part of the HRD and no WR types are formed (Fig. 5b).
- The evolution of stars with initial mass larger than 40–50 M_{\odot} depends on the LBV mass loss and in particular on how Z affects the \dot{M} during this phase. As for the Galaxy, we first assume that the LBV mass loss is large enough to prohibit redward evolution for stars with initial mass larger than 40–50 M_{\odot} . We then lower the mass loss rate by a factor 3 and apply the RSG SW formalism. The overall evolutionary behaviour is very similar to that of the Galaxy. When stars are allowed to move to the red, due to the dependence of the SW mass loss on Z , the RSG phase is longer.

2.5. Post-CHeB evolution

The present state of post-CHeB evolution has been extensively studied by Woosley (1986), Woosley and Weaver (1995), Woosley et al. (1993, 1995). Since the evolution of the final CO core should be largely independent from the mass layers outside this core, the final mass of the FeNi core in our evolutionary calculations can be estimated from the results of Woosley (1986). Table 2 shows the relation between the initial ZAMS mass, the final mass of the star just before the SN explosion and the final mass of the CO core for galactic stars. For the $20 M_{\odot}$ and $15 M_{\odot}$ star, we also give the results when the RSG SW mass loss rate is a factor 2 smaller than predicted by Equation (1.2). We conclude:

comparison of the mass of the final FeNi core with observed masses of neutron stars show that probably all single stars with mass larger than 20–30 M_{\odot} collapse to form a BH.

It is conceivable that in this case no SN explosion happens (Burrows, 1987; Woosley and Weaver, 1995), i.e. the mass of the BH equals the final mass of the whole star and thus that stars more massive than $\sim 20 M_{\odot}$ do not contribute to the chemical enrichment of the interstellar medium (Maeder, 1992). Notice that with the SW mass loss rate of WR stars discussed in Sect. 1.2, our evolutionary computations predict the existence of BHs with mass larger than $10 M_{\odot}$.

Table 2. The pre-SN mass M_{sn} , the CO-core mass M_{CO} and the final FeNi-core mass M_{FeNi} for stars with ZAMS mass between $20 M_{\odot}$ and $60 M_{\odot}$. For the $15 M_{\odot}$ and the $20 M_{\odot}$ model, we also give the results when the RSG SW mass loss is a factor 2 smaller

M_{ZAMS}	M_{sn}	M_{CO}	M_{FeNi}
15	5/8	2.5/3	1.5/1.65
20	5/7	3.5/4.3	1.7/2.0
40	8	6.5	2.9
60	10	8	3.1

2.6. The effect of rotation on massive single star evolution

The effect of rotation on stellar evolution has been studied by [Maeder (1998), Meynet (1998), Talon et al. (1997)] and by [Langer & Heger (1998), Heger et al. (1998)]. The assumptions behind the calculations of both groups are rather different:

The first group uses a parametrized model to describe the transport of angular momentum in the stellar interior. The meridional circulation transports matter from core to the surface along the polar axis. This material then moves across the surface to the equator, increasing its angular momentum. Finally, it transports this momentum inwards along the equatorial plane.

The second group assumes that rigid rotation is a good approximation to describe the redistribution of angular momentum in the stellar interior during the CHB phase (their assumption is based on the study of Zahn, 1994). They therefore implicitly assume that momentum is transported from the stellar core towards the stellar surface.

Despite the different treatment of the process, two effects are common:

- due to rotation, chemically enhanced layers from the convective core are transported outwards. In this way, a rotating stellar model acquires an atmosphere that is enriched in He and N, depleted in C and O,
- fast rotating cores are larger and more massive than slow rotating ones, i.e. the effect of rotation on stellar evolution is similar to the effect of convective core overshooting during CHB in non-rotating models; models that rotate faster correspond to non-rotating models with larger convective core overshooting and this means that (see Sect. 2.2)
 - fast rotators have a longer CHB time scale
 - fast rotators are overluminous compared to non-rotating stars
 - the CHB band of fast rotators may be wider

2.7. Comparison to observations

2.7.1. The HR diagram

A comparison between the observations of stellar aggregate members in the Solar neighbourhood (Fig. 1) and theoretical evolution, reveals the following two discrepancies:

- when we define the end of the ‘observed’ CHB sequence in the HRD as the region where the number of stars drops significantly, we have to conclude that at least in the mass range $10\text{--}25 M_{\odot}$ the observed CHB sequence is broader than the predicted one. Part of the problem may be due to the temperature scale used to construct the HR diagram. The T_{eff} of most of the stars is based on the B-V color - T_{eff} relation and the difference in B-V is merely 0.04 if T_{eff} changes from 30 000 K to 20 000 K. However if we take the HRD position for granted, we are left with a real problem when only single star evolution with small convective core overshooting is considered.
- It is clear that observations of massive stars younger than 1–2 million years are lacking, i.e. we miss $\sim 20\text{--}30\%$ of the O-type stars.

The reason for the latter effect could be intrinsic to the formation mechanism of stars, illustrated by the following experiment.

Suppose we have a gas cloud with mass M leading to the formation of a star with mass M . Contraction is initiated at the center, and a core with mass M_c is formed. Now the cloud starts contracting and the mass of the core increases at a rate \dot{M} . Typical values for the mass gain rate (mass accretion rate) have been computed by Myers & Fuller (1992) and range between $10^{-5}\text{--}10^{-4} M_{\odot}/\text{yr}$. This means that in order to form a $10 M_{\odot}$ star, accretion has to go on for about one million years (using an accretion rate of $10^{-5} M_{\odot}/\text{yr}$). Since the total CHB lifetime of a $10 M_{\odot}$ star ≈ 30 million years ($X = 0.7$, $Z = 0.02$), we can expect that a $10 M_{\odot}$ star will start its evolution almost as a normal ZAMS star. When the accretion rate is $\sim 10^{-4} M_{\odot}/\text{yr}$, also the formation time scale of the more massive stars is considerably smaller than their evolutionary time scale so that the evolutionary tracks are almost entirely similar to those of Fig. 5. The situation changes significantly when the accretion rate is $10^{-5} M_{\odot}/\text{yr}$, e.g. it takes about 4 million years to form a $40 M_{\odot}$ star. Since its CHB lifetime ≈ 4.5 million years, it can be expected that a $40 M_{\odot}$ star does not start its evolution exactly at the ZAMS. To illustrate the effect we first compute a homogeneous ZAMS model of a $10 M_{\odot}$ star with $X = 0.7$ and $Z = 0.02$, and we then follow its evolution by adopting

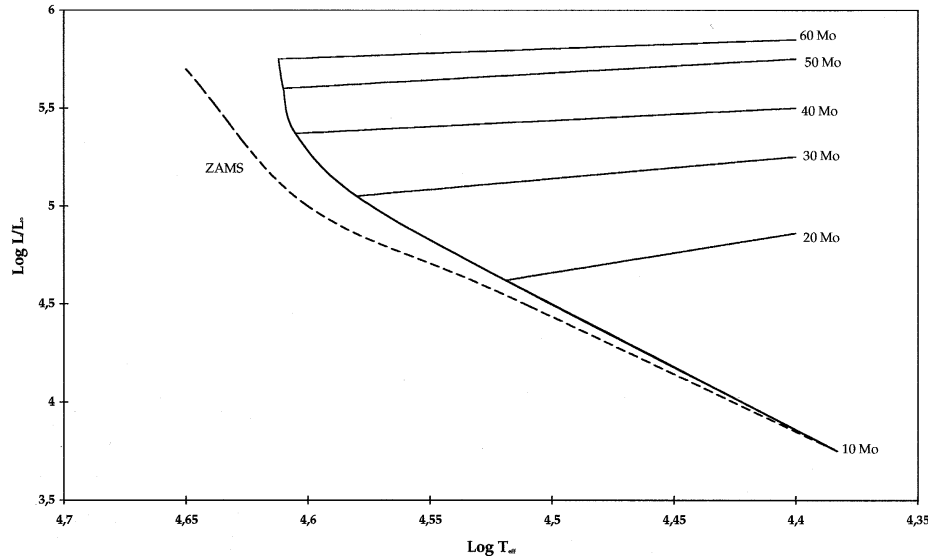


Fig. 6. Starting from a homogeneous ZAMS model of a $10 M_{\odot}$ star with $X = 0.7$ and $Z = 0.02$, we follow its evolution by adopting an accretion rate of $10^{-5} M_{\odot}/\text{yr}$. When the mass of the star equals $20 M_{\odot}$, $30 M_{\odot}$, $40 M_{\odot}$, $60 M_{\odot}$, we stop the accretion and the evolution of the star is continued in a normal way, including the effect of stellar wind mass loss

an accretion rate of $10^{-5} M_{\odot}/\text{yr}$. When the mass of the star equals $20 M_{\odot}$, $30 M_{\odot}$, $40 M_{\odot}$, $60 M_{\odot}$, we stop the accretion and the evolution of the star is continued in a normal way, including the effect of stellar wind mass loss. A very simple accretion model is used (similar to the ‘standard accretion model’ of Neo et al. (1977) also used in binary computations, Sect. 4.1.3). The model assumes that matter falls gently onto the underlying star with very small velocity and with an entropy which is larger than or equal to the entropy of the envelope of the star. The latter means that accretion of matter does not initiate large scale convection of the envelope, i.e. the evolutionary computations are performed assuming that the outer layers of the massive accreting star are in radiative equilibrium and remain so during the whole accretion phase. Evolutionary tracks are shown in Fig. 6, whereas Table 3 gives the numbers. It can be seen that the process explains the lack of massive stars close to the theoretical ZAMS. These computations confirm the results of Bernasconi and Maeder (1996).

However, the model described above may be too simple. Hydrodynamic computations of protostellar spherical symmetric accretion (Shu & Lubow, 1981) predict that, after passing through a shock front, matter settles down onto the underlying star with significantly reduced entropy. This may initiate convective mixing possibly of the whole star. As an example, we have followed the formation of a $30 M_{\odot}$ star (starting from a $10 M_{\odot}$ star and an accretion rate of $10^{-5} M_{\odot}/\text{yr}$, similar as above) but we have assumed efficient mixing of the whole star. At the end of accretion, the $30 M_{\odot}$ star has a $\log T_{\text{eff}} \approx 4.6$ and $\log L/L_{\odot} \approx 5$ which is very close to the position of a normal ZAMS $30 M_{\odot}$ star. If this model is correct, then the reason why very few stars are observed close to the ZAMS could be that the star, once it is formed, is still embedded into the remains of the protostellar cloud and will therefore only be visible in the infrared.

Particularly interesting is the chemistry of the massive star when the latter formation process applies. The layers of the original core are mixed with the surface layers. The hydrogen/helium abundances are only slightly affected ($X = 0.68$, $Y = 0.3$); however the CNO elements are significantly modified (N enriched, CO depleted). The model therefore predicts that a significant fraction of the O-type stars have altered CNO abundance's, also the luminosity class V and IV stars. As these stars evolve they will become giants or supergiants with a N enriched/CO depleted atmosphere.

Table 3. Starting from a $10 M_{\odot}$ ZAMS star, using an accretion rate of $10^{-5} M_{\odot}/\text{yr}$, a $20 M_{\odot}$ (resp. $30 M_{\odot}$, $40 M_{\odot}$) is formed after 1 (resp. 2, 3) million years. The table gives the values of the evolutionary parameters at the moment the stars are formed and at the end of CHB

Mass (M_{\odot})	t (10^6 yrs)	X_c	$\log T_{\text{eff}}$	$\log L/L_{\odot}$
10	0	0.70	4.39	3.73
20	1	0.68	4.52	4.62
19	10.8	0.00	4.36	4.97
30	2	0.63	4.58	5.07
27.7	7.8	0.00	4.38	5.33
40	3	0.58	4.60	5.38
36.2	6.8	0.00	4.34	5.57

2.7.2. The position of RSGs and WR stars

In Fig. 7 we compare the overall HRD position of the WR stars and the RSGs with our single star evolutionary tracks. When at least part of the WR stars (especially the WN types) with the smallest luminosities are single stars, it looks as if galactic (and LMC) single stars with initial mass as low as $20 M_{\odot}$ (and even lower) evolve into WR stars. This is the case with our evolutionary models where the RSG mass loss is determined by Equation (1.2).

An initial WR-progenitor mass as small as $15\text{--}20 M_{\odot}$ has been suggested by Massey & Johnson (1998). They note that the presence of luminous RSGs and WR stars is extremely well correlated for the OB associations in M31 and M33. To the extent that an association is strictly coeval, this argues that some stars of $15 M_{\odot}$ and above indeed do go through both a RSG and a WR phase.

Let us just remind that, based on population number synthesis of WR and O-type stars, it was suggested already a few years ago by one of us (Vanbeveren, 1991, 1995) that the minimum initial progenitor mass of WR single stars may be as small as $20 M_{\odot}$ (and even smaller).

2.7.3. The BHG

The observed star distribution in the HRD region occupied by stars with initial mass between $\sim 10 M_{\odot}$ and $\sim 25 M_{\odot}$ appears to extend more or less continuously down to the G-type supergiants with a maximum density in the A-type supergiant region. This effect is visible in the Galaxy as well as in the MCs.

The latter cannot be explained by the present single star evolutionary computations.

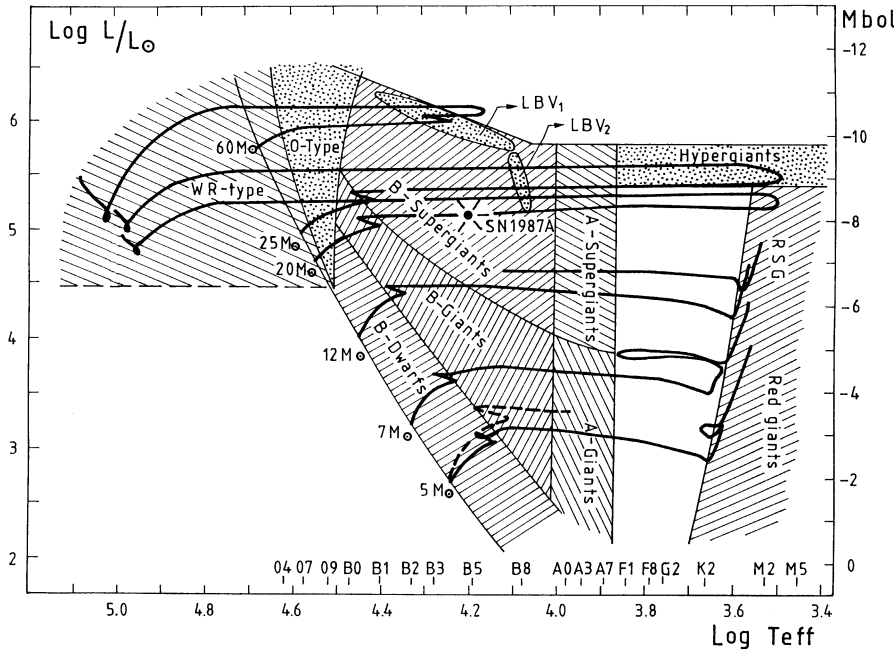


Fig. 7. The overall observed HRD compared to massive single star evolution for the Solar neighbourhood. Since the HRD and the evolution of massive stars in the LMC and in the Solar neighbourhood are very similar, we also show the position of the blue progenitor of SN 1987A

The existence of the BHG and the difficulty in explaining it, led Alongi et al. (1991) to suggest that convective envelopes in RSGs overshoot at their bottom over a large distance. The main effect is the occurrence of extended blue loops during CHB for stars with initial mass up to $\sim 20 M_{\odot}$. However if indeed the SW mass loss rates during the RSG phase of a star are as large as predicted by Equation (1.2), blue loops are largely suppressed and the problem of the BHG reappears again.

In chapter II dealing with close binaries, we will discuss an alternative possibility to explain the stars in the gap.

2.7.4. The effects of rotation compared to observations

One of the main ‘observable’ effects of rotation may be the altered chemistry in the atmospheres of supergiants. However, as outlined in Sect. 1.3, the present situation is unclear as far as observations are concerned.

The rotation period of pulsars may give information about the rotation and the evolution of the rotation of the convective core during CHB.

We follow the same reasoning as in Vanbeveren et al. (1998b). Let us assume for the moment that there is no transport of angular momentum from core to external layers and vice versa. The rotational angular momentum J of a rigidly rotating convective core with rotational period P_{cc} , with radius R_{cc} and mass M_{cc} can be written as $cM_{cc}R_{cc}^2 \frac{2\pi}{P_{cc}}$. We assume that c is constant in time. This is certainly not true but for the present purposes it is more than sufficient. A mass shell leaving the retreating

core has a rotational angular momentum $dJ = \frac{2}{3}dMR_{cc}^2 \frac{2\pi}{P_{cc}}$. If $M_{cc,f}$ = the mass of the final FeNi core ($\approx 1.5M_{\odot}$) and $M_{cc,0}$ = the mass of the convective core on the ZAMS, it follows that

$$\frac{J_f}{J_0} \approx \left(\frac{M_{cc,f}}{M_{cc,0}} \right)^{\alpha} \quad (2.7)$$

J_f = the rotational angular momentum of the FeNi core, J_0 = the rotational angular momentum of the convective core on the ZAMS, $\alpha = \frac{2}{3c}$. Typical values of c range between 0.2 (convective cores of ZAMS stars) and 0.4 (incompressible compact spheres, appropriate for cores at the end of a star's life) and therefore a generous upper limit is $\alpha = 4$.

If it can be assumed that the momentum of the FeNi core does not change as a consequence of the instantaneous SN explosion, J_f can be replaced by the rotational angular momentum of a neutron star $= \frac{2}{5}M_{NS}R_{NS}^2 \frac{2\pi}{P_{NS}}$ ($M_{NS} \approx 1.5 M_{\odot}$), $R_{NS} \approx 10$ km) and therefore

$$P_{cc,0} = \frac{5c}{2} \left(\frac{R_{cc,0}}{R_{NS}} \right)^2 \left(\frac{M_{NS}}{M_{cc,0}} \right)^{\alpha-1} P_{NS} \quad (2.8)$$

Most of the periods of ~ 900 known pulsars range between 0.1 s and 1 s. Even accounting for the fact that shortly after the formation of the pulsar, the rotation period may increase quite rapidly due to magnetic dipole radiation (Pacini, 1967), it seems very plausible that most pulsars have a spin period at birth larger than 0.01 s (Sect. 1.7.1). A massive ZAMS star has a core mass of a few solar masses and a core radius of a few solar radii. Equation (2.8) then implies that most of the ZAMS stars should have a very slowly rotating convective core. We therefore conclude

the rotational periods of pulsars indicate that either convective cores of the majority of the massive core hydrogen burning stars rotate extremely slowly (and thus the evolution of the majority of the massive stars is only marginally affected by rotation), or that there must be a very efficient mechanism to transport rotational angular momentum from the core towards the outer layers of a star.

The evolutionary models with rotation discussed in Sect. 2.6 do not indicate that an efficient mechanism to transport momentum from core towards the outer layers is present. We are therefore inclined to accept the possibility that the evolution of only a small fraction of the massive stars is significantly affected by rotational processes.

2.7.5. The runaway ζ Pup as massive single star

We ask ourselves the following question (see also Sect. 1.6):

along the kinematic path of the runaway ζ Pup, do we find the remains of a massive star cluster which had the dimensions of a few parsec at the moment ζ pup formed?

Using Hipparcos data, Fig. 8 illustrates the present state. As can be noticed, the distance between the stars is sufficiently large to assure that gravitational interaction can be neglected. It is straightforward then to calculate the kinematics of this region a few million years ago (if ζ Pup is a single star, it formed ~ 2 – 3 million years ago). This is shown in Fig. 8 as well. It is clear that

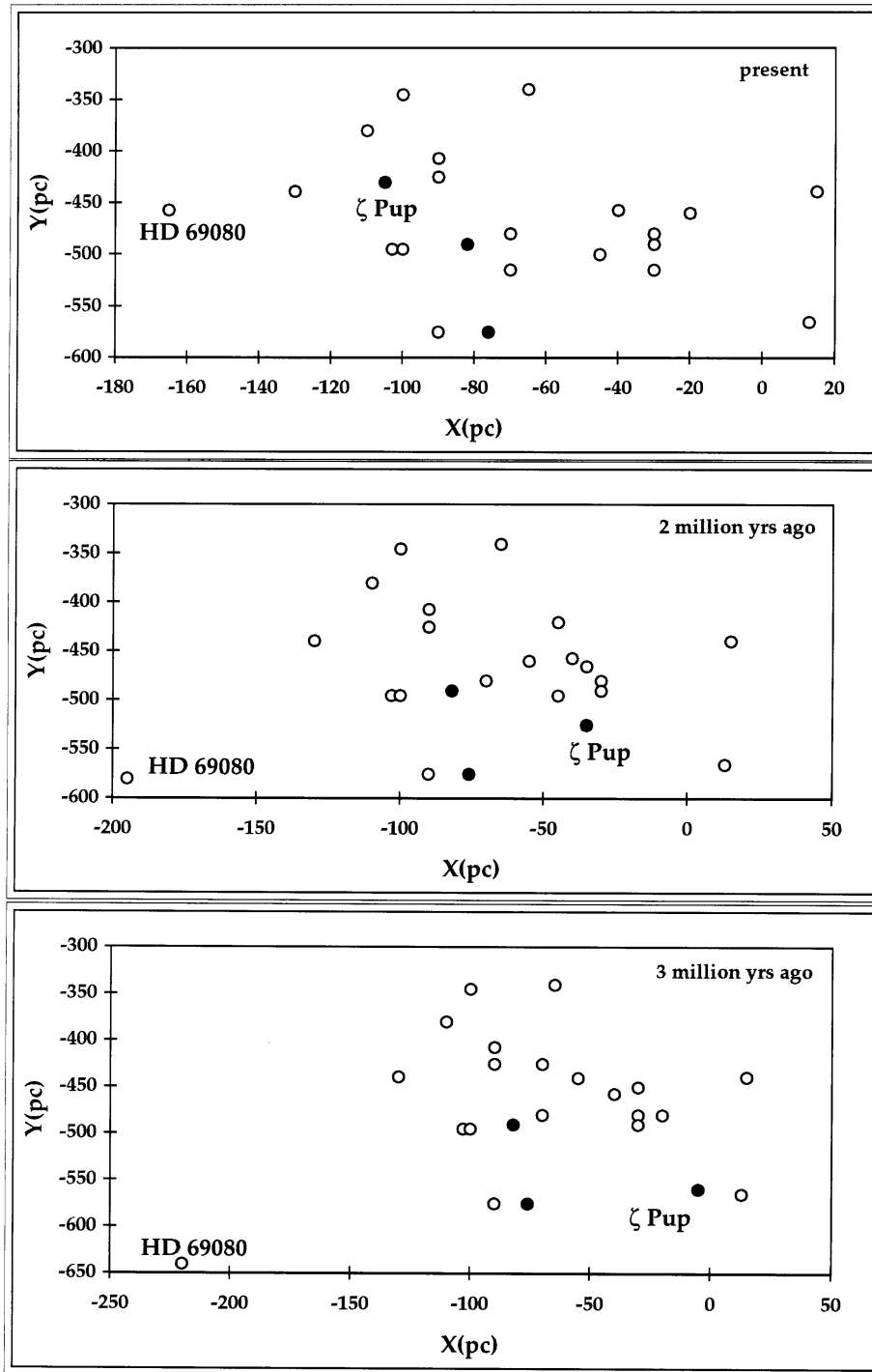


Fig. 8. The kinematic path of ζ Pup compared to the kinematics of the stellar neighbours

Hipparcos data do not support the hypothesis that ζ Pup became a single star runaway as a consequence of close encounters of binaries and single stars in a very dense cluster.

The only remaining possibility then is the supernova explosion in binaries (Sect. 6.4) indicating that ζ Pup may have had an evolutionary history that differs entirely from a classical single star scenario.

II. Massive close binaries

3. General

Primary and secondary: definition. The components in a binary are designated as primary and secondary. In this work we use the classical evolutionary definitions, i.e. the primary (resp. the secondary) is always the star which was initially the most massive component (resp. the less massive). Notice that this may be different from the definition sometimes used by observers. They classify the most luminous component as the primary. For most of the binaries this definition is the same as the evolutionary one. However, in many WR+OB binaries the OB star is by far the most luminous one but it is the secondary from evolutionary point of view.

The binary mass ratio: definition. The mass ratio q of a binary is always defined as the ratio of the secondary mass/primary mass. The mass ratio of WR+OB binaries is therefore the mass of the OB star/mass of the WR star. In binaries where one of the components is a neutron star (NS) or a black hole (BH) and the other a normal star, the mass ratio would be the mass of the normal star/mass of the compact star. However, for these binaries we make an exception, i.e. the mass ratio is defined as the mass of the compact star/mass of the normal star.

The Roche model. The evolution of binary components differs from the evolution of corresponding single stars because of the existence of three points where the mechanical force is zero (the Lagrangian points). Of particular importance are the first one (L_1) and the second one (L_2). The first point is located in between both components. It is important to notice here that such a point always exists, independent from whether or not both components rotate synchronously with the orbit or whether or not the binary orbit is eccentric.

A binary component expands during its evolution and when the orbital period is not too large, the outer layers may approach L_1 ; mass loss must occur and the binary is called an ‘interacting binary’ or ‘close binary’. The mass loss process is known as Roche lobe overflow (RLOF). A massive close binary (MCB) is a binary which was initially a close binary and where initially one or both components were massive stars. The binary component that is losing mass by RLOF is called the ‘mass loser’. The lost mass may be trapped in the potential well of the companion and can possibly be accreted by the latter. The companion can therefore also be called the ‘mass accretor’ or the ‘mass gainer’.

A star always tries to fill an equipotential surface; the surface passing through L_1 is called the Roche surface and the radius of a sphere with the same volume as the

volume enclosed by the Roche surface is called the Roche radius. An interpolation formula for the Roche radius R_{Roche} as a function of mass ratio has been presented by Eggleton (1983):

$$\frac{R_{\text{Roche}}}{A} = \frac{0.49}{0.6 + q^{2/3} \ln(1 + q^{-1/3})} \quad (3.1)$$

Case A, case B and case C binaries: definition. The evolution of a massive star is characterized by three major expansion phases: during CHB, during HSB, during He shell burning. When the orbital period is such that the RLOF starts during one of these phases, the binary is classified as a case A, case B, case C respectively (Kippenhahn & Weigert, 1967; Lauterborn, 1969). Using the evolutionary computations of single stars discussed in Sect. 2, we can conclude that

- in binaries with a primary mass smaller than $40 M_{\odot}$, RLOF occurs in MCBs with periods up to 3000 days.
- most MCBs (with a primary mass smaller than $40 M_{\odot}$) with period smaller than 2–4 days (resp. between 4 and ~ 1000 days, between ~ 1000 and 3000 days) will evolve according to case A (resp. case B, case C).

Binaries where the primary is initially more massive than $40 M_{\odot}$ may experience a large LBV type stellar wind mass loss and therefore

- the LBV phase of a primary with a mass larger than $40 M_{\odot}$ may significantly reduce the importance of the RLOF as mass loss process. MCBs with a primary more massive than $40 M_{\odot}$ will be called ‘Very Massive Close Binaries’, abbreviated as VMCBs.

Due to YSG/RSG mass loss, a star with initial mass between M_{min} and $40 M_{\odot}$ does avoid the He shell burning expansion and therefore case C will not occur. The value of M_{min} obviously depends on the YSG/RSG stellar wind mass loss rates. With our formalism [Equation (1.2)], $M_{\text{min}} \approx 15\text{--}20 M_{\odot}$ in the Galaxy and the LMC. When RSG mass loss depends on the metallicity as predicted by the radiatively driven wind theory [Equation (1.4)], $M_{\text{min}} \geq 40 M_{\odot}$ in the SMC.

One expects a different evolutionary behaviour of the primary in binaries where RLOF starts when the latter has a mostly radiative envelope (case B_r) compared to binaries where RLOF starts when the mass loser has a deep convective envelope (case B_c). The reason is the adiabatic reaction of a star with a convective envelope to mass loss, i.e. the larger the mass loss rate the faster the star’s expansion. The evolutionary computations of single stars (Sect. 2) reveal that among all case B types, case B_r binaries are the most frequent ones.

The separation (in terms of period and mass ratio) between case A and case B_r, between case B_r and case B_c, for binaries with primary mass smaller than $40 M_{\odot}$, is very similar for the Magellanic Clouds. The separation between case B_c and case C which is affected by the RSG stellar wind mass loss and the effect of LBV mass loss when the primary mass is larger than $40 M_{\odot}$ obviously depends on the relation between the metallicity and the SW rates.

The MCB evolutionary scenario: the early days. In Fig. 9 we show the qualitative evolutionary scenario of MCBs first introduced by Paczynski (1967) and completed later on by Van den Heuvel and Heise (1972). The primary is a massive star and

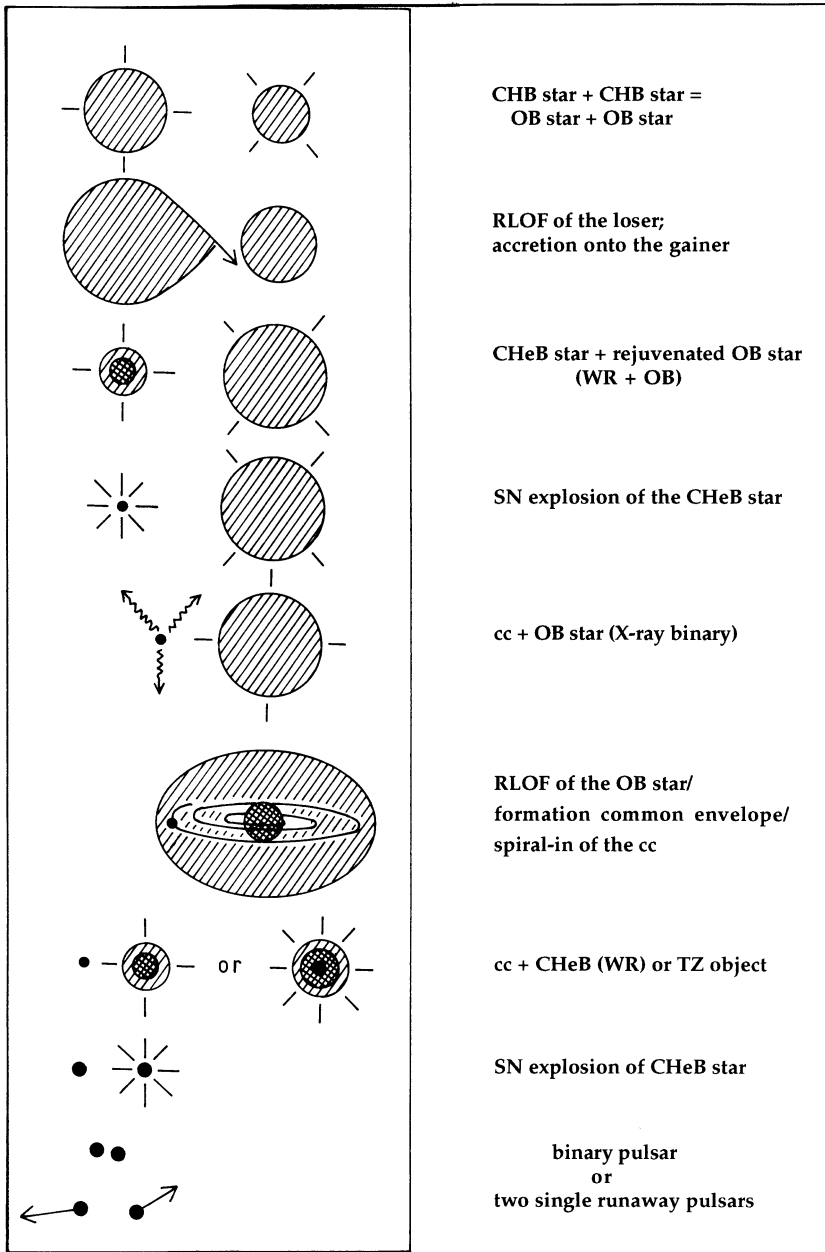


Fig. 9. The qualitative MCB scenario as it was introduced by Paczynski (1967) and completed by Van den Heuvel & Heise (1972)

possibly also the secondary. Both components first evolve as single stars, independent from each other. As the most massive star expands faster than its companion, it first reaches its critical radius and the RLOF starts. When the mass loser has lost most of its hydrogen rich envelope, an overall contraction phase sets in and the RLOF stops. The system then consists of a hydrogen deficient CHeB star and an OB-type star that has accreted part or all the mass lost by the loser; it was first suggested by Paczynski (1967) that this phase corresponds to the observed WR+OB binaries. Shortly after core helium exhaustion, the He star explodes. If the SN explosion does not disrupt the binary, the post SN-binary resembles an OB+cc binary; Van den Heuvel & Heise (1972) linked this phase to the observed massive X-ray binaries. As the OB-type mass gainer further evolves, it expands and its radius may also reach a critical value: a second RLOF starts but due to the extreme mass ratio of the binary, the low mass compact star will be dragged into the envelope of the OB star and it will start spiralling in (Sects. 4.2 and 4.4.4). The result of this process may be a very close binary (period of a few hours) consisting of a helium star and a cc. At the end of the evolution of the helium star, a second SN occurs. In most of the cases, the system will be disrupted leaving behind two single runaway pulsars. There is, however, a non-zero probability that the binary remains bound, in this way forming a binary pulsar like PSR 1855-09.

4. Binary evolutionary processes

We separately consider

- the RLOF of mass losers in case A/case B_r MCBs with initial $q > 0.2$, the resulting mass transfer, the effect of mass accretion on the evolution of the mass gainer and the formation of contact binaries
- the evolution of case A/ case B_r binaries where the mass ratio ≤ 0.2 : the spiral-in process (SpI process)
- the RLOF of mass losers in case B_c/case C MCBs and the formation of a common envelope (CE)
- the evolution of the binary period
- the effect of the supernova explosion of one of the components of a MCB on the system parameters

4.1. The RLOF process in case A/case B_r MCBs with initial $q > 0.2$

4.1.1. The mass loser

The RLOF starts when the stellar radius becomes larger the Roche radius. In general, the following method is applied in evolutionary computations to determine the mass loss rate:

- *assume that the interior structure of the primary can be computed using the same set of stellar structure equations derived for single stars*
- *compare the radius of the star to the Roche radius determined by Equation (3.1)*
- *if the stellar radius is larger than the Roche radius, determine the mass loss rate by imposing the condition that the stellar radius equals the Roche radius.*

When the Roche radius of a binary component is determined by Equation (3.1), one assumes that the binary is circularized, whereas the star rotates synchronously.

This may not be correct. However, anticipating, detailed evolutionary computations reveal that (see also Sect. 5.1)

knowing that there exists a critical radius is much more important than knowing its precise value.

Therefore, equalling the stellar radius to the canonical Roche radius derived from the binary period and mass ratio, gives very reasonable mass loss rates of the mass loser and leads to fairly good evolutionary tracks of the binary.

4.1.2. Mass transfer

Mass transfer has been studied hydrodynamically by Lubow & Shu (1975) assuming that the forces exerted by the radiation field of both components on the gas-stream can be neglected. A general conclusion:

matter lost by the loser during its RLOF falls on the gainer (depending on the initial binary period, either directly or through a Keplerian disc around the gainer); due to the large angular momentum of this matter, at least the outer layers of the gainer will spin up.

Is it possible that radiation forces in MCBs change the picture sketched above? It is quite clear that only detailed hydrodynamic computations, similar to the case of stellar winds, but adapted for a non-spherical gas-stream, can give an answer. This has not been done until now. The effect can be estimated as follows.

Typical RLOF mass loss rates in MCBs are in the range 10^{-4} – $10^{-3} M_{\odot}/\text{yr}$. Assuming a (cylindrical symmetric) gas-stream across L_1 with a typical radius of the order of a solar radius and with a temperature equal to the surface temperature of the mass loser (\sim a few 10^4 K), since the velocity of the matter in the stream is of the order of the sonic velocity, straightforward calculations show that the densities in the gas-stream should be $\sim 10^{-7}$ – 10^{-6} gr.cm^{-3} . Under these circumstances the main opacity is electron scattering. It is quite easy to demonstrate that electron scattering radiation forces do not significantly modify the streamlines in between the two components and they are certainly unable to drive the gas-stream out of the binary.

One could be worried about the effects of the collision of the gasstream with a possible stellar wind of the gainer. Again, only explicit hydrodynamics can be entirely conclusive. However, one may wonder what a supersonic spherical stellar wind with small density can do against a very dense gasstream? We are inclined to believe that the stream will cut through the wind like a knife through butter.

4.1.3. The mass gainer

Accretion of matter in a binary is always local (hence non-spherical). However it is assumed that the redistribution of the mass all over the stellar surface occurs very rapidly so that the effect of accretion may be estimated by adopting a spherical symmetric formalism.

The main effect of mass accretion is then the compression of all mass layers in the stellar interior due to the increase of gravity leading to the release of gravitational energy of all these layers. We consider two cases:

a. The standard accretion model (Neo et al., 1977). When dealing with MCBs, it can be assumed that the envelope of the mass gainer is in radiative equilibrium and has a positive entropy gradient. In the ‘standard accretion model’ it is assumed that the radiative equilibrium of the outer layers is not affected by accretion. This applies when the entropy of the in-falling matter is equal or larger than the entropy of the envelope of the mass gainer and when the effect of rotation (thus of rotational mixing) is neglected.

Of particular importance is the reaction of the convective core of a mass accreting star when the standard accretion model applies. A secondary in an interacting close binary may have already performed a significant part of its own CHB at the onset of the RLOF of the primary and thus at the onset of the mass transfer phase. This means that it has built up a molecular weight gradient in its interior. Increasing the mass of the star results into an increase of the stellar convective core. However, this immediately leads to the formation of a molecular weight barrier at its border which may prohibit a fast increase of the convective core when the stellar mass increases.

The way convection and semi-convection are treated is of fundamental importance here.

When the diffusion process in the semi-convective layers on top of the convective core is very fast, independently of the existence of a molecular weight gradient, the convective core boundary can be determined by the Schwarzschild criterion.

However, when the diffusion process is slow, compared to case 1, we obviously expect a much slower increase of the convective core when the star accretes mass and a situation can arise where the convective core does not increase at all.

During its RLOF, a primary may lose mass layers which have been nuclearly processed during an earlier evolutionary phase (the CHB phase). These layers have a molecular weight which is larger than the molecular weight of the outer layers of the mass gainer. This means that if at least part of the nuclearly processed matter is accreted by the gainer, it acquires an inverted μ -gradient. This situation is unstable and initiates mixing. The process which is commonly known as ‘thermohaline convection’, has been studied by e.g. Zahn (1983) and by Kippenhahn et al. (1980) who conclude that it is a very fast process which allows us to treat it as an instantaneous one. The numerical procedure to determine the consequences of this fast mixing is then straightforward: mix the accreted mass with the outer layers of the gainer until a situation occurs in which the molecular weight of the mixed layers is equal to the molecular weight of the layer just below the mixed region. It is clear that this process will produce stars with increased N and depleted C and O at their surface.

b. The accretion induced full-mixing model (Vanbeveren et al., 1994; Vanbeveren & De Loore, 1994). Mass accretion implies accretion of angular momentum; consequently a mass gainer spins up. Rotation induces mixing, i.e. radiative equilibrium is destroyed. Furthermore, if unlike the assumption made in the standard accretion model, the entropy of the accreted matter is significantly lower than the entropy of the envelope of the gainer, convection will start smearing out the entropy profile. This convection zone will develop inwards as long as its specific entropy exceeds that of the matter which is accreted on top of it. The limiting situation is of course a complete mixing of the whole star: the ‘accretion induced full mixing model’.

It is quite obvious that in the fully mixed case considered here, the way how semi-convection is treated is much less important than in the standard accretion model.

The existing hydrodynamic studies of accretion and accretion discs do not allow to make a distinction between both accretion models. Therefore, one can study the evolution of mass gainers by adopting both models and by using different values for the diffusion coefficient in semi-convective layers. A comparison with observations may then hopefully favor one of these models.

4.1.4. The formation and the evolution of contact binaries

When accretion of mass is treated in the standard way, a mass gainer expands during the accretion phase and the expansion rate is larger the larger the mass gain rate. The expansion may be so large that both stars come into contact. The evolutionary computations of MCBs performed in Brussels reveal that

if, during mass transfer, accretion is treated in the standard way, the mass gainers in all MCBs expand and most (all) of them reach their own Roche limit during the fast phase of the RLOF, i.e. the majority (all) of the MCBs evolve into a contact system.

Pols (1994) made a detailed study of the evolution of case A and case B MCBs and concluded that only binaries with large mass ratio may avoid contact if accretion is treated in the standard way. His conclusion was based on evolutionary computations performed with old opacity tables (Cox & Stewart, 1969). With new OPAL tables, also systems with large mass ratio become contact binaries.

Note that when the accretion induced full mixing model applies, the expansion is not that rapid and contact may be avoided.

The further evolution of contact binaries is not straightforward. One needs an evolutionary code where both components are followed simultaneously. For the RLOF, the following model is a possibility:

- start with a conservative RLOF where the mass loss rate of the primary (and thus the mass gain rate of the secondary) is determined by imposing the condition that the primary radius must be equal to the Roche radius; remember that although the assumptions of circularization and/or synchronization may not be 100% valid, this approximation will give very reasonable mass loss rate values,
- when due to mass transfer/accretion, both components come into contact, determine the mass loss rate of the primary (= mass gain rate of the secondary) by imposing the condition that both components are filling a common equipotential surface. Since evolutionary models are spherical symmetric whereas common equipotentials are not, approximations have to be used. A criterion has been proposed by Packet (1988), i.e. the mass loss/gain rate is determined by imposing the condition

$$M_1 \left(\frac{1}{R_{1c}} - \frac{1}{R_1} \right) = M_2 \left(\frac{1}{R_{2c}} - \frac{1}{R_2} \right) \quad (4.1)$$

where M_1 (resp. M_2), R_1 (resp. R_2) and R_{1c} (resp. R_{2c}) are the mass, the radius and the critical Roche radius of the mass loser (resp. mass gainer),

- when both stars overflow the equipotential surface defined by L_2 , calculate the mass loss rate of the primary by imposing the condition that the star must remain inside this surface, compute the mass gain rate by imposing the condition that the mass gainer must remain inside this surface; the difference then determines the amount of mass that has to be removed from the binary through L_2 resulting in a period variation discussed in Sect. 4.4.2.

It is clear that these computations are very time-consuming and depend on the initial mass ratio and period of the binary. A few test computations have been performed in Brussels, but a systematic investigation is still lacking. However, from these computations we can already conclude that when the accretion process is treated with the standard model, all MCBs with primary mass larger than $\sim 20 M_{\odot}$ evolve into deep contact during RLOF and will lose mass through L_2 . Our computations reveal that this deep contact is avoided when during the rapid phase of the RLOF 50% of the mass lost by the primary during its RLOF also leaves the binary. During the slow phase, a conservative assumption is perfectly possible.

We have also studied the early case B_r evolution of MCBs with primary mass smaller than $20 M_{\odot}$ and mass ratio q close to unity. These systems seem to be able to survive a conservative RLOF.

4.1.5. The effect of an LBV type stellar wind

When the most massive component in a binary has a mass larger than $\sim 40 M_{\odot}$, stellar wind mass loss at rates appropriate for LBVs may significantly affect its evolution and in particular it may largely reduce the importance of RLOF (and thus of mass transfer). Accounting for the uncertainties in the observed stellar wind rates of LBVs, it can not be excluded that the star does not reach L_1 and thus that the RLOF phase will not start.

4.2. The evolution of case A/case B_r MCBs where the mass ratio ≤ 0.2

Binaries where the mass ratio ≤ 0.1 meet the Darwin instability (Darwin, 1908; Kopal, 1972; Counselman, 1973; Sparks & Stecher, 1974). Instead of a classical RLOF, the low mass star is engulfed by the high mass component.

The evolutionary computations discussed in Sect. 5 indicate that although the star with a radiative envelope shrinks in response to mass loss, it may not be able to shrink fast enough to keep up with the rapid shrinkage of the Roche lobe when initially the binary has a mass ratio $0.1 < q \leq 0.2$. Also in this case, the low mass component will be dragged into the envelope of its high mass companion.

It is therefore conceivable that in most of the binaries with initial mass ratio $q \leq 0.2$, where the high mass star has a radiative envelope, the low mass star will be engulfed by the former at some evolutionary phase. The further evolution will then be governed by viscous forces and the low mass star will spiral-in (Sect. 4.4.4). In most of the cases, this SpI process leads to a merging of both stars.

When the low mass component was a neutron star or a black hole, merging means that spiral-in will continue until the compact star reaches the center of the star and a Thorne-Zytkow object (TZO) (Thorne & Zytkow, 1977) is formed. Computations were performed by Biehle (1991) and Cannon et al. (1992). It follows that TZOs have the structure of a RSG. Due to SW mass loss, first the hydrogen rich layers will be stripped off; when its mass and SW are large enough, the star may be observed as a 'weird' WR star (WR_{TZ}). Most probably this mass loss dominated evolution continues until the whole stellar mass has been blown away and the cc becomes visible again.

When the low mass component was a normal star, merging means that both stars will be mixed to form one star with mass equal to the sum of both masses. The consequences of this process can be studied assuming that the effects of merging are

similar to the effect of accretion (matter with mass equal to the mass of the low mass star is accreted on the more massive component). It is important to notice here that since case B_r binaries are expected to be the most frequent class of binaries, this type of merging will happen when the high mass star is a post-CHB, hydrogen shell burning star, i.e. the effect of merging may resemble the effect of accretion of mass on a post-CHB, hydrogen shell burning mass gainer.

A criterion for merging will be discussed in Sect. 5.3.

4.3. The RLOF process in case B_c/case C MCBs

The numerical procedure discussed in Subsect. 4.1.1 works well when the following conditions are satisfied:

- the response of the star to mass loss implies a decrease of its radius,
- due to mass loss, the radius of the star decreases faster than the Roche radius.

This is always the case when the massive star has a (mainly) radiative envelope. The procedure discussed above does never work when the star has a deep convective envelope (red supergiants), i.e. in case B_c/case C binaries. When a RSG is subjected to mass loss due to RLOF [on a time scale which is shorter than its thermal time scale], its adiabatic response will be an increase of the radius. Therefore, it may be expected that the star will experience a very violent mass loss phase, on a dynamical time scale which is of the order of hours. Due to the increase of the star's radius, the secondary star will be engulfed by the primary; this phase is known as the 'common envelope phase' (CE phase) of a binary.

4.4. The variation of the binary period due to mass loss

The variation of the binary period depends on the following mass loss processes:

- Spherically symmetric stellar wind mass loss
- The SpI process in case A/case B_r binaries with mass ratio ≤ 0.2
- The RLOF in case A/case B_r binaries with initial mass ratio $q > 0.2$
- The CE phase in case B_c/case C binaries

4.4.1. Spherical symmetric stellar wind mass loss

We assume that

- the orbit is circular and remains circular during the mass loss phase. The mathematics in the non-circular case are somewhat more complicated but the general behaviour of the period is very similar to the one we will describe here,
- the stellar wind mass loss is spherically symmetric.

It is straightforward then to prove that the orbital period varies according to

$$\frac{P}{P_0} = \left(\frac{M_{1_0} + M_{2_0}}{M_1 + M_2} \right)^2 \quad (4.2)$$

where the subscript 'o' stands for values at the beginning of the stellar wind mass loss phase. We thus conclude that

the period of a binary increases with the square of the sum of the masses of both components when one or both components lose mass by stellar wind.

In binaries where the primary is more massive than $\sim 40\text{--}50 M_\odot$, the LBV type stellar wind mass loss rate can be so large that the RLOF phase never starts. Using the single star evolutionary results of Sect. 2, Equation (4.2) then predicts a period increase by a factor 2 to 3.

4.4.2. The RLOF in case A/case B_r binaries with initial mass ratio $q > 0.2$

It is customary to define a parameter β describing the fraction of the mass lost by the mass loser that is accreted by the mass gainer, i.e. if \dot{M}_1 (resp. \dot{M}_2) denotes the mass loss (resp. mass gain) rate of the mass loser (resp. mass gainer), it follows that

$$\dot{M}_2 = -\beta\dot{M}_1, \quad 0 \leq \beta \leq 1 \quad (4.3)$$

In most of the MCBs (except the VMCBs), SW mass loss is not sufficiently large to allow the primary to escape RLOF. Due to RLOF, the primary loses matter at very high rates ($\geq 10^{-3} M_\odot/\text{yr}$). When this is accreted by the secondary, the latter starts expanding and both stars may enter a contact phase. A possibility (may be the only one) by which matter can leave a case A/case B_r MCB with synchronized period in an efficient way at rates similar to the mass loss rate of the primary due to RLOF, is mass loss through L_2 ; in this case it can be expected that a ring is formed around the binary with a radius L_2C with C the center of mass (see also Fig. 10).

We then derive the following formulae for the period variation:

if $\beta = 1$ (conservative RLOF)

$$\frac{P}{P_0} = \left(\frac{M_{1_0} M_{2_0}}{M_1 M_2} \right)^3 \quad (4.4)$$

if $0 < \beta < 1$ (non-conservative RLOF, mass lost through L_2)

$$\frac{P}{P_0} = \left[\frac{M_1 + M_2}{M_{1_0} + M_{2_0}} \right] \left[\frac{M_1}{M_{1_0}} \right]^{3[\sqrt{\eta}(1-\beta)-1]} \left[\frac{M_2}{M_{2_0}} \right]^{-3[\sqrt{\eta}\frac{1-\beta}{\beta}+1]} \quad (4.5)$$

where $\eta = L_2C/A$ (A = distance between both components). For a wide range of binary mass ratios, $L_2C \sim 1.3A$ and therefore η can be kept constant ($= 1.3$) during RLOF

if $\beta = 0$, with $\eta = 1.3$,

$$\frac{P}{P_0} = \left(\frac{M_1 + M_2}{M_{1_0} + M_{2_0}} \right) \left(\frac{M_1}{M_{1_0}} \right)^{0.42} e^{3.42 \frac{M_1 - M_{1_0}}{M_2}} \quad (4.6)$$

In the foregoing formulae, the subscript ‘o’ denotes values at the beginning of the RLOF phase.

Anticipating, when we use the results of MCB evolutionary computations, we conclude that

as a consequence of conservative RLOF, the period of the binary after RLOF is always larger than the period before RLOF; however, a significant fraction of the mass lost by a primary due to RLOF in a case A or case B_r binary, can be removed from the binary at the expense of a reduction of the available orbital energy, leading to a decrease in the orbital period.

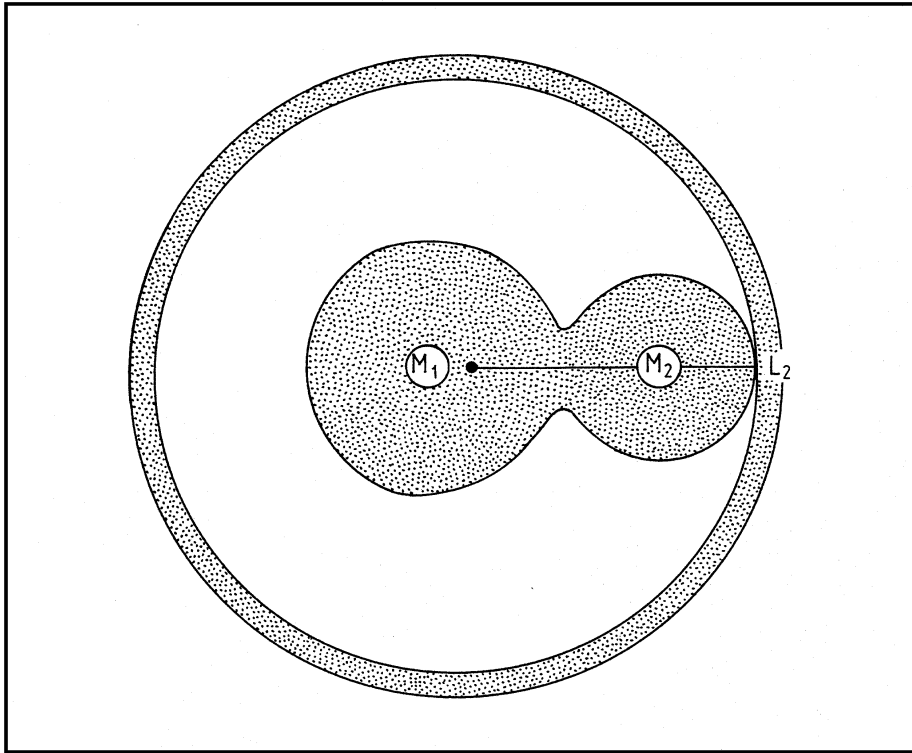


Fig. 10. Mass loss from the system through L_2 and the formation of a ring around the binary, during the RLOF of the primary in a case A/case B_r binary

4.4.3. The CE phase in case B_c/C binaries

We know of two energy sources in a massive binary which are able to remove matter from the CE: stellar nuclear energy and orbital energy.

Stellar nuclear energy is able to drive a SW from the CE. It can reasonably be expected that the rate is similar to that of supergiants, of the order of a few times 10^{-6} – $10^{-5} M_{\odot}/\text{yr}$.

An efficient use of orbital energy may result into larger mass loss rates. The idea: due to viscosity, orbital energy of the secondary is transformed into thermal energy of the CE and the secondary spirals-in into the envelope (a CE phase is thus always accompanied by a SpI process). Part of the thermal energy is radiated away, part is used to drive the matter of the CE out of the binary. Computations have been presented by Taam et al. (1978) and by Meyer & Meyer-Hofmeister (1979). They introduce a parameter L_{fric} (the friction luminosity) which is related to the variation of the orbital energy ε_{tot} according to the relation

$$L_{\text{fric}} = \frac{d\varepsilon_{\text{tot}}}{dt} \quad \text{with} \quad \varepsilon_{\text{tot}} = \varepsilon_{\text{pot}} + \varepsilon_{\text{kin}} = -G \frac{M_1 M_2}{2A} \quad (4.7)$$

The value of L_{fric} is uncertain. Despite this uncertainty, we can try to answer the following general question:

if viscosity between the secondary and the envelope of the primary is able to transform orbital energy into thermal energy of the envelope in an efficient way, how much orbital energy is required to remove this envelope?

We follow a similar prescription as proposed by Webbink (1984). When $\Delta\varepsilon_b$ is the binding energy of the envelope, the total orbital energy (potential + kinetic) $\Delta\varepsilon_{\text{tot}}$ needed to remove this envelope, can be determined from the relation

$$\Delta\varepsilon_b = \alpha \Delta\varepsilon_{\text{tot}} \quad (4.8)$$

where the parameter α expresses the fraction of the orbital energy (which is first transformed into thermal energy) that is not radiated away, and hence is effectively used to drive mass from the star ($0 < \alpha \leq 1$).

Generally, a star stops expanding (i.e. the RLOF or CE phase stops) when most of the hydrogen rich layers (with $X \geq 0.2$ – 0.3) have been removed (Sect. 5.1). It is then customary to introduce a parameter λ so that

$$\Delta\varepsilon_b = G \frac{M_{1_0}(M_{1_0} - M_{1_e})}{\lambda R_0} \quad (4.9)$$

with M_{1_e} = the final mass of the star after the removal of the hydrogen rich layers, and R_0 = the stellar radius at the onset of the CE/SpI phase. Since the primary is a RSG $\lambda = 0.7$ – 1.5 is a fair estimate.

In combination with the expressions for the orbital energy of the binary (relation 4.7) Equations (4.8), (4.9) and Kepler's law give the period variation.

To illustrate: using the overall evolutionary conclusions discussed in Sect. 5.1 and the period formalism discussed above with $\alpha = 1$ and $\lambda = 1$, a $20 M_\odot + 16 M_\odot$ (resp. $30 M_\odot + 24 M_\odot$) binary with a period $P = 600$ days will evolve into a $7 M_\odot + 16 M_\odot$ (resp. $12 M_\odot + 23 M_\odot$) post-common envelope binary with period $P = 14$ d (resp. 19 d). The $7 M_\odot$ (resp. $12 M_\odot$) component may be observed as a WR star.

4.4.4. The SpI process in case A/case B_r binaries with mass ratio ≤ 0.2

When the primary is a blue star with a radiative envelope and when spiral-in is a consequence of the fact that the secondary is a low mass companion, $\Delta\varepsilon_b$ in Equation (4.8) can be approximated by the binding energy of the hydrogen rich layers prior to the spiral-in phase. We therefore need the mass concentration $M(r)$ in the stellar interior at the onset of the mass loss process and thus (neglecting the effect of the low mass companion)

$$\Delta\varepsilon_b = \int_{M_{1_e}}^{M_{1_0}} G \frac{M(r)}{r} dM \quad (4.10)$$

Using the evolutionary computations of massive stars, Equation (3.11) can be approximated by expression (4.9) if $0.3 \leq \lambda \leq 0.5$ and the period variation can be calculated in a similar way as during the CE phase in case B_c/C binaries.

To illustrate the consequences of this SpI process, consider a $20 M_\odot$ OB type star ($\lambda \approx 0.4$) with a $2 M_\odot$ companion and assume maximum efficiency for the transformation of orbital energy into escape energy, i.e. $\alpha = 1$. Since $M_{1_e} \approx 7 M_\odot$ (Sect. 5.1), it follows from the foregoing formalism that the removal of $13 M_\odot$ implies a binary period decrease by a factor 2000. We therefore conclude that

the spiral-in process in a binary with very small mass ratio is able to remove a significant fraction of the mass of the mass loser at the expense of a very large reduction of the orbital separation (orbital period).

The large period reduction implies that

most of the case A/case B_r MCBs with mass ratio ≤ 0.2 will merge as a consequence of the spiral-in process of the small mass component into the envelope of the high mass one.

4.5. *The effect of the supernova explosion of one of the components of a MCB on the system parameters*

When a massive star does not end its life as a BH, it encounters a SN event. The effect on binary parameters has been discussed by Sutantyo (1978) (see also Verbunt et al. 1990; Wijers et al. 1992; Tauris & Takens 1998). We recall a few important properties.

- The effects of the SN shell on the companion star will generally be small (Fryxell & Arnett, 1981).
- If the SN explosion is not entirely spherically symmetric, the remaining neutron star will receive a kick velocity with a magnitude depending on the degree of anisotropy of the SN.
- If the SN explosion is spherically symmetric (and thus the kick velocity is zero), the binary remains bound if the SN shell has a mass less than half the total mass of the pre-SN binary; evolutionary calculations reveal that this is the case in most of the MCBs when the primary explodes.
- If the SN explosion is not spherical symmetric, the probability for a binary to remain bound is a very sensitive function of the kick velocity; if Equation (1.6) describes the distribution of kick velocities, it follows that most of the MCBs will be disrupted during the SN explosion of the primary.
- Due to the SN explosion of one of the components of a MCB, the center of mass of the system achieves a ‘runaway velocity’ for which analytic expressions can be derived. The value depends on the kick velocity and its direction.
- The space velocity of a NS after binary disruption is a combination of the kick velocity due to the asymmetric SN explosion and of the pre-SN orbital velocity of the exploding star. It can readily be understood that, depending on the orientation of the asymmetry,

large kicks may produce single pulsars with small space velocity., i.e. pulsars with small space velocity are not necessarily the result of a spherically symmetric SN explosion.

5. MCB evolutionary computations

A large number of detailed evolutionary computations of MCBs has been presented in numerous papers the last three decades. Mainly (only) case A and case B_r binaries with initial mass ratio $q > 0.2$ were considered. The reason is that the knowledge of the evolution of the latter can be used to simulate the final result of the CE and SpI phases. An extended review was presented by Van den Heuvel (1993). The present

state of MCB evolution has been discussed in extenso in a monograph ‘The Brightest Binaries’ (Vanbeveren, Van Rensbergen and De Loore, 1998). We summarize here a few conclusions.

5.1. The mass loser

Conclusion 1. A star in an interacting binary keeps its tendency to expand (and thus mass loss due to RLOF will continue) as long as the star has a hydrogen rich envelope.

This means that the RLOF in a case A/Case B_r binary, the CE phase in a case B_c/case C binary or the SpI phase in a binary with mass ratio ≤ 0.2 , will stop when both stars merged or when most of the hydrogen rich layers of the loser are removed (detailed calculations reveal that the mass loss processes stop when the atmospheric hydrogen abundance of the mass loser $X_{\text{atm}} \leq 0.2\text{--}0.3$).

Conclusion 2. In most of the MCBs (case B/C) the RLOF is very short ($\leq 20\,000$ yrs); the later the RLOF starts (i.e. the larger the orbital period) the shorter it is; the time scale reaches a minimum in case B_c/C binaries where it is of the order of the dynamical time scale resulting in the formation of a common envelope

General consequences.

- When merging is avoided, the final mass of the loser after the RLOF/CE/SpI phases is largely independent of the detailed physics of the mass loss process itself, and is largely independent of the initial mass ratio and period of the binary; the following relations (with coefficient of correlation ≥ 0.95) hold between the mass (M_b) before and the mass (M_a) after the mass loss process:

$$\begin{aligned} \text{for the Galaxy: } M_a &= 0.093M_b^{1.44} \\ \text{for the LMC: } M_a &= 0.085M_b^{1.52} \\ \text{for the SMC: } M_a &= 0.048M_b^{1.7} \end{aligned} \quad (5.1)$$

- The knowledge that at a given moment during the evolution of the loser it will lose its hydrogen rich layers on a very short time scale, is much more important than knowing the details of the mass loss process.
- The removal of almost all hydrogen rich layers on a very short time scale implies a large mass loss rate ($> 10^{-3} M_{\odot}/\text{yr}$); this mass loss rate is larger in binaries where the RLOF starts later, e.g. in binaries with larger initial orbital period.
- At the end of the mass loss process, when merging does not occur, the loser is a hydrogen deficient star at the beginning of CHeB. Shortly after the mass loss process, the star reaches a stage of thermal equilibrium. Its equilibrium radius satisfies the relation (coefficient of correlation ≥ 0.95)

$$R_e = 0.62 \cdot 10^{-4} M^3 - 0.49 \cdot 10^{-2} M^2 + 0.18M + 0.17 \quad (5.2)$$

R_e in R_{\odot} , M in M_{\odot} . Relation (5.2) also holds for evolutionary computations with lower metallicity.

Remarks.

1. The total mass lost by the loser during the CE phase in a case B_c/case C obviously depends on the adopted stellar wind mass loss formalism during the RSG phase. To illustrate, using Equation (1.2), accounting for the metallicity effect [Equation (1.4)], a case B_c/case C binary where the mass loser has an initial mass $> 20 M_{\odot}$ may never encounter a CE phase.
2. Also a star with mass larger than $40 M_{\odot}$, losing mass by stellar wind at very large rates appropriate for LBVs, stops expanding when the atmospheric hydrogen abundance has dropped below $X_{\text{atm}} = 0.34\text{--}0.4$. If this star is a binary component and if the LBV mass loss cannot entirely prevent RSG formation, the star experiences a normal RLOF and similar theorems and conclusions hold as the ones listed above. However, the LBV stellar wind may reduce the total amount of matter lost by the RLOF process.

In Fig. 11 we summarize the evolution of the mass losers with chemical abundances holding for the Solar neighbourhood and for the SMC.

5.2. The mass gainer

It is very unlikely that significant mass accretion occurs during CE evolution and/or during the SpI phase. It may however be very important during the RLOF of a case A/case B_r binary.

Knowing typical mass loss rates due to RLOF of a primary in a MCB, we can study from a phenomenological point of view the behaviour of a star when it gains mass at these rates. As discussed in Sect. 4.1.3, we need to distinguish the following cases:

- case 1a: accretion with the standard model, very fast diffusion process in semi-convective layers,
- case 1b: accretion with the standard model, very slow diffusion process in semi-convective layers
- case 2: accretion induced full mixing model.

We list a few important conclusions.

5.2.1. Accretion case 1a

- When the accretion time scale ($\sim M/\dot{M}$) is larger than the thermal time scale $\tau_{\text{th}} = 3.1 \cdot 10^7 \frac{M^2}{RL}$ of the CHB star, the mass gainer always occupies a position in the HR diagram which is very close to the HRD position of a normal CHB single star with the same mass and chemical composition; after the accretion phase, the further evolution of the star is almost entirely the same as the evolution of a normal single star with the same mass.
- When the accretion time scale is smaller than the thermal time scale, the mass gainer becomes overluminous for its mass and its radius increases significantly. When this happens in a binary, also the mass gainer may reach its critical Roche radius and a contact system is formed
At the end of the rapid accretion phase, the star regains its thermal equilibrium very fast and moves in the HRD to the position of a normal single star with the same mass and chemical composition. Again its further evolution is normal.

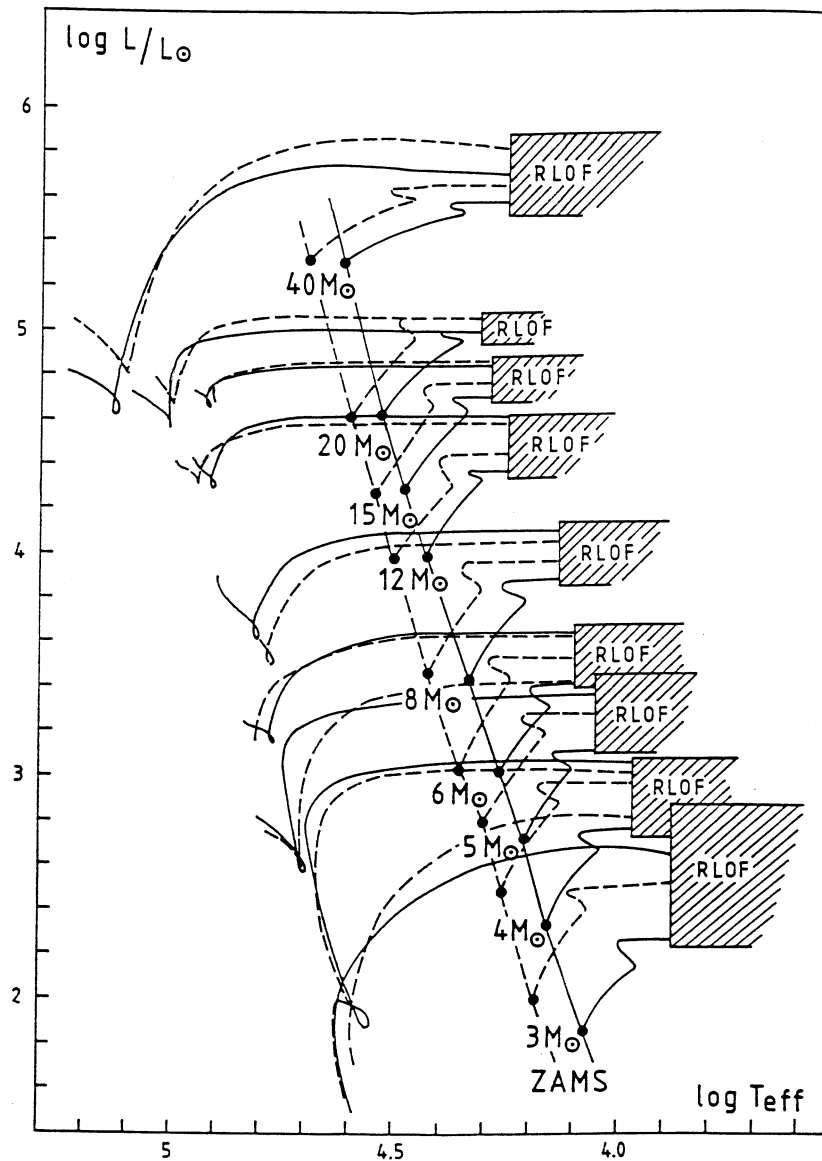


Fig. 11. The overall evolutionary behaviour of primaries of case B_r close binaries with galactic (full lines) and SMC (dashed lines) initial chemical composition (De Loore and Vanbeveren, 1995)

- After accretion, the stars are rejuvenated. This means that in the HRD, they are on a time-isochrone with a time scale smaller than their real lifetime.
- When the mass ratio of a binary is close to one, the RLOF starts when the secondary is also a HSB star. Since the He core is fixed and somehow protected by the hydrogen burning shell, accretion does not enlarge the core but instead produces an extended fully convective region on top of the hydrogen burning

shell. After the accretion phase the star is (slightly) underluminous for its mass. Evolutionary calculations were presented by De Loore & Vanbeveren (1992) and Podsiadlowski et al. (1992). The most important difference when compared to a CHB mass gainer is the further evolution of the gainer after the accretion process. The star has a He core which is small for its mass whereas due to the large convection region on top of the burning shell, the shell has a lot of fuel at its disposal and a rapid expansion of the star does not occur during the HSB and CHeB phase. As a consequence the star stays in the blue part of the HRD and does not make an excursion towards the RSG region.

5.2.2. Accretion case 1b

When the diffusion in semi-convective layers is very slow, the formation of a molecular weight-barrier on top of the convective core wright from the beginning of the accretion phase prevents a rapid core mass increase. Therefore even when the gainer is a CHB star, a situation can be encountered which is similar to the one described above when the accretion case 1a applies and when the gainer is a HSB star. Detailed computations were performed by Braun & Langer (1995). We conclude:

- after accretion, the stars are underluminous and are less rejuvenated compared to case 1a. Even when the gainer was a CHB star at the onset of mass transfer, it can remain a blue star during its entire further evolution after accretion. Furthermore, although the stellar mass increased considerably, its core mass remained almost the same as before the accretion process. Its further lifetime (and certainly its CHeB lifetime) may therefore be considerably larger than that of a normal single star with the same mass. This scenario explains (at least partly) the large number of AB-type supergiants observed in the BHG in the HR diagram.

5.2.3. Accretion case 2

The effect has been studied by Vanbeveren et al. (1994) and by Vanbeveren & De Loore (1994). Conclusions:

- Obviously, when the whole star is mixed, the way semi-convection is treated is of no importance.
- As expected, the rejuvenation of a mass gainer is very pronounced with the accretion induced mixing model.
- When accretion started during the second half of the CHB phase of the gainer, the post-accretion star is significantly overluminous and remains overluminous during its further evolution.

5.2.4. The variation of the chemical abundance at the surface of a mass gainer

- During the second part of the RLOF phase, the primary loses CNO processed matter and thus mass transfer due to RLOF and thermohaline mixing produces stars with surface layers which are significantly N enhanced (more than a factor 2) and CO depleted.
- If, due to accretion, the star is mixed completely (the accretion induced full mixing model), the effect is obviously much more pronounced.

- The surface hydrogen abundance in mass gainers is hardly affected in the standard case. However with the accretion induced full mixing process, the gainer can have a significantly reduced hydrogen abundance in its outer layers.

5.3. The binary after the RLOF/CE/SpI process: a CHeB+OB binary or a merger?

To decide upon the remnant system after the mass loss process, one may proceed as follows:

- knowing the mass that will be lost by the primary before it becomes a hydrogen stripped CHeB star, the period (orbital separation) of the binary after the mass loss process, and thus the final Roche radii of the binary, can be estimated, using the formalism outlined in Sect. 4.4,
- when the final Roche radii are larger than the equilibrium radii of both stars [for the hydrogen stripped primary, one can use Equation (5.2)], we are left with a binary consisting of a hydrogen deficient CHeB star and an OB component,
- when one of the Roche radii is smaller than the equilibrium radius of the corresponding component, it is plausible that both stars merged before the end of the mass loss process. To calculate the matter $\Delta M = M_{10} - M_1$ that will be removed during a CE/SpI process before both stars merge, the following scenario is a possibility. It is probable that the merging process will happen from the moment that the secondary itself fills its Roche lobe. Since its radius R_2 and mass M_{20} are not expected to change during the SpI process, the two equations that allow to estimate ΔM are

$$R_2 = R_{\text{Roche}}(M_1, M_{20}, A) \quad \text{and} \quad G \frac{M_{10} \Delta M}{\lambda R_0} = \alpha \left[\frac{M_{10} M_2}{2A_0} - \frac{M_1 M_2}{2A} \right] \quad (5.3)$$

5.3.1. The evolution of mergers

In most of the MCB mergers, merging occurs while the primary is a hydrogen shell burning star. If the effect of merging resembles the effect of accretion case 1 (Sects. 5.2.1 and 5.2.2), it can be argued that mergers will remain blue stars during most of their CHeB phase and may thus populate the BHG, together with the post-accretion stars discussed in Sects. 5.2.1 and 5.2.2.

5.3.2. The evolution of a CHeB+OB binary

When merging is avoided, the further post-RLOF/post-CE/post-SpI evolution of the loser depends critically on the adopted stellar wind mass loss rate formalism. Similarly as for single stars, when the mass loser satisfies the definition of a WR star, one can use Equation (1.3).

Table 4 illustrates the large effect of possible small uncertainties in the adopted mass loss rates of WR stars on the WR, WN and WC time scales. As usual, a WR star is classified as a WN (resp. WC) star when the outer layers are composed mainly of CNO (resp. triple-alpha) processed material. It can be concluded that

Table 4. The WN timescale compared to the WC timescale of a $30 M_{\odot}$ primary in a case B_r binary, when the stellar wind mass loss rate is calculated with relation (1.3), with relation (1.3) but multiplied by 0.5 and 1.5

\dot{M}^* correction	$T_{\text{WN}}/T_{\text{WC}}$
0.5	1.6
1	0.6
1.5	0.3

the observed WC/WN number ratio limits the possible stellar wind mass loss rate formalisms during CHeB.

Of particular importance is the existence of a very tight mass-luminosity relation for massive hydrogen poor CHeB remnants after RLOF losing matter by SW at rates typical for WR stars. Such a M-L relation has been derived by Vanbeveren & Packet (1979). It has been studied over again by Maeder (1983), Langer (1989), Vanbeveren (1991), Schaerer & Maeder (1992). All proposed relations closely match the original one, although different assumptions were made concerning a number of uncertainties during CHeB (e.g. different SW mass loss rate formalisms, different CO reaction rates, etc.).

Since massive hydrogen deficient CHeB stars are stars in thermal equilibrium, their M-L relations are largely independent of the evolution of their progenitors, i.e. the way the hydrogen rich envelope was removed from the progenitor. This explains why the M-L relation of hydrogen deficient CHeB binary components is very similar to the one of single stars where the matter was lost by SW during the LBV phase and/or the RSG phase (Sect. 2).

The M-L (in solar units) relations (coefficient of correlation ≥ 0.9) hold for WR masses between $5 M_{\odot}$ and $\sim 30 M_{\odot}$:

$$\begin{aligned}
 \text{WNL} \quad \log M &= -1.691 + 0.524 \cdot \log L \\
 \text{WNE} \quad \log M &= -1.658 + 0.520 \cdot \log L \\
 \text{WC} \quad \log M &= -1.822 + 0.542 \cdot \log L
 \end{aligned} \tag{5.4}$$

Primaries with initial mass smaller than $15 M_{\odot}$ develop hydrogen deficient CHeB remnants with mass $< 5 M_{\odot}$. Habets (1985, 1986) computed the evolution of helium stars with $2 \leq M/M_{\odot} \leq 4$ up to neon ignition, assuming that for these stars the SW mass loss during CHeB is small and does not significantly affect the further evolution of the star. Of particular importance is the variation of the radius as a function of core mass. It can be concluded that

- the CHeB stars with $2 \leq M/M_{\odot} < 2.9$ (corresponding to primaries in a case B/late case A binary with initial mass $< 15 M_{\odot}$) expand significantly during the He shell burning phase, after CHeB. It can be expected that they will overflow their critical Roche lobe for a second time: the process is known as case BB RLOF. As a consequence of case BB RLOF a star will lose the remaining hydrogen and most of the helium layers (those on top of the He burning shell).

The mass loss rate during the case BB phase is obviously much lower than during the previous one, so that most probably case BB RLOF is conservative. Since in

that case the period varies according to Equation (4.4), even the small mass variation during the case BB RLOF results into a very large period increase as illustrated by the following example:

consider a $10 M_{\odot} + 9 M_{\odot}$ case B_r binary; after the first conservative RLOF, we obtain a $2.3 M_{\odot} + 16.7 M_{\odot}$ system and after the second case BB RLOF a $1.7 M_{\odot} + 17.3 M_{\odot}$ system; during this second RLOF, the period has increased by a factor 2.2.

Remark. The existence and/or importance of case BB RLOF depends on the stellar wind mass loss during CHEB. One generally assumes that when the mass of the star is smaller than $5 M_{\odot}$ (and thus the star does not belong to the WR class), SW mass loss is too small to affect the CHEB evolution. However, the latter assumption is ad hoc. To illustrate: a constant SW mass loss rate as small as $10^{-6} M_{\odot}/\text{yr}$ is sufficient to prevent case BB RLOF.

5.4. The final fate of primaries of MCBs

- Primaries with initial mass $\sim 40 M_{\odot}$ (resp. $30 M_{\odot}$) develop a CO core with mass $\sim 3.8 M_{\odot}$ (resp. $3 M_{\odot}$). Using the computations of Woosley (1986), a CO core mass of $3.8 M_{\odot}$ (resp. $3 M_{\odot}$) corresponds to a FeNi core mass of $\sim 1.8 M_{\odot}$ (resp. $1.6 M_{\odot}$). We therefore conclude that

evolutionary computations of massive close binaries with small convective core overshooting show that primaries with initial mass up to $30\text{--}40 M_{\odot}$ may end their life as a NS (accompanied by a SN explosion)

Note the difference with single stars (Sect. 2).

- Primaries with initial mass $> 30\text{--}40 M_{\odot}$ have quite massive CO cores. The corresponding mass of the iron core is large enough to make them potential candidates for BH formation.

For the primaries with initial mass $< 15 M_{\odot}$, one can again use the results of Habets (1986); they allow the conclusion that

- in all helium stars with mass $> 2.2 M_{\odot}$, the heavy element core becomes larger than the Chandrasekhar mass; these stars are therefore expected to run into a SN event leaving behind a compact star. A $2.2 M_{\odot}$ CHeB remnant after RLOF results from a $10 M_{\odot}$ primary in a case B or late case A binary if convective core overshooting during CHB is negligible.

5.5. The evolution of a MCB after the collapse of the core of the primary

The evolution of the primary comes to an end when its core is composed mainly of iron and nickel, and nuclear processing ceases. The core collapses and becomes a BH or a NS accompanied by a SN explosion. The latter event could disrupt the binary. It is clear that in this case, the further evolution of the OB component is that of a single star but, due to accretion, with a chemical composition that may differ from the chemical composition of a normal single star. Note that, when the initial mass ratio of the progenitor binary is close to one (the exact value depends on the treatment of

semi-convection, Sect. 5.2), the gainer can remain a blue star during its entire life and thus populate the BHG. These stars will then explode as blue supergiants, producing events like SN 1987A.

The evolution of an OB+BH or an OB+NS binary (both are designated as OB+cc binaries) depends on the orbital period, on the mass of the OB component but also on the initial mass ratio of the system, since this determines the evolutionary phase of the mass gainer at the onset of mass transfer.

When the mass of the OB type component is larger than the minimum mass of LBVs ($\sim 40\text{--}50 M_{\odot}$ for the Galaxy), the OB star will lose most of its hydrogen rich layers first by a LBV type SW possibly followed by a spiral-in phase. The total mass lost by the OB star as a consequence of the latter process is largely reduced due to the preceding SW mass loss. It may be expected that the binary will evolve into a CHeB+cc (WR+cc) binary. It is obvious that such systems are rare. As an illustration, let us consider a $60 M_{\odot} + 50 M_{\odot}$ binary. After two LBV phases (possibly followed by a RLOF or a spiral-in with reduced total mass loss), the system evolves into a $28 M_{\odot}$ (WNL) + $10 M_{\odot}$ (BH) binary with a period of the order of days to decades.

When the mass of the OB type component is smaller than $\sim 40\text{--}50 M_{\odot}$ and accretion started late enough, similarly as in the disrupted case, the OB star will remain blue during its remaining lifetime and populate the BHG. One may expect that SpI will not happen (or will be very inefficient). The explosion of the OB component will be a type II SN event but from a blue progenitor, much like SN 1987A.

When, after accretion the OB star evolves more or less as a normal star and the period of the OB+cc binary is small enough to allow the OB star to fill its critical Roche volume before it becomes a RSG, the further evolution of the binary is governed by the SpI process. When the cc is a NS, the process is characterized by a very large period reduction. All OB+NS binaries with period smaller than ~ 100 days will merge before the removal of the whole hydrogen rich envelope, i.e. the system consists of a massive (HSB) star with a compact star in its He core: a Thorne-Zytkow object (Sect. 4.2).

When merging due to the SpI of the compact star is avoided and a CHeB + (NS or BH) is formed, depending on its mass the CHeB star becomes a WD, a NS (with SN explosion) or a BH, i.e. the binary ends its life as

WD + (NS or BH) binary
or
NS + (NS or BH) binary if the SN explosion did not disrupt the system
or
two single compact stars if the SN explosion disrupted the binary
or
BH + (NS or BH) binary

5.6. The effect of rotation on the evolution of a MCB

5.6.1. The primary

First notice that if the primary in a MCB is initially a rapid rotator, accounting for the orbital periods of most of the binaries, tidal torques will slow down most of these primaries, i.e. the effect of rotation on the structure and evolution of a star is expected

to be smaller when this star is a primary in a close binary compared to the case where it is a single star.

Probably the most important consequence of fast rotation for primaries in MCBs, is the enlargement of the convective core. This will not affect the qualitative evolutionary behaviour of the primary discussed in the previous subsections, although the final mass after RLOF/LBV/Spl/CE will be larger compared to the non-rotating case. This means that similarly to single stars

the effect of fast rotation on the evolution of primaries in MCBs \approx the effect of large(r) convective core overshooting.

A few conclusions:

- the total mass lost by RLOF (and transferred) of a fast rotating primary is smaller than that of a slowly rotating one,
- given the mass of the hydrogen deficient post-RLOF CHeB remnant (a WR if its mass is large enough), the mass of the pre-RLOF progenitor is smaller if it was a rapid rotator compared to the case where it was a slow rotator,
- similarly as for single stars, the minimum mass of a binary component that will collapse into a NS will be smaller if the star was a rapid rotator during its CHB phase compared to the case where it was a slow rotator.

5.6.2. The secondary

Accretion of matter lost by the primary during its RLOF may spin-up the outer layers of the secondary. If the whole star spins up, it is obvious that the further evolution of the secondary will be affected by rotational mixing. Accounting for the discussion in Sect. 6 we can expect that

- a rapidly rotating secondary will evolve at a larger luminosity compared to a slow rotator producing stars that are overluminous with respect to their mass; in the case of the accretion induced full mixing model, this overluminosity will obviously be very large,
- due to mass transfer the secondary may already have an altered surface abundance; dredge-up of CNO processed material continues when the star is a rapid rotator.

6. Observations of MCBs

The data of extra-Galactic MCBs are scarce. Therefore, how the binary properties such as binary frequency, mass ratio distribution, period distribution etc., depend on the metallicity is unknown. Even more, for the Solar neighbourhood only (≤ 3 kpc), MCB data are reasonably complete. Whether or not the statistics apply for the whole Galaxy (for the whole cosmos?) is uncertain.

We distinguish the following classes of massive binaries (MBs):

- MBs where both components are OBA-type stars (OBA+OBA),
- MBs with a WR star component and an OBA-type component (WR+OBA),
- the X-ray binaries for which we separately consider the high mass X-ray binaries (HMXB) where the optical component is an OB-type star, a Be type star or a WR star and the companion is a NS or BH, and the low mass X-ray binaries (LMXB) with a massive binary evolutionary history,

- binary pulsars where at least one component is a NS or a BH; the other component is either a low mass white dwarf or a NS (BH).

Owing to the SN explosion of one of the components in a binary, the remaining component may acquire a large space velocity and the star may be classified as a ‘runaway’ star. Therefore, when discussing observations which may be important for MCB evolutionary computations, we have to add

- the runaways.

6.1. Massive OBA+OBA binaries

The class of massive OBA+OBA binaries can be subdivided into:

detached binaries: both components are smaller than their critical Roche lobes,

semi-detached binaries: one component fills its Roche lobe

contact binaries: both components fill their Roche lobe.

Of particular importance are the OBA+OBA binary frequency, the mass ratio and period distribution.

6.1.1. The OBA+OBA mass ratio distribution

The observed mass ratio distribution of non-evolved O-type binaries has been discussed by Garmany et al. (1980). It was concluded that

- systems with q in the range $[0-0.2]$ are rare,
- systems with two components of similar mass (q in the range $[0.8-1]$) are remarkably frequent.

A similar analysis but for the early B-type binaries reveals that

- every possible mass ratio occurs with an almost constant probability; the same is true for the late B type binaries.

A binary with mass ratio close to one is obviously easier to detect than a binary with very unequal component masses. A detailed study of the implications of this selection effect on the q distribution of all spectroscopic binaries in the DAO8 catalogue (Batten et al., 1989) has been presented by Hogeveen (1991, 1992) (see also Halbwachs, 1987). He concludes that the true overall q distribution for all spectroscopic binaries can be described by the relation:

$$\Phi(q) \begin{cases} \propto q^{-2} & \text{if } 0.3 \leq q \leq 1 \\ = C & \text{if } q < 0.3 \end{cases} \quad (6.1)$$

If this is correct, then comparison with the observed distribution forces us to conclude that there is still a large number of stars to be recognized as components of binary systems.

6.1.2. The OBA+OBA period distribution

The observed period distribution of the unevolved O type binaries and of the early B type (B0-B3) and late B type binaries from the DAO8 catalogue are given in Fig. 12.

Comparing the periods of the unevolved MCBs in our sample with the minimum period a binary must have in order to avoid RLOF, we conclude that most of them will interact.

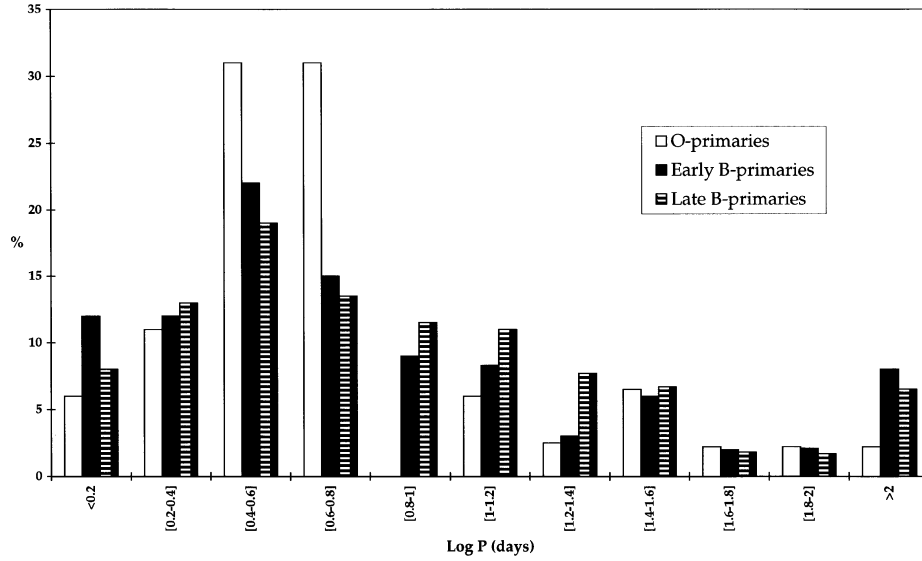


Fig. 12. Observed periods of binaries with an O type primary, an early B type primary and a late type B primary

Figure 12 shows that MCBs with observed period larger than ~ 100 days are very scarce. This may be due to observational selection.

According to Popova et al. (1982) (see also Vereshchagin et al., 1987, 1988), the semi-major axis A of the relative orbit of (all) binary systems, is distributed according to:

$$\Pi(A)dA \propto \frac{dA}{A} \quad (6.2)$$

and thus the period (P) distribution according to:

$$\Pi(P)dP \propto \frac{dP}{P} \quad (6.3)$$

extending up to periods of 10 years.

It is not meaningful to make such a detailed statistical study for the O type and the early B type binaries separately, since their number is too small. However, if the foregoing distributions also apply there, similar to the conclusion made in the previous subsection, there are still a significant number of OBA binaries waiting to be discovered (Mason et al., 1998).

6.1.3. The OBA+OBA binary frequency

First remark that the binary frequency should not be confused with the frequency of stars in binaries. The latter obviously accounts for the secondaries, i.e. the frequency of stars (of a certain subtype) in binaries is larger than the binary frequency.

Garmany et al. (1980) studied the binary frequency among all known O type stars brighter than $m_V = 7$ and north of -50° (a total of 67 O type single stars or primaries of binaries). Deleting the O type HMXBs from the sample, one concludes that among the O-type stars the observed MCB frequency $\sim 33\%$ ($\pm 13\%$ accounting for small number statistics).

In order to get an idea of the observed binary frequency in the B0-B3 spectral range we proceed as follows: if N is the number of stars, d the distance of the star (relative to the observer) and adopting a disc-like homogeneous space distribution

$$\frac{dN}{dr} \propto d \quad (6.4)$$

The apparent magnitude m_V of the star depends on its distance d

$$m_V = M_V - 5 + 5 \log d(\text{pc}) \quad (6.5)$$

and thus

$$\frac{dN}{dm_V} \propto 10^{\frac{2}{5}m_V} \quad (6.6)$$

The ‘Bright Star Catalogue’ = BSC (Hoffleit & Warren, 1991) contains 511 B0-B3 [III-IV-V] stars. The observed number distribution as a function of m_V can be compared to the prediction (6.6) and it follows that

- the number of B0-B3 stars in the BSC is complete up to $m_V = 6$ (a 95% confidence hypothesis),

There are 59 B0-B3 binaries in the DAO8 (Batten et al., 1989) brighter than $m_V = 6$. The BSC (which is complete up to $m_V = 6$) contains 348 B0-B3 stars, i.e. $\sim 17\%$ of the B0-B3 stars in the BSC are primaries of close binaries listed in the DAO8.

However, the DAO8 catalogue appears to be very incomplete. This is illustrated in Fig. 13 where we give the number of B0-B3 primaries in the DAO8 catalogue as a function of m_V . Furthermore, a significant number of binaries, listed in the BSC are not in the DAO8. As an illustration, counting all B0-B3 stars in the BSC which are classified as binaries in this catalogue, again restricting to $m_V = 6$, it follows that the binary frequency $\sim 66\%$ (using $m_V = 6.5$ as limit one obtains 61%; considering all stars, one arrives at a $\sim 60\%$ binary frequency).

Of course the BSC catalogue also contains the wide binaries which may not interact and we are obviously interested in the interacting binary frequency. In order to obtain a more realistic number we proceed as follows.

In Fig. 13 we have also drawn the expected ($N - m_V$) distribution under the assumption that the DAO8 is complete for $m_V < 5$ and we correct the number of stars in the m_V -bin [5-6] assuming a binary fraction independent of m_V and a disc distribution for all early Bs. From this, we conclude that there should be 127 spectroscopic binaries (most of them interacting) with $m_V \leq 6$ and with properties which are similar to the properties of the 59 binaries which are contained in the DAO8.

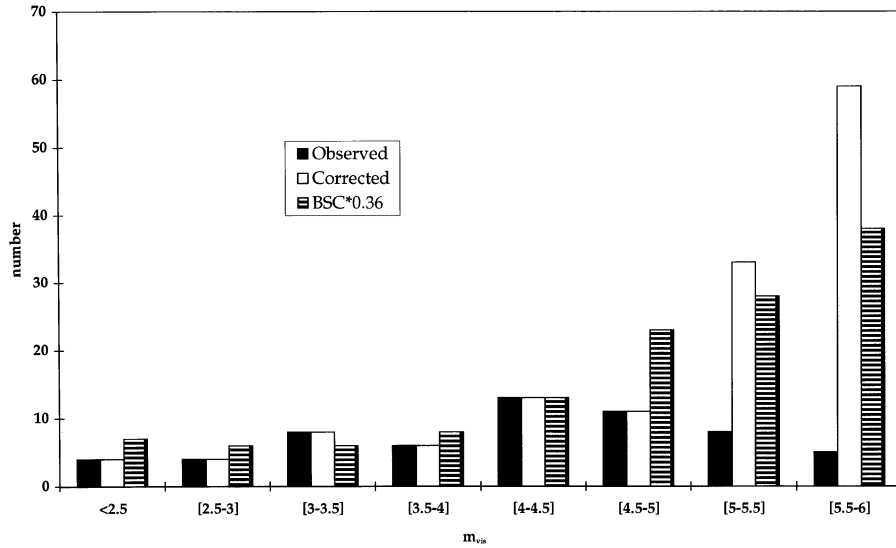


Fig. 13. The number of observed early B primaries in the DAO8 is incomplete above $m_V = 5$. Correcting for incompleteness enhances the fraction of binaries up to $\sim 36\%$. The number of early B primaries being $\sim 36\%$ of the number of early B stars in the BSC is also shown

This means that among the B0-B3 sample, the real interacting binary frequency is more like 127/348, i.e. $\sim 36\%$.

This number could be biased, since a primary is brightened by the presence of its companion. If one assumes a mean brightening with $0^m 25$ (a brightening with $0^m 75$ would be achieved when all secondaries and primaries have the same magnitude), one should rather compare the number of binaries brighter than $m_V = 5.75$ to the number of single stars brighter than $m_V = 6$. Extrapolated from the DAO8 catalogue one obtains for a complete sample 104 binaries brighter than $m_V = 5.75$, whereas the complete sample from the ‘Bright Star Catalogue’ contains jointly 120 singles brighter than $m_V = 6$ and 201 binaries brighter than $m_V = 5.75$.

With these assumptions, and using the same method as described above, we conclude that $\sim 32\%$ of the B0-B3 stars are primary of an interacting close binary. It is interesting to notice that this is remarkably similar to the observed binary frequency for the O-type stars.

Due to selection effects, the real MCB frequency may be much larger than the observed values quoted above.

Suppose that we detected all massive systems with mass ratio between 0.6 and 1. If Equation (6.1) applies for the mass ratio distribution, we expect about 2.5 times more stars in the $0.3 \leq q \leq 0.6$ range compared to the number of stars with $q \geq 0.6$. From the observed mass ratio distribution, we conclude that we are missing at least 30–40% of the binaries, i.e. starting from the observed 33%, the frequency now reaches a value $> 60\%$ and we yet have not counted the possible number of binaries with small mass ratio ($q < 0.3$).

If the period distribution of OB type binaries follows Equation (6.3) as well, we have to conclude again that we are missing at least another $\sim 30\%$ of the interacting MCBs.

Furthermore, the observed binary frequency can differ significantly from the binary frequency at birth of a population of stars. Binaries where both components merged will be observed as single stars but have had a binary history. Single stars that became single due to the fact that the SN explosion of the primary disrupted the binary, have had a binary history (and may have experienced mass accretion).

Accounting for the foregoing discussion we conclude

Probably the majority of the massive stars are formed as binary components; the fraction of massive stars that are formed as real single stars is very small.

6.1.4. Special cases

In the present section we will compare the evolutionary computations discussed in Sect. 5 with observations of specially interesting OBA+OBA binaries listed in Table 5 where mass loss due to RLOF/CE evolution happens or has happened.

Table 5. A representative set of evolved OB+OB binaries; (1) = Batten et al. (1989), (2) = Harries et al. (1997), (3) = Gies et al. (1998), (4) = Hutchings (1975), (5) = Dudley and Jeffery (1990); (6) = Hilditch (1974)

HD (name)	Sp. type	P (days)	e	$f(M)$ (M_{\odot})	M (M_{\odot})	Ref.
190967(V448 Cyg)	B1Ib+O9.5V	6.5	0.04		14.0+25.2	(2)
209481	O9V+O9V	3.1	0.03		6.2+2.9	(6)
12323	ON9V	3.1	0.21	0.0034		(1)
14633	ON8V	15.3	0.68	0.019		(1)
163181(V453 Sco)	BN0.5Iae+OBN	12	0.08		13.0+22.0	(1,4)
193516	BN0.7IV	4.0	0.06	0.043		(1)
ν Sgr	AI+B4/6	138	0.0		2.5+4*	(5)
Φ Per	sdO6+B0.5Ve	126	0.02		1.14+9.3	(3)
25638	O9.5V+B0	2.7	0.0		17.0+4.3	(1)

HD 163181 and HD 190967

HD 163181 is an eclipsing binary with a period $P = 12$ days, with a nitrogen enriched BN0.5Ia primary. Hutchings (1975) derived masses for the components, i.e. $M_1 = 13M_{\odot}$ (the primary) and $M_2 = 22M_{\odot}$. The secondary star (M_2) is 1.5–2 mag fainter than the primary and it looks also nitrogen enhanced, indicating that mass transfer has occurred. The primary is largely overluminous for its mass (it has a luminosity matching a normal $30 M_{\odot}$ star). We consider this as evidence that the star is a CHeB star, in the slow phase of the RLOF, close to the end. Its actual mass suggests an initial mass of $\sim 30 M_{\odot}$.

MCB evolutionary computations predict that the BN0.5 Ia star has an atmospheric hydrogen abundance $X_{\text{atm}} \leq 0.3$, whereas the ratio N/C should correspond to CNO equilibrium, i.e. the supergiant has all the evolutionary properties to be a WR star, but it is not. We therefore conclude that in order for a star to be a WR type, being a hydrogen deficient massive CHeB star is a necessary but not a sufficient condition.

The binary HD 190967 is very similar as the previous one. The fact that the secondary is a O9.5 V star means that it has been rejuvenated, hence that mass transfer has occurred

The orbits of both systems are eccentric although the binaries are very close and RLOF/mass transfer has occurred. This indicates that

a binary with a period of the order of a decade where RLOF has occurred will not necessarily be circularized.

Φ Per

The binary Φ Per is classified as sdO6+B0.5Ve with a period $P = 126$ days. In correspondence with the evolution of MCBs, the O6 subdwarf has to be a CHeB remnant after a previous RLOF whereas the B-type companion is a former mass gainer which has acquired a large rotation as a consequence of mass accretion and therefore shows the e-feature. The orbital masses are $1.14 M_{\odot} + 9.3 M_{\odot}$ (Gies et al., 1998) for resp. the subdwarf and the Be component.

If these masses apply we propose a model where the sdO6 star is at the beginning of CHeB.

A binary with initial masses $6 M_{\odot} + 5 M_{\odot}$ with a period $P = 13.5$ days, where the RLOF is conservative, reproduces the present system parameters (Fig. 14). A B0.5V star in general corresponds to a star with mass $\sim 15 M_{\odot}$, i.e. the star is undermassive (or overluminous) and this may indicate that accretion induced mixing has occurred (Sect. 5.2).

Particularly interesting is the further evolution of the binary. The sdO6 component will evolve into a White Dwarf (with mass $\approx 1 M_{\odot}$) and the binary may become a low-luminosity X-ray source (X-ray luminosity in the range $10^{29} - 10^{33}$ erg/s) when the WD accretes mass from the Be component, similar to the Be+WD candidates μ^2 Cru and HR 4804 (Waters et al., 1989).

Notice that it is impossible to find a matching evolutionary model with large convective core overshooting.

HD 12323, HD 14633 and HD 193516

The three systems have an OBN V or IV optical component. Their mass function suggests a lower mass companion. We propose two evolutionary scenarios.

a. The systems are post-CE/SpI. As an example, consider a $15 M_{\odot} + 3 M_{\odot}$ CB with a period of the order of 2–3 years. The SpI of the $3 M_{\odot}$ component removes the hydrogen rich envelope of the primary. At the end, the system has a period of the order of days, the secondary has remained a $3 M_{\odot}$ late B-type and the primary has evolved into a $\sim 5 M_{\odot}$ hydrogen deficient ($X_{\text{atm}} \approx 0.2-0.3$) CHeB star with CNO equilibrium abundances. It is highly overluminous for its mass ($\log L/L_{\odot} \approx 4.5$), it may show up as an ONV star on its way to become a subdwarf similar to the O6 component in Φ Per but more massive.

b. The systems are comparable to Φ Per. In this case the OBN components are accretion stars in an OBe ‘off’ phase. The overabundance of N is due either to thermohaline mixing when the standard accretion model applies, or to the accretion induced full mixing. In the latter case the stars are expected to be overluminous. The companion may be a subdwarf, a WR-like star like in the binary V Sagittae (Herbig et al., 1965), or it can be a compact star.

HD 25638

The spectral type and the orbital masses of both components and the magnitude of the B0 star are strong indicators that the system is a post-RLOF binary (the B0 is

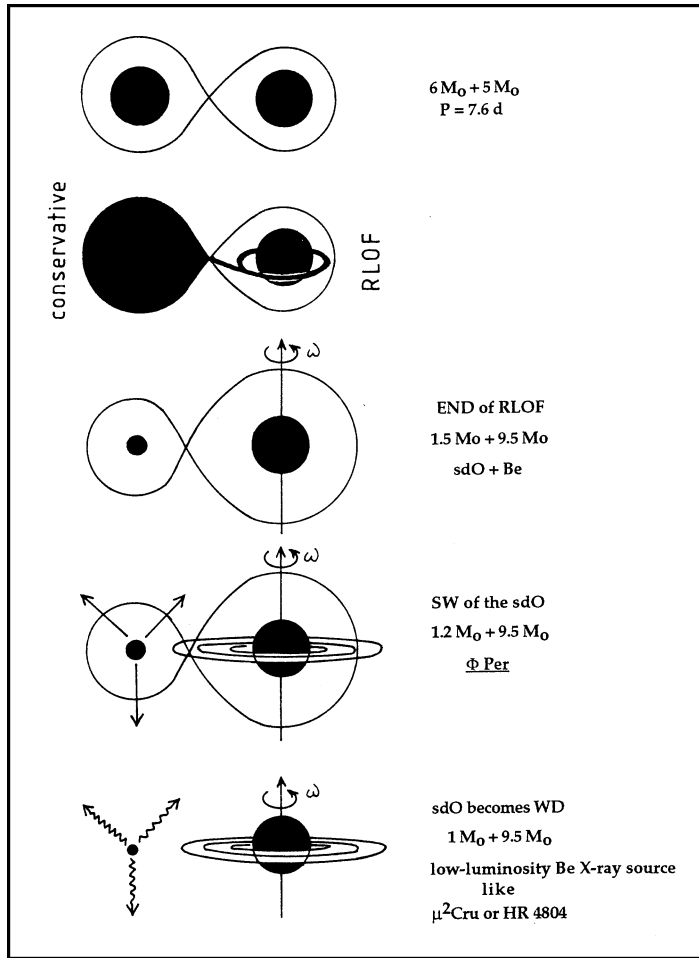


Fig. 14. The evolutionary scenario of Φ Per

a post-RLOF remnant). Accounting for the present period, we propose a $12 M_{\odot} + 10 M_{\odot}$ case A progenitor. Although the age of the system is ~ 20 million years, the O9.5 component has luminosity class V. This indicates that mass accretion and rejuvenation have played a very important role in its evolution; the star could be a fast rotator.

If the B0 star is post-RLOF, it can be expected that it has a significantly reduced hydrogen abundance. The star may evolve into a sdO or WR type.

HD 209481

Both components are classified as O9V although their masses differ by a factor 2 at least. The most plausible explanation is that the binary went through a mass transfer phase. The most massive star is the accretor and the lower mass star is the mass loser. Since both stars do not differ much in magnitude, we expect the loser to be close to the end of its RLOF.

The gainer is classified as luminosity class V and therefore, despite accretion, it is close to thermal equilibrium. Adopting a normal mass-spectral type relation, the mass of the gainer equals $\sim 24 M_{\odot}$ and thus the mass of the loser $\sim 11 M_{\odot}$. Evolution predicts that the latter should be hydrogen deficient, on its way to become a WR star in the near future (probably in less than 20 000 yrs from now)

v Sgr

The $\geq 2.5 M_{\odot}$ primary is an A type supergiant that has lost most of its hydrogen rich layers ($n_{\text{H}}/n_{\text{He}} < 10^{-4}$, Schönberner & Drilling, 1983). The very small hydrogen abundance, the mass of the secondary and the 138d orbital period indicate that either the system went through a case C CE phase, or through a case B_c CE phase where the remnant system experienced further mass loss due to SW or due to a second case BB RLOF.

A $2.5 M_{\odot}$ He core (no hydrogen left) corresponds to a primary with initial mass $\sim 12 M_{\odot}$ (small convective core overshooting during CHB). We propose a $12 M_{\odot} + 4 M_{\odot}$ progenitor binary with a period $\sim 2-3$ years. When the $12 M_{\odot}$ star becomes a RSG, SW mass loss (Equation 1.2) first removes $5-6 M_{\odot}$ (implying a period increase as predicted by Equation 4.2) before the CE phase starts. The latter process then removes another $3-4 M_{\odot}$, reducing the period (Equations 4.8 and 4.9) to a value comparable to the observed one.

It is important to realize here that it is very hard to find a binary evolutionary model for *v Sgr* where SW during the RSG phase is assumed to be very small, i.e. the existence of this system can be considered as indirect evidence that also for stars with initial mass $\sim 12 M_{\odot}$ SW during the RSG phase is sufficiently large to remove a significant fraction of their mass.

Let us finally remark that beside *v Sgr*, there are three other candidate binaries with an evolved very hydrogen deficient (probably CHeB or hydrogen shell burning) component, i.e. KS Per (Plavec, 1986), LSS 1922 and LSS 4300 (Drilling et al., 1985; Jeffery et al., 1987). Whether or not these are MCB products is unclear at present.

6.2. WR+OB binaries

Frequently asked questions during the last decade:

1. Are the WR components in WR+OB binaries formed by stellar wind mass loss or by binary mass loss processes (RLOF or CE)?
2. If RLOF happened in WR+OB binary progenitors, was it accompanied by mass transfer and mass accretion?

Primaries of MCBs with mass exceeding $\sim 40-50 M_{\odot}$ may lose mass by SW at very large rates (LBV rates). If the rate is large enough, the RLOF can be avoided. Obviously accretion (and thus rejuvenation) does not occur whereas the binary period increases significantly [Equation (4.2)]. To find candidates among the observed WR+OB binaries, we then have to look for binaries with sufficiently large period and with OB components that are preferentially giants or supergiants; HD 68273 (γ^2 Vel; new orbital parameters were presented by Van der Hucht et al., 1997) and HD 190918 satisfy both criteria. It must be noted, however, that CE evolution can explain both systems as well. To illustrate, a $35 M_{\odot} + 27 M_{\odot}$ binary with initial period $P = 900$ days, evolving through a CE phase, reproduces the orbital parameters of γ^2 Vel.

Obviously, when the binary period was very large, a massive primary with initial mass smaller than $40\text{--}50 M_{\odot}$ may become WR due to RSG stellar wind mass loss, similarly as single stars. This could have been the scenario for the large period WR-systems HD 137603 (Niemela, 1995), HD 192641 (Annuk, 1991) and HD 193077 (Annuk, 1995).

However,

if indeed the WR components in the binaries discussed above have been formed mainly by stellar wind mass loss during an LBV and/or RSG phase, why don't we see small shell like structures around them, much like around many 'single' WR stars (Sect. 1.5)?

Accounting for the binary period evolution during the different mass loss phases of a star (Sect. 4.4) and accounting for the effect of mass accretion on the evolution of a binary mass gainer, it can be concluded that

a WR+OB binary with a period of the order of days must have experienced a RLOF or common envelope phase

and

the progenitor of a WR+OB binary where the OB star has luminosity class V or where the O component is an early O-type star, most likely underwent RLOF and mass transfer, causing the rejuvenation of the gainer.

As a prototype, we consider **V444 Cyg (HD 193576)**.

Facts (Cherepaschuk, 1975)

- the observed mass of the WNE component $\approx 9M_{\odot}$; its progenitor must therefore have had a mass of $\sim 30 M_{\odot}$ and thus the age of the binary is ~ 7 million years,
- the OB companion is an O6 star. Since the age of a normal O6 star is $\sim 1\text{--}2$ million years, the OB star must have been rejuvenated, i.e. mass transfer must have occurred,
- the binary period is 4.2 days, which excludes a stellar wind mass loss scenario

A conservative RLOF scenario

In order to obtain the observed post-RLOF component masses and the orbital period with a conservative RLOF, the progenitor system must have been a $30 M_{\odot} + 12 M_{\odot}$ case A binary with a period of ~ 3 days. Evolutionary tracks are presented in Fig. 15.

Note, however, that when accretion is treated in the standard way, very soon after the onset of the mass transfer phase also the mass gainer fills its Roche lobe and a contact binary is formed. We continued our computations as if there was no contact, however. We may conclude that, when mass accretion is treated in the standard way, a conservative scenario for the progenitor binary of V444 Cyg is rather improbable.

A quasi-conservative RLOF scenario.

A probable quasi-conservative MCB evolutionary model is illustrated in Fig. 16 (during CHB, convective core overshooting is small).

We show the evolutionary behaviour of the gainer when the accretion induced mixing process applies and when accretion is treated in the standard way. The progenitor system is a $30 M_{\odot} + 20 M_{\odot}$ MCB with initial period $P = 12$ days. Due to

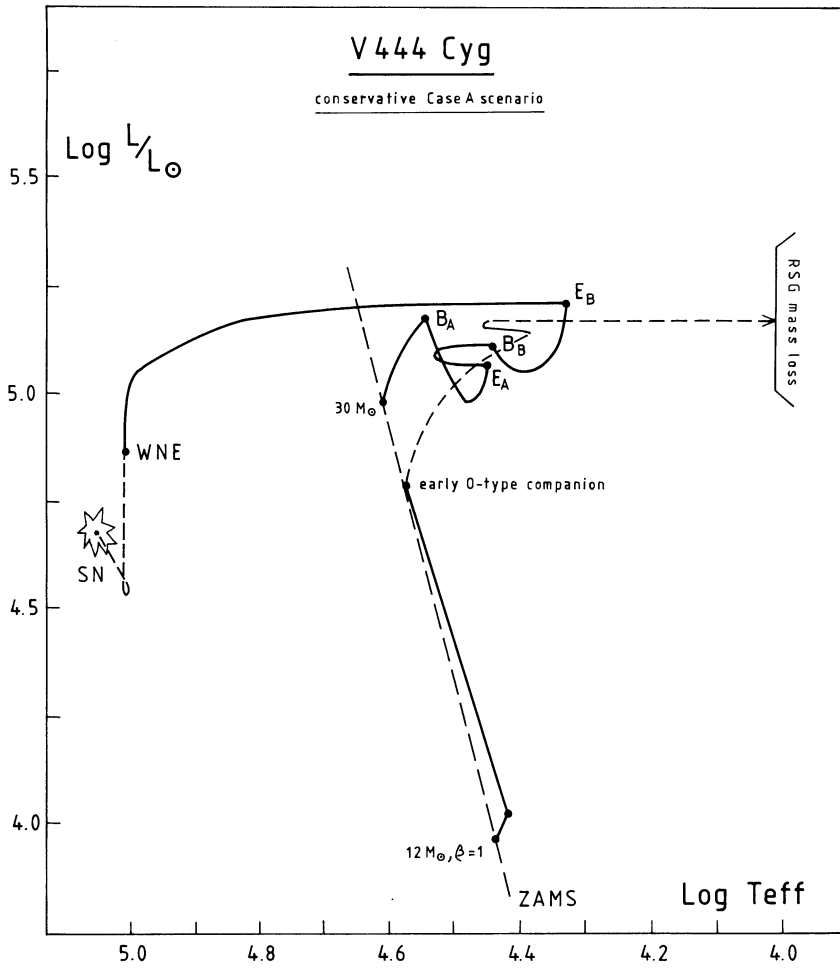


Fig. 15. The theoretically predicted case A evolution of the WR+OB binary V444 Cyg under the assumption that the RLOF process was conservative; B_A = beginning of the case A RLOF, E_A = end of case A RLOF, B_B = beginning of the case B RLOF, E_B = end of case B RLOF. The dashed part of the tracks is the expected further evolution of the binary

SW during CHB, the orbital period increases slightly to 14 days. The theoretically predicted masses of both components of V444 Cyg equal the observed masses if it is assumed that $\sim 50\%$ of the mass lost by the primary during its RLOF also leaves the binary. Note however that this '50%' depends on the choice of the initial mass of the secondary. If we started with a $16 M_\odot$ secondary and a smaller orbital period, the masses and present period of V444 Cyg are recovered with $\beta = 0.8$.

Using Equation (4.5), the period at the end of the RLOF (mass transfer) = 3.5 days: the system resembles a WNL + OB binary. Further mass loss by SW removes the remaining hydrogen rich layers. When the WR star has evolved into a WNE star (with mass $9 M_\odot$), the period = 4.2 days.

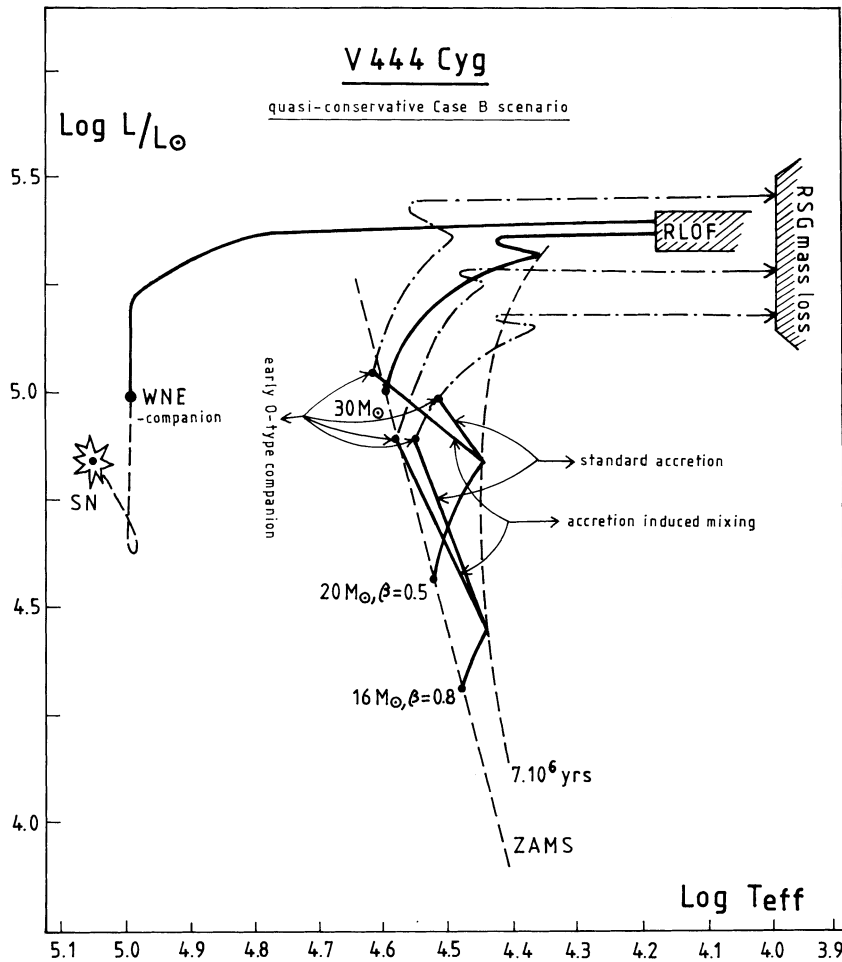


Fig. 16. The theoretically predicted case B evolution of the WR+OB binary V444 Cyg when it is assumed that the RLOF process was quasi-conservative and convective core overshooting during CHB is small

At the end of the mass transfer, when the secondary has been entirely mixed, the O6-type component may be an overluminous star with mass $M = 26M_{\odot}$ and a homogeneous composition $(X, Y, Z) = (0.5, 0.48, 0.02)$.

The future of V444 Cyg

Figure 16 also illustrates the theoretically expected further evolution of V444 Cyg. The WR star will explode as a SN leaving a NS as remnant. We computed the effect of the SN explosion using the kick velocity distribution given by Equation (1.6) and assuming isotropic direction of the kicks. In this case, the binary is disrupted with a probability of $\sim 60\%$. The single OB-type star has a space velocity > 30 km/s and will be classified as a runaway. The star evolves into a RSG where mass loss by SW removes the hydrogen rich layers and it becomes a WR star with mass between 10–14 M_{\odot} .

When the binary is not disrupted (40% probability), it will evolve through a spiral-in phase. Our calculations reveal that in 95% of the cases, the NS will spiral-in completely and a TZO will be formed. Further SW mass loss during the RSG phase of this TZO may remove the hydrogen rich layers: a WR_{TZ} is formed. The remaining 5% may survive the spiral-in phase and a WR+NS system with a period of the order of hours is a possibility.

Can we imagine an evolutionary model in which no mass transfer occurred in the progenitor of V444 Cyg?

When one accepts the possibility that no mass transfer happened in the progenitor of V444 Cyg, one also has to accept that

- the secondary should be an early B-type supergiant rather than an O6-type, which is not overluminous for its mass,
- there should be a $14 M_{\odot}$ ring/shell around the binary,

however there is no observational evidence for this. The latter consequence can be generalized, i.e.

the fact that only a few (no?) short period WR+OB binaries show some evidence of shell/ring-like structures with small diameter can be considered as an indication that the secondaries in massive case A/case B_r binaries act as efficient vacuum cleaners, and that the RLOF process is quasi-conservative.

Obviously, the absence of evidence has to be confirmed by more observations. Since we consider V444 Cyg as a prototype WR+OB binary, we conclude that

'quasi-conservative' RLOF occurred in a large number of case A/case B_r progenitors of WR+OB binaries.

Remark. Larger convective cores during CHB of the primary (possibly as a consequence of rapid rotation of the star) imply a larger post-RLOF mass for a given pre-RLOF mass. It can readily be checked then that

the larger the enlargement of the convective core of the CHB progenitor of the WR component of V444 Cyg, the more conservative the RLOF and the mass transfer must be to explain all observations of the system.

6.3. The X-ray binaries

6.3.1. The OB-type high mass X-ray binaries (HMXB)

The observations of the optical components of HMXBs may give important clues to understand the evolution and mass transfer in MCBs. We will restrict the discussion to the standard HMXBs where the X-rays are formed through the accretion of mass by the compact star from the stellar wind of the OB stars (Davidson & Ostriker, 1973).

For evolutionary purposes, the three HMXBs Vela X-1, Wray 977 and Cyg X-1 are particularly interesting.

Vela X-1

The observations

A comparison between a high S/N spectrum and NLTE calculations gives $T_{\text{eff}} = 26000$ K, $\log g = 2.7$ and $\varepsilon = N_{\text{He}}/(N_{\text{H}} + N_{\text{He}}) = 0.28$ for the B0.5Ib optical component. (Vanbeveren et al., 1994).

A projected rotational velocity of $125 \text{ km}\cdot\text{s}^{-1}$ was derived from eleven metal lines of C, N, O, Si and Mg. Since the inclination angle of the binary is very large ($> 70^\circ$), v_{rot} is not much larger than its projection.

From the orbit and X-ray eclipse one obtains the mass and radius of the supergiant: $R = 28\text{--}35 R_{\odot}$, $M = 21.5\text{--}26.5 M_{\odot}$ (these values are 95% confidence limits, Rappaport and Joss, 1983; Joss and Rappaport, 1984).

Combining the NLTE results, the orbital and X-ray eclipse observations, it follows that $\log L/L_{\odot} = 5.5\text{--}5.7$ and therefore, from the relation $M_V = m_V + 5 - 5 \log d$, d has to be in the range 1.8–2 kpc.

The evolutionary model

When the HRD position of the B0.5 supergiant is compared with evolutionary tracks of mass gainers we conclude:

- evolutionary prediction of mass gainers where accretion is treated in the standard way is unable to reproduce the observed HRD position of the optical component of Vela X-1; even accounting for thermohaline mixing, the predicted H and He abundance is very close to solar and this differs significantly from the ε value derived with actual NLTE atmosphere codes.
- with the accretion induced full mixing model, we can not only reproduce the observed HRD position of the B0.5 supergiant of Vela X-1, but we also explain the ε value.

Wray 977

The X-ray source is a pulsar, indicating that it is a NS, and together with 4U1700-37, it has the highest-mass optical companion known. Sato et al. (1986) propose a mass of $\sim 38 M_{\odot}$. However, Kaper et al. (1995) re-investigated the system and concluded that it is probably a hypergiant with a minimum mass of $\sim 48 M_{\odot}$.

Accounting for the mass of the optical component, from comparison with evolutionary computations of MCBs it can be concluded that

- if 50% of the mass lost by the primary during its RLOF also leaves the case B_r binary, the primary of the progenitor binary must have had a mass larger than $40 M_{\odot}$; if the RLOF is assumed to be conservative, this minimum mass equals $33 M_{\odot}$,
- the previous conclusion means that primaries in interacting binaries with initial mass up to $\sim 30 M_{\odot}$ (and possibly up to $\sim 40 M_{\odot}$) may end their life as NSs (accompanied by a SN explosion),

Remark. When the cc in the HMXB 4U1700-37 is a NS, a similar analysis with similar conclusions can be performed as for Wray 977.

Cyg X-1

A detailed analysis has been presented by Gies & Bolton (1986). Herrero et al. (1995) studied the spectrum between 4000 \AA and 5000 \AA of the optical component of the

HMXB and compared selected hydrogen and helium lines with theoretical prediction using a NLTE, spherical model atmosphere including the effects of SW mass loss. Accounting for all uncertainties, combining both studies, the following parameters can be proposed

- the optical star is a O9.7 Iab type star with $28\,000\text{ K} \leq T_{\text{eff}} \leq 33\,000\text{ K}$
- $\log L/L_{\odot} \approx 5.4$
- the mass of the optical component $M \geq 17M_{\odot}$; most probably (accounting for its luminosity), the mass $\sim 30M_{\odot}$,
- He may be overabundant (?)
- $M_{\text{cc}} \geq 7M_{\odot}$; the most probable mass ranges between $10 M_{\odot}$ and $16 M_{\odot}$.

Particularly interesting is the mass M_{cc} of the compact star. Its value exceeds by far the maximum mass of a stable NS and it can therefore be considered as one of the best BH candidates.

The observations of the HMXB Wray 977 seem to indicate that primaries with initial mass as high as $30\text{--}40 M_{\odot}$ end their life as a NS. This means that the BH in Cyg X-1 originated from a star with initial mass $> 30\text{--}40 M_{\odot}$ and if the probable mass value quoted above is confirmed, it tells us that

some massive stars with initial mass $\geq 30\text{--}40 M_{\odot}$ end their life with a mass larger than $10 M_{\odot}$.

6.3.2. The low mass X-ray binaries (LMXB)

A LMXB is an X-ray binary where the optical component is a low mass star. A majority of the LMXBs are old binaries belonging to Globular Clusters. Most probably they are formed by tidal capture or by exchange collisions of an old NS passing by (Verbunt, 1990; Bhattacharya & Van den Heuvel, 1991).

There are, however, a few LMXBs, located in the galactic disc, which are in our opinion of fundamental importance in shedding some light onto MCB evolution, i.e. the X-ray pulsar Her X-1 and the LMXB BH candidates.

Her X-1

This LMXB consists of an X-ray pulsar (a NS with a 95% probability mass of $1.4 \pm 0.3M_{\odot}$, Van Kerkwijk et al., 1995) and an A-type companion with a mass $\approx 2 M_{\odot}$. Her X-1 is located at a height $z = 3$ kpc out of the galactic plane. Since a $2 M_{\odot}$ star has an age around 800 million years, starting from inside the galactic disc, the z -component of its velocity at the moment of explosion must have been larger than 120 km/s in order to reach its present height against the gravitational pull of the Galaxy.

The only binary model that explains the observed properties of the LMXB Her X-1 is similar to the original suggestion made by Sutantyo (1975) (see also Verbunt et al., 1990). The initial system consists of a massive star with mass around $15 M_{\odot}$ and a $2 M_{\odot}$ companion, with a period larger than 1 year. The system evolves through a CE phase and at the end of it, it consists of a $\sim 4 M_{\odot}$ CHeB star and a $2 M_{\odot}$ A-type star with a period ~ 1 day. The CHeB star explodes leaving behind a NS with mass $\sim 1.4 M_{\odot}$ in an eccentric orbit around the A-type star. The system will acquire a peculiar space velocity of the order of 100 km/s. As the A-type companion evolves and reaches its own Roche lobe, the initial stage of the mass transfer transforms the NS into a X-ray source.

LMXBs with a BH component

There are 7 LMXBs known with a BH candidate component, i.e. Nova Muscae 1991 (Remillard et al., 1992), A0620-00 (Marsh et al., 1994), GS2000+25 (Harlaftis et al., 1996), GS2023+338 (Sanwal et al., 1996), Nova Ophiuchi 1977 (Remillard et al., 1996), GRO J0422+32 (Filippenko et al., 1995), GRO J1655-40 (Orosz & Baylin, 1997). The optical stars have an average mass $\sim 0.7 M_{\odot}$ whereas the proposed masses of the compact components range between $4 M_{\odot}$ and $9 M_{\odot}$ (possibly up to $12.5 M_{\odot}$), which is considerably above the maximum mass for NSs.

If the minimum mass for BH formation in a MCB component $\geq 30\text{--}40 M_{\odot}$, we propose two possible scenarios for these LMXBs (Fig. 17). The first one with a $30\text{--}40 M_{\odot}$ primary is comparable to the suggestion made by De Kool et al. (1987). The system has a low mass secondary and a period of ~ 500 days. Due to the extreme mass ratio, the binary evolves through a CE phase. The latter phase stops when the primary has lost most of its hydrogen rich layers. Using the evolutionary computations of Sect. 5, it then has a mass $\geq 18 M_{\odot}$ and resembles a WNL star whereas the binary period ~ 0.25 days. The star starts losing mass by SW at a rate which is typical for a WR star. Just prior to the collapse of the FeNi-core, the remaining mass of the star is $\sim 5 M_{\odot}$. If the collapse results in the formation of a BH, no SN occurs and thus the system remains bound.

In the second scenario the initial primary mass equals $50 M_{\odot}$ and the initial period $P = 5$ days. The primary evolves through a LBV phase but we assume that the SW is not large enough to avoid the common envelope phase completely. The total mass lost during the latter is very much reduced due to the previous SW phase, and although we started with a binary with a period of 5 days, the period at the end of the common envelope/LBV phase ~ 0.4 days. From thereon, the evolution is similar to the first scenario.

It is important to realize that

- if stars with initial mass $> 40 M_{\odot}$ lose a significant part of their hydrogen rich layers by a LBV type SW and end their life as a BH, most of the binaries with a $> 40 M_{\odot}$ primary and a low mass secondary will avoid merging (which would occur if the binary went through a normal CE/SpI phase), and most of them will become a LMXB with a BH component.

Overall conclusion concerning the LMXBs

Accounting for the fact that most of the binaries with small mass ratio, progenitors of Her X-1 like systems, will merge during spiral-in, or will be disrupted during the SN explosion, the existence of only few which survived the SpI and the SN can be considered as an indication that a large number of MCBs with small mass ratio exist.

Also the LMXBs with a BH candidate suggests the existence of very massive close binaries with very small mass ratios.

6.4. The O type runaway ζ Pup as a binary component

Let us first remark that accounting for the asymmetry of the SN explosion, a large fraction of the OB type stars which became runaway as a consequence of the SN explosion in a binary, are expected to be really single.

In Sect. 2.7.5, we concluded that it is difficult to explain the peculiar space velocity of the O-type star ζ Pup with the cluster ejection model.

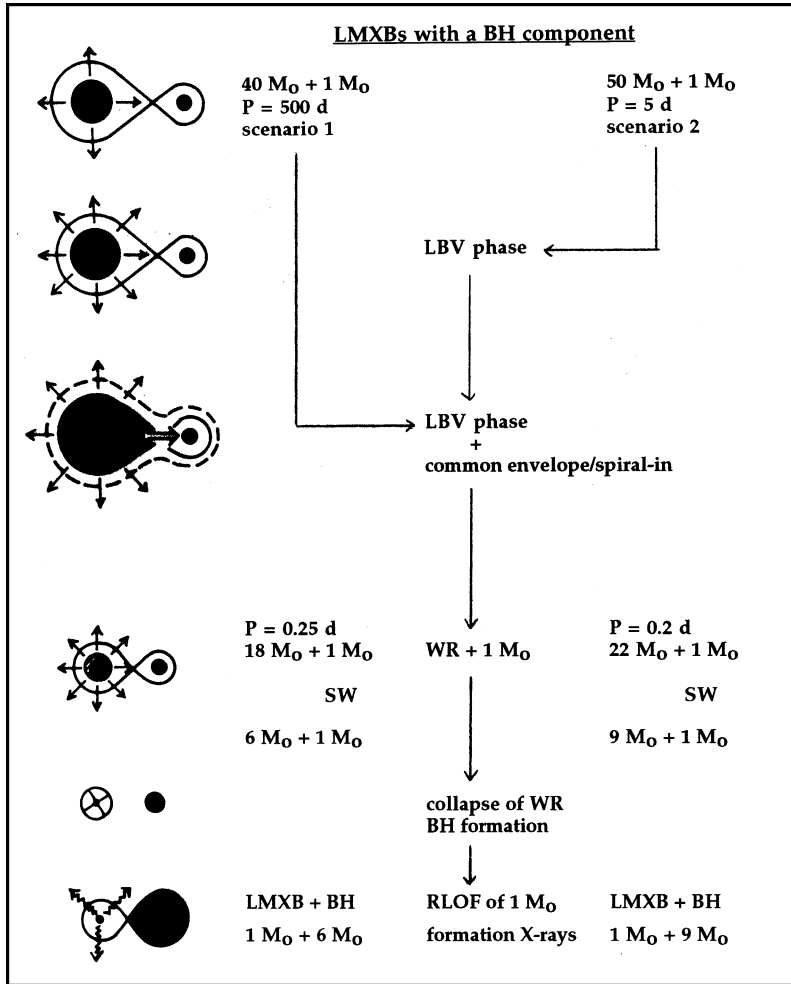


Fig. 17. Two possible evolutionary scenarios for the LMXBs with a BH component

A MCB evolutionary scenario for ζ Pup

Since there is no signature for the presence of a compact companion, we assume that the SN explosion disrupted the binary.

The observed hydrogen abundance is very low and we therefore assume that extended mixing occurred during the accretion process. Figures 18 gives a possible evolutionary history of the runaway. The star started as the secondary of a $40 M_{\odot} + 38 M_{\odot}$ MCB. After RLOF, the binary consists of a $18 M_{\odot}$ WNL star and a $44 M_{\odot}$ early O type dwarf. After the removal of the remaining hydrogen rich layers by SW mass loss, the binary becomes a WC+early O. We assume that the SN explosion of the WC star disrupts the system.

The mass transfer mixed the gainer thoroughly, explaining the overluminosity of ζ Pup and the high surface helium abundance. Due to this mixing process, the further evolution of the star is similar to the evolution of a single star but with initial (X, Y)

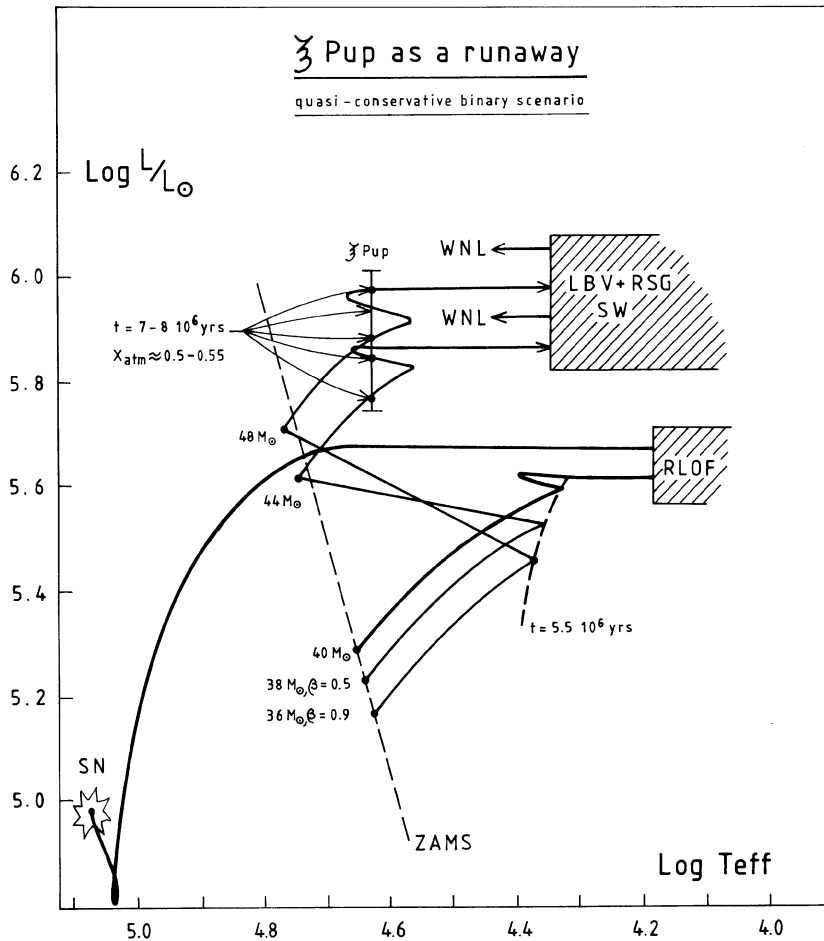


Fig. 18. The theoretically predicted evolution in the HRD of a MCB meeting the observational constraints of the runaway ζ Pup. The bold track traces the evolution of the $40 M_{\odot}$ primary. We consider two possible mass gainers meeting the observed HRD position and the atmospheric chemical abundance of ζ Pup

abundances which differ significantly from normal i.e. $(X, Y) = (0.5-0.55, 0.48-0.43)$. After the removal of $\sim 15 M_{\odot}$ due to a LBV and/or RSG type SW, it will evolve into a $25 M_{\odot}$ WNL star. We expect that ζ Pup will end its life as a massive BH.

Notice the similarity with the evolution of the optical component of the HMXB Wray 977.

6.5. Critical remarks

All evolutionary models of accretion stars predicting a significantly increased helium abundance at the surface, also predict a significantly increased surface N abundance (factor 5 larger than solar) and depleted C and O (factor 4 to 5 smaller than solar).

The optical stars of the HMXBs and the OB runaway discussed in the two previous subsections have been extensively observed and their spectra have been studied in detail.

Why then have these stars never been classified as OBN types?

The actual NLTE model atmosphere code of Munich, upon which most of the ϵ values quoted above are based, does not account for the effect of microturbulence. In a recent paper (McErlean et al., 1998) it was concluded that at least in early B-type supergiants microturbulence may be very important with microturbulent velocities close to the sound velocity. One of the main effects (important for stellar evolution) is that the hydrogen and helium lines in the spectra can be explained without drastically increasing the helium abundance. Although none of the stars considered above were included in the study of McErlean et al., it is interesting to discuss qualitatively the consequences, if in reality they would all have normal helium abundance in their surface (and thus also normal CNO).

First, if helium is normal, we must conclude that accretion was not able to mix the whole star. It is straightforward to understand that, except for quantitative differences, the overall model for the runaway ζ Pup is very similar as the one proposed in Sect. 6.4. If the star is a post-SN runaway, since the star is a rapid rotator, we conclude that binary mass transfer occurred causing rejuvenation and spin-up but no extended mixing.

The evolutionary scenario of the HMXB Vela X-1 depends explicitly on the value of ϵ . The position in the HRD of the B0.5Ib supergiant hardly depends on the NLTE analysis, so that the overluminosity remains a fact independent from whether or not He is overabundant in the atmosphere. The question then is:

if the surface helium abundance in the optical star of the HMXB Vela X-1 is normal, what causes its overluminosity (with respect to the orbital mass)?

At present, we have found no evolutionary model (with or without rotation) meeting all observations of Vela X-1 but where the optical star has a normal He abundance at the surface. We are therefore inclined to conclude:

if the overluminosity of the optical component of the HMXB Vela X-1 is confirmed, evolution is able to explain the system only if its surface helium abundance is significantly larger than normal; we thus expect the atmosphere to be rich in N, depleted in C and O.

6.6. The descendants of OB+cc binaries: the CHeB (WR)+cc candidates

If the OB+cc binary survives the SpI phase, the remnant will be a CHeB+cc binary where the CHeB component may show up as a WR star.

We consider the three WR+cc candidates Cyg X-3, HD 50896 and HD 197406.

Cyg X-3

Cyg X-3 is an X-ray binary discovered in 1966 (Giacconi et al., 1967). The X-ray flux shows a 4.8 hour period modulation and it has been classified as a WR+cc system by Van Kerkwijk et al. (1992). The WR classification is based on I- and K-band spectra where WR-like features have been detected but an unambiguous classification similar to other WR stars is still lacking.

It is possible to give an answer to the following question:

accounting for all observed features of the HMXB Cyg X-3, is it possible to find a model where the optical component is a ‘normal’ Population I WR star with a spherically symmetric stellar wind?

The observations

Apart from the variation as a function of orbital phase, the X-ray flux varies in time (see e.g. the review of Bonnet-Bidaud & Chardin, 1988). Using a distance of ~ 10 kpc (Dickey, 1983) its 2–20 keV X-ray luminosity varies between $\sim 10^{37}$ erg/s (low state) and $\sim 2 \cdot 10^{38}$ erg/s (high state). Here, we will focus on the high state.

The absence of an X-ray eclipse in the quasi-sinusoidal variation of the X-ray emission – with Period = orbital period of ≈ 0.2 days – indicates a rather low inclination ($i = 20\text{--}60^\circ$) although Van Kerkwijk (1993) argues a value $i = 74^\circ$.

Schmutz et al. (1996) derived a velocity amplitude $K = 480 \pm 20$ km/s. The mass function $f(m) = 2.3 M_\odot$. With a realistic WR mass value, it follows that the mass of the cc is significantly above the mass value of all known NSs, and it can therefore be considered as a BH candidate. The former result is still quite uncertain so that we have chosen two models: one where we ignore the mass function and simply assume that the compact star is a NS with mass equal to $1.4 M_\odot$, and a second model where we account properly for the mass function and where the cc is assumed to be a BH candidate.

Van Kerkwijk et al. (1992) measured the variation of the orbital period $\dot{P} = 1.6 \cdot 10^{-6} \text{yr}^{-1}$. If the optical star is losing mass by a spherically symmetric stellar wind, it follows from Equation (4.2) that there is a relation between the mass loss rate and \dot{P} , which in the case of Cyg X-3 corresponds to

$$\dot{M} = 0.8 \cdot 10^{-6} (M_1 + M_2) \quad (6.7)$$

the masses in M_\odot , \dot{M} in M_\odot/yr .

Formation and absorption of X-rays

When matter lost by the optical component is trapped gravitationally by the relativistic component, to obtain X-rays, it is necessary that an accretion disk can be formed (Shapiro & Lightman, 1976), and/or a very strong magnetic field is present (Langer & Rappaport, 1982). The former condition is particularly important when the compact component is a BH which cannot support a magnetic field. In this case, a Keplerian disk can be formed when the specific angular momentum of the accreted matter exceeds the specific angular momentum of the matter in the last stable orbit in the disk. When the BH accretes matter from a spherical symmetric SW, the latter condition is fulfilled when (e.g. Illarionov & Sunyaev, 1975)

$$P < 4.8 \cdot 10^{-12} M_{\text{BH}} v_{\text{wind}}^{-4} \delta \quad (6.8)$$

(the orbital period P in hours, M_{BH} in M_\odot , the wind velocity v_{wind} at the orbital distance A in km/s, δ is a dimensionless parameter of order 1). Since the WR wind velocity is typically of the order of 1000 km/s, condition (6.8) is satisfied in the case of Cyg X-3.

When the conditions for the formation of X-rays are fulfilled, we use the model of Davidson & Ostriker (1973) to compute the X-ray luminosity when a cc accretes mass from the stellar wind of the WR star.

The X-ray opacity in a wind of a massive star has been computed in detail by Vanbeveren et al. (1982) using an admixture of *moderately ionized species* in the wind. This applies for a wind where the temperature is not higher than 10^5 K.

Stevens & Willis (1988) remade these calculations for the absorption in the wind of the WR-star HD 50896. They argued that the ionization should be calculated in detail. However, such calculations have never been done in the wind of a WR star.

We have repeated the Vanbeveren et al. (1982) computations using updated atomic data. Unlike the statement made by Stevens and Willis, it can be demonstrated that calculations where the detailed ionization balance is not followed in detail, give yet very reasonable results as far as the opacity of X-rays in the > 2 KeV region is concerned, and that

the value of the absorption in the keV region depends only marginally on the ionization equilibrium actually attained. Significant changes occur only when dominant chemical species turn into hydrogenic ions or are completely stripped off.

Since the ionization in the WR wind will only be moderately high

a reliable estimate of the hard X-ray spectrum of a HMXB produced by accretion of stellar wind mass by a compact star can be calculated without knowing the detailed ionization balance in the wind.

The observed X-ray luminosity after absorption is called $L_{X,\text{obs}}(2\text{--}20 \text{ keV})$.

The theoretically predicted X-ray luminosity of Cygnus X-3

We use bremsstrahlung to describe the intrinsic X-ray spectrum since this explains the observations for energies $E > 20 \text{ keV}$ best.

We have computed the expected value of $L_{X,\text{obs}}(2\text{--}20 \text{ keV})$ as a function of the parameters in the model. In a first attempt, we have chosen different values for the stellar wind mass loss rate independently of the constraint given by Equation (6.7). Furthermore, although the masses of most of the WR stars in binaries are larger than $5 M_{\odot}$, we also allow for models where the WR mass is smaller than $5 M_{\odot}$. Apart from all parameters in the model of Davidson and Ostriker, we then looked for solutions in the following parameter space:

- model 1: the mass of the compact star equals $1.4 M_{\odot}$
- model 2: the mass of the compact star satisfies the mass function of the system,
- the mass of the WR star ranges between $1 M_{\odot}$ and $20 M_{\odot}$,
- \dot{M} of the WR star ranges between $5 \cdot 10^{-7} M_{\odot}/\text{yr}$ and $5 \cdot 10^{-5} M_{\odot}/\text{yr}$,

Comparison with the observed value of $2 \cdot 10^{38} \text{ erg/s}$ already excludes a large number of parameter values. For the models that are left, we then calculate the expected X-ray spectrum which would be observed after absorption through the WR-wind and compare it with the observed spectrum. The results are shown in Fig. 19 for two typical models with $L_{X,\text{obs}}(2\text{--}20 \text{ keV}) = 2 \cdot 10^{38} \text{ erg/s}$. The figure illustrates why again a large number of parameter sets are unlikely.

From the models that remain after the comparison, we conclude that

- the observed X-ray luminosity and distribution of X-rays over energies in Cyg X-3 can be explained only if the compact star is a BH with a mass that satisfies the mass function proposed by Schmutz et al. (1996) and if the SW mass loss rate of the CHeB component $< 10^{-6} M_{\odot}/\text{yr}$.

The best correspondence is achieved when the WR star has a mass equal to $2 M_{\odot}$ (analogous to the WR like star in the binary V Sagittae, Herbig et al., 1965) and the compact companion has a mass $\approx 8 M_{\odot}$.

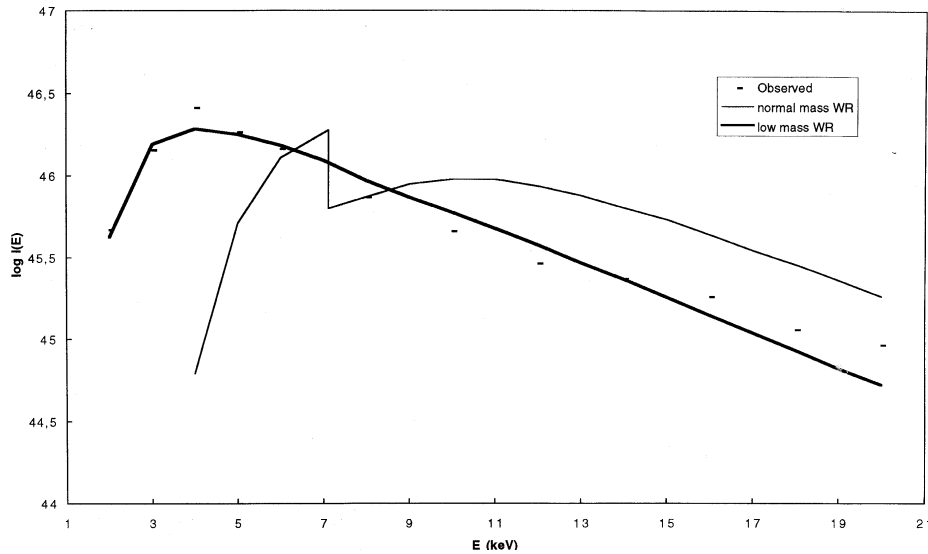


Fig. 19. The observed [2–20] keV spectrum of the HMXB Cyg X-3 compared to the theoretically predicted one for two models: the full bold line is considered as a good fit and holds for the parameters [$M_{\text{BH}} = 8M_{\odot}$, $M_{\text{WR}} = 2M_{\odot}$, $\dot{M}_{\text{WR}} = 5 \cdot 10^{-7} M_{\odot}/\text{yr}$] and the accretion model parameters (Davidson & Ostriker, 1973) [$\xi = 0.35$, $v_{\text{w}}(A) = 1000$ km/s, $v_{\infty} = 1500$ km/s]; the thin line is representative for a bad fit and corresponds to [$M_{\text{BH}} = 14.6M_{\odot}$, $M_{\text{WR}} = 10M_{\odot}$, $\dot{M}_{\text{WR}} = 10^{-5} M_{\odot}/\text{yr}$] and accretion model parameters [$\xi = 1$, $v_{\text{w}}(A) = 1000$ km/s, $v_{\infty} = 2000$ km/s]

However, this best model (as well as all other models with a small stellar wind mass loss rate that explain more or less the observed X-ray luminosity and distribution of X-rays over energies) does not meet the constraint given by Equation (6.7), so that we are forced to admit that

it is not possible to find a model that meets all observed properties of the HMXB Cyg X-3 where the optical component is a ‘normal’ Population I WR star with a spherically symmetric stellar wind.

The latter corresponds to the conclusion of Mitra (1996) who used a simplified absorption mechanism.

An alternative model for Cyg X-3 is the following: the optical component is a $\leq 2M_{\odot}$ WR-like star similar to the one in the binary V Sagittae. If the star is at the end of its CHeB it will expand, reach its Roche lobe for a second time (case BB) and start mass transfer. The very strong X-rays may be capable of driving part of the mass lost by the CHeB component out of the binary. If it is assumed that Cyg X-3 is in this phase, Equation (6.7) is obviously no longer valid and the constraint against a small stellar wind mass loss disappears.

A MCB evolutionary model

A probable evolutionary scenario is sketched in Fig. 20. We start with a binary with a secondary with mass $\sim 10M_{\odot}$ and a $50 M_{\odot}$ primary. The primary first loses a lot of mass during its LBV phase, but since its initial mass is not too different from $40 M_{\odot}$, we assume that despite the LBV SW mass loss, a SpI phase occurs but with a largely reduced efficiency of course. At the end of its evolution, the primary collapses

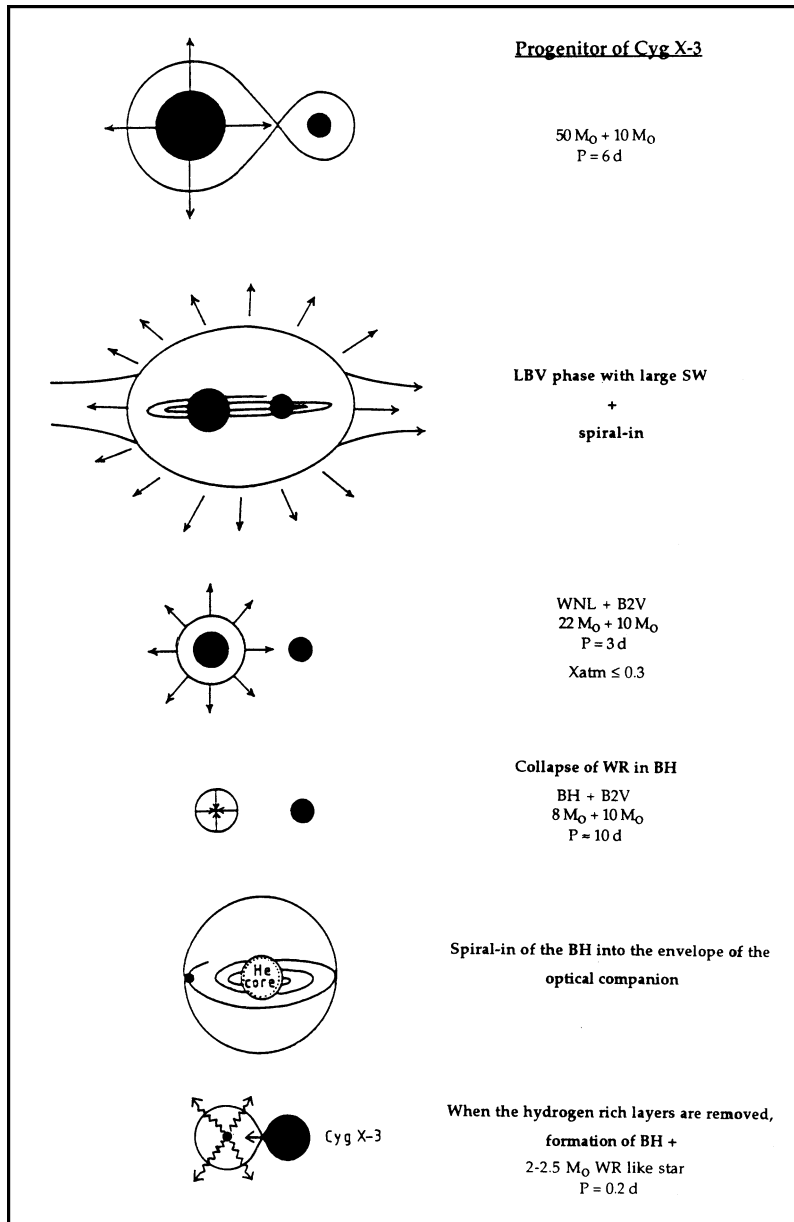


Fig. 20. An evolutionary model for the MCB producing a system like Cyg X-3

into a $8 M_{\odot}$ BH (thus no SN). When the $10 M_{\odot}$ secondary reaches its Roche lobe, the further evolution is governed by the CE/SpI process. When most of the hydrogen rich layers of the secondary are removed, we are left with a $2\text{-}2.5 M_{\odot}$ CHeB star which may show up (in the IR) as a WR like star.

At the end of CHeB (during He shell burning), the CHeB star expands, reaches its Roche lobe and start losing mass (case BB). The X-rays are the result of the accretion by the BH of part of this lost mass.

Together with RLOF mass transfer, the WR like star may lose mass by a spherically symmetric SW, but the \dot{M} must be smaller than $10^{-6}M_{\odot}/\text{yr}$ to assure a small X-ray absorption efficiency.

The SN explosion of the WR like star will be a type I and when the binary is not disrupted, a NS+BH binary is formed.

HD 50896

Observational facts

The WR star is a WNE type with peculiar space velocity $\sim 80 \pm 60$ km/s and can thus be classified as a runaway.

A detailed wind model of the WR star yields a luminosity $\log L/L_{\odot} \approx 5.6-5.7$ (Schmutz, 1997). From evolutionary calculations it follows then that if the WR star is a real single star, its age is $\sim 6-7$ million years. Using the Hipparcos data and performing a similar kinematic analysis as for ζ Pup (Sect. 2.7.5), the past path of HD 50896 approaches the stars of the two clusters Col 359 and Sco OB2. However, Col 359 hardly meets the conditions necessary for the cluster ejection model whereas a most luminous star in Col 359 (HD 164353) has a spectral type B5Ib indicating that the cluster has an age $\sim 12-14$ million years. The number of massive stars in Sco OB2 is also quite small whereas the cluster seems to contain a M1Ib (i.e. HD 148478, Humphreys, 1978). This would mean that the cluster is older than 20–30 million years, much older than HD 50896. Therefore, we are inclined to conclude that

Hipparcos data does not support the hypothesis that the WR star HD50896 became a single star runaway as a consequence of close encounters of binaries and single stars in a very dense cluster.

The WR star is associated with the nebula S 308 which is due most probably to pre-WR mass loss phases.

A 3.7 day period variation has been reported by different authors. Firman et al. (1980) proposed a low mass binary component (possibly a relativistic object) to explain these variations although alternatives appeared in literature as well (St.-Louis et al., 1993).

Interestingly, the WR star has not been detected as a hard X-ray source.

Interpretation of HD 50896 as a WR+cc binary

Let us accept the WR+cc hypothesis and study the consequences. Absorption of X-ray with energies > 2 keV by the stellar wind of the WR star is not sufficient to explain the lack of X-radiation (Vanbeveren et al., 1982). This was confirmed by Stevens & Willis (1988) and by Vanbeveren et al. (1998a). The only way to explain the observations then is adopting a model where the cc is a NS that is spinning fast enough to prevent accretion of mass from the stellar wind of the WR star. The following scenario is a possibility (see also Ergma & Yungelson, 1998).

If HD 50896 is a WR+NS binary with an orbital period $P = 3.6$ days, the pre-spiral-in period of the OB+NS progenitor must have been of the order of a few hundred days. Suppose now that the NS is born with a typical spin period of $\sim 0.01-0.1$ sec and accretes mass from the stellar wind of the OB star. Due to the large separation between the OB star and the NS, the accretion rate (computed with the

model of Davidson & Ostriker, 1973) is very small, too small to change drastically the spin period of the NS due to the action of magnetic torques during pre-spiral-in lifetime of the OB component. It is therefore conceivable that at the beginning of the spiral-in phase, the NS still rotates very fast. Assume that, during the spiral-in phase, the NS accretes mass at the Eddington rate ($\sim 2 \cdot 10^{-8} M_{\odot}/\text{yr}$). When the NS star has a magnetic field (in Gauss) $\log B = 12$ which is typical for pulsars (Sect. 1.7.1), using the formalism of Stella et al. (1986), the NS will reach an equilibrium period $P_{\text{eq}} = 0.2$ s on a short time scale. The spiral-in phase stops when the OB star has lost most of its hydrogen rich layers and it becomes a WR star (with mass $\sim 10\text{--}15 M_{\odot}$). The accretion rate onto the NS from the fast stellar wind of the WR star is significantly lower than during the previous spiral-in phase and this means that, for this situation, the NS is spinning too fast to allow accretion and X-ray formation is prevented.

HD 197406

The WR star shows a 4.32 day period variation and when it is due to the presence of a compact companion, the resulting mass function suggests a BH component (Drissen et al., 1986).

Condition (6.8) is not fulfilled for HD 197406 and this could explain why the system is not a hard X-ray emitter.

III. Massive star population synthesis

7. General

Population number synthesis (PNS) of massive stars can be defined as a comparison between the observed number of stars with common observational characteristics and a theoretical number. To calculate the latter, one needs

- an evolutionary model for massive single stars
- an evolutionary model for massive close binaries (MCB)
- an unambiguous definition of when a massive star calculated with an evolutionary code will be observed as a star belonging to the class of stars that is studied, and the lifetime of single stars and of binary components during such an evolutionary phase,
- input parameter distributions for stellar objects at birth, i.e.
 - the IMF of single stars and of primaries of binaries
 - the binary frequency
 - the period (P) and mass ratio (q) distribution of binaries
 - a parameter distribution describing the asymmetry of the supernova (SN) explosion
 - the distribution of the spin period of the NSs at birth and of the magnetic field of NSs

The evolutionary models are summarized in Fig. 21a–e where we use the following abbreviations:

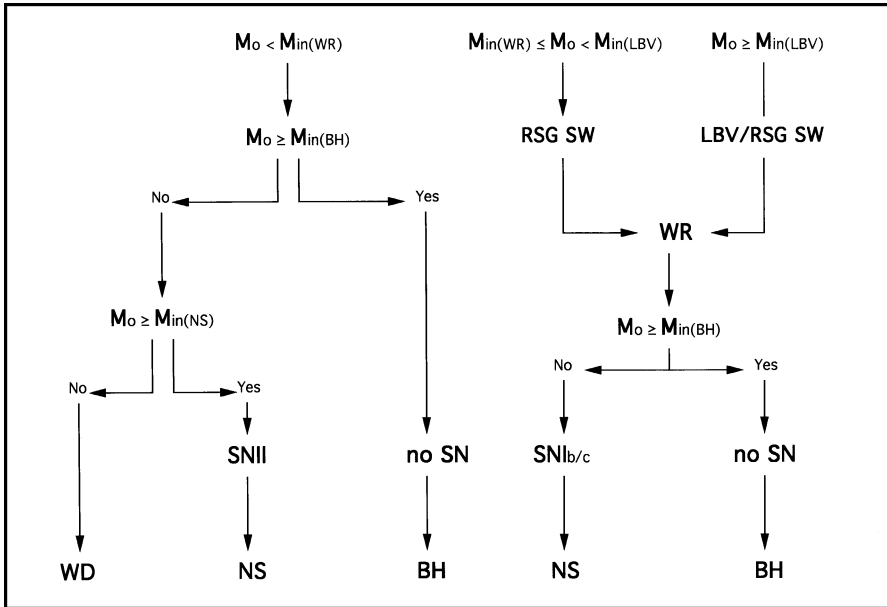


Fig. 21a. The overall evolutionary model of massive single stars

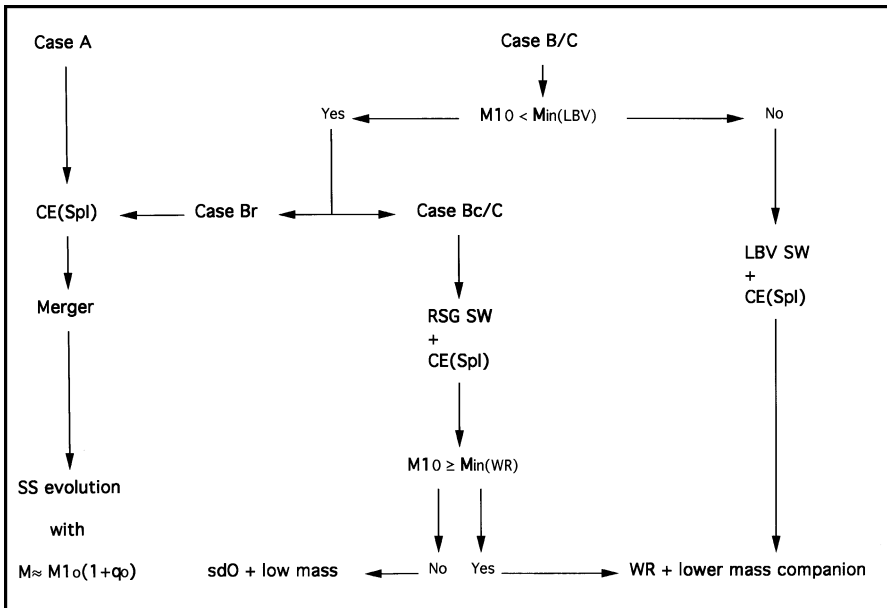


Fig. 21b. The overall evolutionary model of MCBS with initial mass ratio $q \leq 0.2$, prior to the first SN explosion

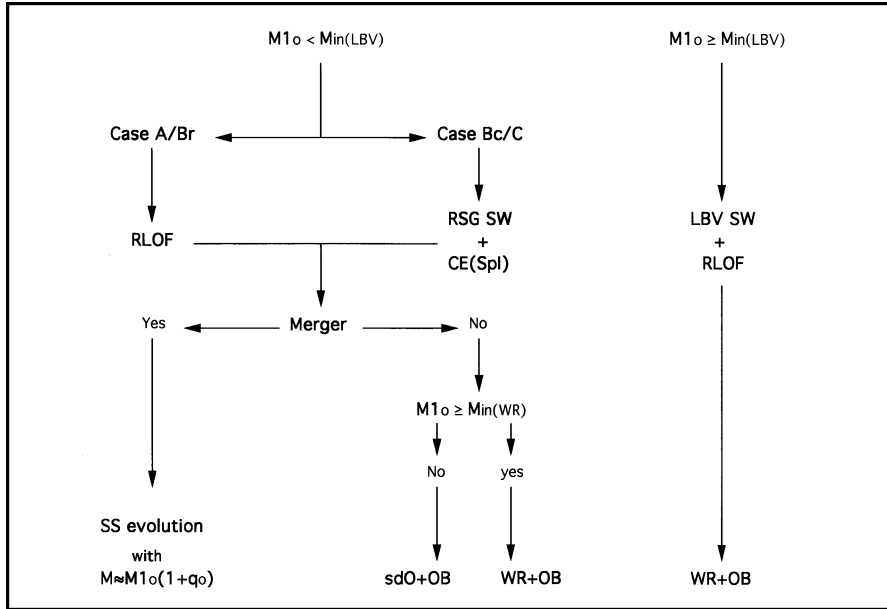


Fig. 21c. Similar as Fig. 21b but for initial $q > 0.2$

- Min(WR) = the minimum initial mass a star must have to lose most of its hydrogen rich layers and to evolve into a WR star; if we trust the observed luminosities of WR stars, the minimum mass of a WR star $\sim 5 M_{\odot}$ corresponding to an initial mass $\sim 18 M_{\odot}$.
- Min(LBV) = the minimum initial mass a star must have so that it will lose a significant part of its hydrogen rich layers by a LBV type SW reducing the mass lost by a possible RLOF; for the Galaxy, its value $\geq 40\text{--}50 M_{\odot}$,
- Min(NS) = the minimum mass a star must have to end its life as a NS accompanied by a SN explosion; when convective core overshooting during CHB is small, $\text{Min(NS)} \approx 8 M_{\odot}$ (resp. $10 M_{\odot}$) for single stars (resp. binary components); rapid rotation during CHB may lower this limit,
- Min(BH) = the minimum mass a massive star must have to end its life as a BH; when convective core overshooting during CHB is small, $\text{Min(BH)} \approx 20\text{--}30 M_{\odot}$ (resp. $40\text{--}50 M_{\odot}$) for single stars (resp. binary components); rapid rotation during CHB may lower this limit.

Most of the PNS studies with a realistic binary population published till now, deal with the number of X-ray binaries, the WR-O-RSG population, the formation of single and binary pulsars and, related to the latter, the supernova formation rate.

8. The X-ray binaries

Predicting the number of HMXBs is extremely difficult and the results are highly uncertain. The reason is intrinsic to the formation mechanism of X-radiation which depends on a number of uncertainties, such as the formation of disks around Be stars,

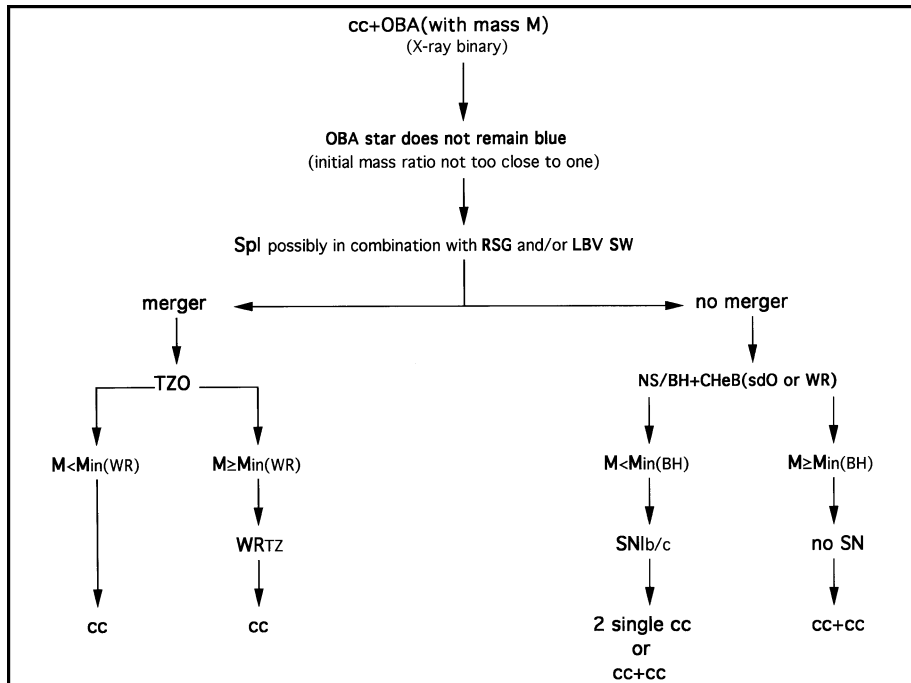
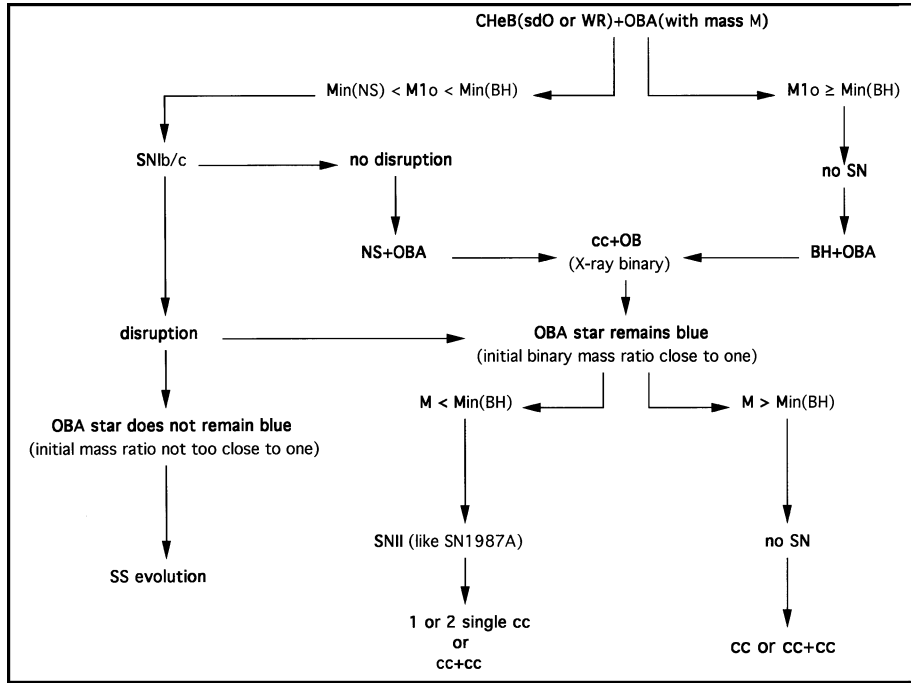


Fig. 21d-e. The evolutionary model of MCBs after the first SN explosion

the initial period- and magnetic field distribution of a neutron star, the evolutionary lifetime of post-RLOF mass gainers etc.

A first step in predicting the number of X-ray binaries is obviously the computation of the number of binaries with a compact companion with a PNS code. Results were presented by Dewey & Cordes (1987), Meurs & Van den Heuvel (1989), Pols et al. (1991), Pols & Marinus (1994), Tutukov et al. (1992), Iben et al. (1995 a,b), Jorgensen et al. (1997), Dalton & Sarazin (1995a, b), Portugies Zwart (1995, 1996), Portugies-Zwart & Verbunt (1996), Ergma & Yungelson (1998).

Two remarks:

- the theoretically predicted number of OB+cc binaries obviously depends on the lifetime and evolution of the OB components. The latter are mass gainers and in most studies cited above, the lifetime is estimated using a qualitative formula originally proposed by Van den Heuvel (1969);
- we have the impression that authors do not always realize that the adopted stellar wind mass loss formalism critically affects the CHB and CHeB evolution of a massive star (massive binary component).

Two examples to illustrate:

- in one of the papers cited above, we read: ... *'we use the CHeB timescales of Iben & Tutukov (1985)'* ... and, in the same paper, to determine the final mass at the end of CHeB and the binary period variation during CHeB ... *'we will use the stellar wind mass loss formalism of Langer (1989)'* ... Obviously, the evolutionary results of Iben and Tutukov were not computed with the SW formalism of Langer.
- In another paper we find the following assumption: ... *'Computations were performed on the assumption that black holes result from objects which have a mass exceeding 7 or 10 M_{\odot} at the end of the helium star stage. Using Langer's (1989) mass loss rates for helium stars, these limits correspond to $M_{\text{ZAMS}} \approx 30$ or $50 M_{\odot}$.* ... However, with the mass loss rates of Langer (1989), all massive stars with initial ZAMS mass larger than $30 M_{\odot}$ end their life with a mass $\sim 4\text{--}5 M_{\odot}$ (this is a fortiori true for MCB components).

The two effects cited above primarily affect the estimated population of O-type stars and WR stars with a NS or a BH companion. They will be discussed in the next section.

Using an extended grid of explicitly calculated post-RLOF evolutionary sequences of mass gainers, the effect of large kicks [Equation (1.6)] on the population of early B+cc [Be + cc] binaries has been investigated by Van Bever & Vanbeveren (1997).

From all the studies listed above, we select the following conclusions.

- If the asymmetry of the SN explosion of a massive star results in a vkick distribution predicted by Equation (1.6), at most 1%–2% of all B-type stars with spectral type earlier the B3, in the Solar neighbourhood, have a NS companion. The latter percentage has to be multiplied by a factor 2–3 if, instead, Equation (1.7) is used predicting a much smaller disruption probability of a MCB due to the SN explosion of the primary.
- At most 20% (and possibly only 5%) of the early Be stars in the Solar neighbourhood are close binary products.

- If the binary formation process is similar in the Magellanic Clouds as in the Solar neighbourhood, the population of early B-type stars with a NS companion is expected to be similar in both environments.

An interesting study on the formation of BHs in LMXBs has been published by Portegies Zwart et al. (1997). They conclude that

- If the minimum mass for BH formation in a close binary component is $\sim 40 M_{\odot}$, then the theoretically predicted formation rate of LMXBs with a BH component is about 1% of the formation rate of LMXBs with a NS. This contradicts the observations which indicate an equal formation rate.

As a solution, a much smaller minimum mass of BH formation is proposed ($\sim 20 M_{\odot}$).

However, the PNS model of Portegies Zwart et al. can be criticized. The LBV stellar wind mass loss rates are large but the exact rates are very uncertain (allowing a large degree of freedom) and it can not be excluded that a star with initial mass $> 40 M_{\odot}$ loses most (all) of its hydrogen rich layers due to this stellar wind. When a star like that has a close low mass companion, although it will be engulfed by the dense stellar wind of the LBV and spiral-in may happen, the efficiency of spiral-in may be much reduced since it is radiation pressure that is capable to drive most of the mass out of the system. It can therefore not be excluded that

the majority of the close binaries with primary mass $> 40 M_{\odot}$ and a low mass secondary will survive the combined action of stellar wind mass loss and spiral-in.

It can readily be checked then that, compared to the results of Portegies et al., the predicted formation rate of LMXBs with a BH component increases by two orders of magnitude. Therefore, lowering the minimum mass for BH formation is not necessary.

9. The WR-O-RSG population

The theoretically predicted distribution of WR and O-type stars in regions of continuous star formation with a realistic frequency of binaries, has been studied by Dalton & Sarazin (1995a,b) and by Vanbeveren (1995). In the former paper, binary evolution was simulated using the single star evolutionary computations of Schaller et al. (1992). The formation and evolution of post-supernova binaries and the effect on the WR and O-type star population was not considered in detail in either of the two papers but was discussed by Vanbeveren et al. (1997) and by De Donder et al. (1997).

The early discovery of galaxies with emission line spectra like those of HII regions (Sargent & Searle, 1970; Searle et al., 1973) started a new era in PNS studies: the evolution of young and massive starbursts and the formation of ‘WR galaxies’ (Conti, 1991, 1994). Theoretical PNS models of starbursts have been calculated by Leitherer and Heckman (1995), Mass-Hesse & Kunth (1991), Cervino & Mass-Hesse (1994), Leitherer et al. (1995), Meynet (1995), however binaries were not included in any of these studies.

Binaries were included in starburst computations by Vanbeveren et al. (1997). Van Bever & Vanbeveren (1998) introduced the concept ‘the rejuvenation of starbursts due to MCB evolution’, making the determination of the age of a starburst not unambiguous.

PNS model computations have been discussed in Vanbeveren et al. (1998b) using the most recent massive single star and MCB evolutionary calculations (Sects. 2 and 5), with the updated stellar wind mass loss rates (Sect. 1.2).

Main results are summarized in the following subsections.

9.1. Continuous star formation regions

9.1.1. The population of O-Type stars

The population of O-type stars consists of:

- O_s = number of O-type single stars, formed as single stars
- O_b = number of O-type primaries in a binary with an OB or a low mass component; we separately consider the number of O-type primaries in a binary with $q \geq 0.2$ and orbital period $P \leq 100$ days. Since it is this number that may be comparable to the observed number, we denote it as $O_{b,o}$.
- O_{+CHeB} = number of O-type mass gainers with a CHeB (WR) companion
- O_{sb} = the number of single post-SN O-type mass gainers where the SN disrupted the binary; we separately consider those with a space velocity ≥ 30 km/s (the runaways)
- O_{cc} = the number of post-SN O-type mass gainers with a compact companion (NS or BH); also here we separately consider those with a NS companion and with a space velocity ≥ 30 km/s (the runaways).

A first important conclusion:

- a comparison between the predicted $O_{b,o}$ numbers and the observed O-type frequency ($33\% \pm 13\%$, Sect. 5.2.2) forces us to conclude that the majority of the O-type stars is formed as binary component in binaries with orbital period between 1 day and 10 years (i.e. the MCB formation rate $f > 0.7$).

To illustrate: $f = 0.8$ means that for 2 O-type single stars, there are 8 O-type primaries of a MCB. These 8 MCBs also have ~ 5 secondaries that are O-type stars (or, due to mass transfer, will become an O-type star). This means that assuming a MCB formation rate $f = 0.8$ means that among all O-type stars, only 10–15% are really formed as single stars.

In the following, the results hold for $f = 0.8$. One should realize that all theoretical percentages of the different types of stars scale linearly with f .

- Between 15% and 25% of all O-type stars are post-SN mass gainers of MCBs; if the kick-velocity distribution has an average value of 150 km/s (resp. 500 km/s), $\sim 40\%$ (resp. $< 12\%$) of these post-SN O-type mass gainers have a NS companion. It is clear then that if the kick-velocity distribution has an average value of 500 km/s, a very significant fraction of the population of 'single' O-type stars are single post-SN O-type mass gainers of MCBs.
- $\leq 10\%$ of the O-type stars are runaways due to a previous SN explosion in a binary; if $\langle v_{kick} \rangle = 500$ km/s (resp. 150 km/s), $< 20\%$ (resp. $> 50\%$) of these runaways have a NS companion. Gies (1987) and Gies and Bolton (1986) investigated the presence of compact companions among O-type runaways and concluded that only a small percentage may hide one. This is predicted by our PNS model provided that the kick velocity during the SN explosion is very large,
- The results for the Magellanic Clouds are very similar.

9.1.2. The WR population

A realistic WR population consists of

- WR_s = number of single WR stars descendent from the O_s class,
- WR_b = number of WR binary components with an OB or low mass component, descendants from the O_b sample; this class can be subdivided into
 - $WR_{b,i}$ = number of WR stars with an OB-type or low mass companion, where RLOF and binary interaction played a dominant role,
 - $WR_{b,LBV}$ = number of WR stars with an OB-type or low mass companion where, due to very large SW during an LBV phase, RLOF and thus binary interaction played only a minor role,
 - $WR_{b,merged}$ = number of (single) WR stars, descendent from those interacting binaries that merge,
 - $WR_{b,RSG}$ = number of WR binaries with an OB-type or low mass companion orbiting with very large period, where interaction did not happen and where the WR star was formed by SW during the RSG stage,
- WR_{sb} = the number of single post-SN WR stars descendant from the O_{sb} class,
- WR_{cc} = the number of WR+cc binaries that survived the spiral-in phase of the O+cc binary,
- WR_{TZ} = the number of WR stars with a cc in their center, descendent from O+cc binaries where during the spiral-in phase a Thorne-Zytkov object is formed.

The Solar neighbourhood

- The observed WR/O and WR+OB/WR number ratios in the Solar neighbourhood can be reproduced if the MCB formation rate > 0.7 .
- In $\sim 70\%$ of the WR+OB binaries (where also the OB star is a massive star) RLOF and mass transfer occurred; the other $\sim 30\%$ evolved either according to the LBV scenario or according to the RSG scenario.
- 3–5% of the WR stars may have a normal intermediate mass or low mass companion.
- At most 3% (resp. 8%) of the WR stars may have a compact star in their center (WR_{TZ}) if the kick-velocity distribution has an average value of 500 km/s (resp. 150 km/s).
- The PNS model predicts a small percentage of WR stars with a compact companion. Depending on the adopted efficiency for converting orbital energy into kinetic energy of the envelope of the OB-type star during the spiral-in of the cc, at most 2% (resp. 8%) of the WR stars may have a NS companion if the kick-velocity distribution has an average value of 500 km/s (resp. 150 km/s). Between 3%–5% of the WR stars may have a BH companion. The WR+BH numbers depend on the value of the minimum mass of BH formation in binaries. They were calculated assuming a minimum mass for BH formation = $40 M_{\odot}$.
- Between 40% and 50% of all WR stars are single WR stars. However, it cannot be excluded that ~ 70 –80% (or more) of these single WR have had a binary history, i.e. are WR stars, descendants from OB type mass gainers in binaries where the SN explosion disrupted the binary, or are WR stars descendants from binaries where during the RLOF both components merged. The latter class is largest when the Hogeveen mass ratio distribution (6.1) applies and/or when the RLOF in case A/case B_r MCBs is highly non-conservative ($\beta \leq 0.5$).

- At most 5% of all WR stars have a space velocity larger than 30 km/s (WR runaway) caused by the recoil of the SN explosion in a binary.

The inner Milky Way

- It is hard to explain the observed WR/O number ratio (≈ 0.2) by means of a continuous star formation model. However, a WR/O number ratio as large as 0.2 is not unusual if, instead of a continuous star formation history, there has been an increased star formation rate a few million years ago.

The Magellanic Clouds

- Adopting a continuous star formation history in the LMC, the theoretically predicted WR/O number ratio ~ 0.04 – 0.05 which is very close to the observed value.

9.1.3. Why the number of Galactic X-ray binaries with a WR type optical component is so small?

- The PNS code predicts that 3%–5% of the WR stars may have a BH companion. Most of them have a period larger than 1 day. Condition (6.8) is never satisfied in this case and X-ray formation is prevented.
- 2%–8% of the WR stars are expected to have a NS companion. Most of these WR+NS binaries are spiral-in survivors and originated from an OB+NS progenitor with orbital period of a few hundred days. Similar arguments as used for HD 50896 (Sect. 6.6) allow to suspect that the NSs in most of these binaries spin too fast for accretion of matter from the stellar wind of the WR star to happen. Therefore, also here hard X-radiation is prevented.

9.2. Starburst regions

9.2.1. The population of O-type stars and WR stars

Figure 22 illustrates the evolution in the HR diagram of a starburst with 1000 massive stars for a starburst which lasted for 1 million years, with the same PNS parameters. We define the O-phase (resp. the WR phase) and the corresponding O-lifetime (resp. WR lifetime) of a starburst as the phase or the time where the starburst shows O-type (resp. WR type) features.

We conclude

- the evolution of a starburst older than $\sim 4 \cdot 10^6$ years depends critically on the binary frequency. If binaries are included, the total elapse of time the starburst shows O-type and WR star features, is much longer than in starbursts where binaries are omitted. This is due to the effect of accretion in MCBs and the appearance of a class of young O-type mass gainers when the starburst is older than $\sim 4 \cdot 10^6$ yrs: we propose to call this the ‘starburst rejuvenation’. Figure 21 shows the situation of a burst of $8 \cdot 10^6$ years old and where, owing to O-type mass gainers, it looks younger than $4 \cdot 10^6$ years.

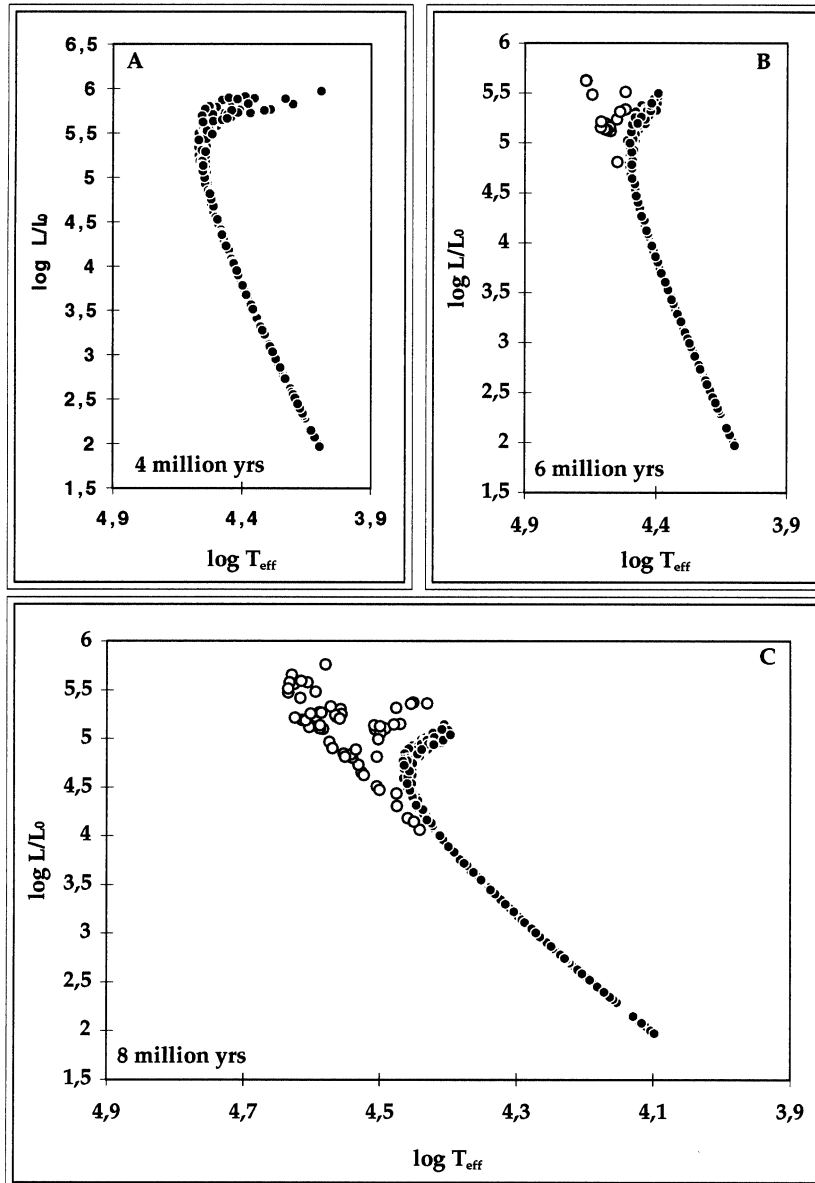


Fig. 22. The evolution in the HR diagram of a starburst with 1000 massive stars for a starburst which lasted for 1 million years. The figures labelled A (resp. B and C) correspond to the burst after 4 million years (resp. 6 and 8 million years) (from Van Bever and Vanbeveren, 1997). The open circles are rejuvenated mass gainers of case A/B; binaries

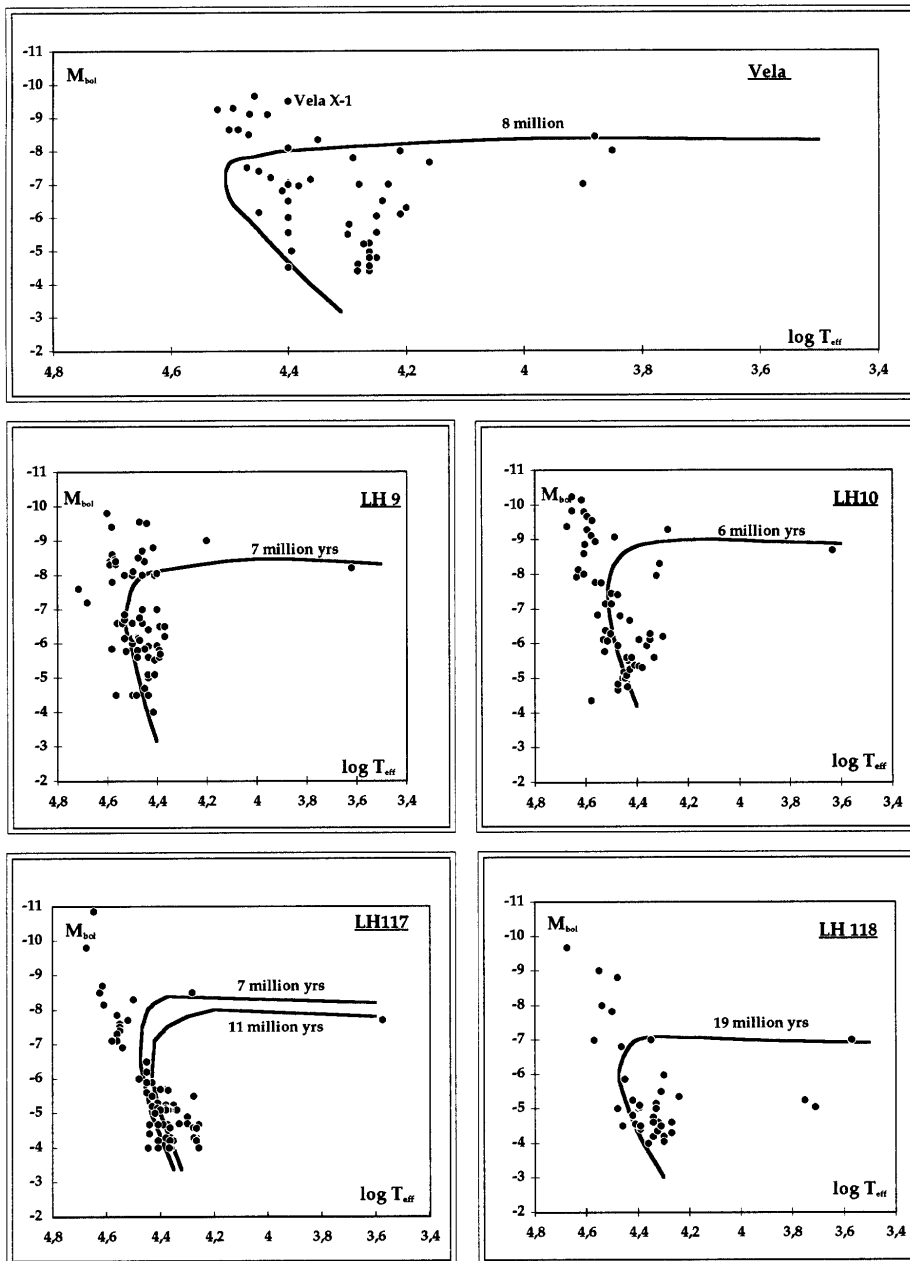


Fig. 23. The HR diagram of the most massive stars in the stellar aggregates Vela OB1 in the Galaxy, LH 9, 10, 117 and 118 in the LMC; data are from Humphreys and McElroy (1984), Parker et al. (1992) and Massey et al. (1989a,b)

- a comparison between theoretical prediction and observations of young starbursts is meaningful only if binaries and the effect of binary evolution are correctly included. Most important is the rejuvenation caused by mass transfer,
- when the observed HR diagram of stellar aggregates in the Galaxy and MCs (Fig. 23) is compared with the predicted HR diagram of starbursts (Fig. 22), although the number of stars is smaller in the former, it looks as if the effects of interaction in binaries offer a natural explanation for the presence of a younger class of stars, bluer and more luminous than the cluster turn-off (blue stragglers).

9.2.2. The population of RSGs and WR type stars in starbursts

- Up to $\sim 4 \cdot 10^6$ years, starbursts show no signature of RSGs. After $\sim 4 \cdot 10^6$ years RSGs and WR stars are simultaneously present. However, although the lifetime of a starburst where WR stars and RSGs are simultaneously present may be comparable to the one where only WR stars (and no RSGs) will be observed, during most of that lifetime, the number of WR stars is larger than the number of RSGs.

10. The pulsar population and the fraction of binary pulsars

With a PNS code, the binary pulsar population can be estimated in a straightforward way. This has been done recently by De Donder et al. (1997, paper 1), Portegies-Zwart & Yungelson (1998, paper 2), De Donder and Vanbeveren (1998a, paper 3). It is encouraging to notice that for similar initial conditions and PNS parameters, the results of papers (1, 3) are similar to the results of paper (2). Similarly as for the WR+NS and O+NS population, the results depend significantly on the adopted kick velocity distribution. In papers (1 and 3), we used the formalism of Sect. 1.7.2 with average $\langle v_{\text{kick}} \rangle = 150$ km/s and 500 km/s.

We summarize:

- The PNS model predicts a Galactic NS+NS formation rate of $\sim 10^{-6}$ – 10^{-5} /yr corresponding to observations. About 60% of these double neutron star systems will merge within a Hubble time possibly producing observable γ -ray bursts.
- The BH+NS formation rate is similar to the NS+NS one. However, most of the BH+NS binaries have periods larger than one day and, therefore, it is expected that only a small fraction will merge within a Hubble time.
- The BH+BH formation rate is surprisingly large (100–1000 times larger than the NS+NS rate). However, almost all of them have periods in excess of 10 days and this means that only few will merge within a Hubble time.

11. The SN rates

Stellar evolution predicts the chemical composition of a star at the moment of the SN explosion and thus it can be decided whether a massive star will explode as type II (hydrogen present) or as type I_{b,c} (no hydrogen present). The PNS code then computes the number ratio (II/I_{b,c}) for different combinations of the model parameters (De Donder & Vanbeveren, 1998a). The following conclusions hold:

- Depending on the minimum mass of BH formation, it is conceivable that only few WR stars contribute to the SN $I_{b,c}$ population; the latter then originate from binaries with primary mass smaller than $\sim 20 M_{\odot}$.
- The number ratio ($II/I_{b,c}$) strongly depends on the adopted MCB formation rate, the binary mass ratio and period distribution.

To estimate the number ratio in one galaxy, data are collected of a large sample of galaxies of the same type. The average value is then considered as representative for all of them. However, accounting for the dependency of the SN ratio on MCB statistics, it follows that

- Estimating the SN ($II/I_{b,c}$) number ratio in a particular galaxy by using the average ratio of a large set of galaxies of the same type, is meaningful only if the MCB formation rate, the binary mass ratio and period distributions are the same in all the galaxies where the average value is based on.

Cappellaro et al. (1993) combined the data of two independent SN searches and derived an average ratio ~ 4 . Since the sample contains 2461 galaxies and since all morphological types are present, this value can be considered as some cosmological average. It can be recovered by PNS calculations adopting a MCB formation rate between 40% and 60%, i.e.

- The cosmological MCB formation rate is $\sim 50\%$.

The early type (resp. late type) spiral galaxies in the sample have an average ratio is ~ 2.3 (resp. ~ 5.5). If this difference is due to a difference in the MCB formation rate, we conclude that

- The MCB formation rate in late spiral galaxies may be a factor 2 smaller than in early type spirals.

References

- Alongi, M., Bertelli, G., Bressa, A., Chiosi, C.: 1991, *A&A* 224, 95.
- Annuik, K.: 1991, in 'WR Stars and Interrelations with other Massive Stars in Galaxies', eds. K.A. Van der Hucht & B. Hidayat, IAY Symp. 143, (Kluwer: Dordrecht), p. 245.
- Annuik, K.: 1995, in 'WR Stars: Binaries, Colliding Winds, Evolution', eds. K.A. Van der Hucht & P.M. Williams, IAU Symp. 163, (Kluwer: Dordrecht), p.231.
- Batten, A.H., Fletcher, J.M., MacCarthy, D.G., 1989, Publications of the Dominion Astrophysical Observatory, Volume XVII: The Eighth Catalogue of the Orbital Elements of Spectroscopic Binary Systems.
- Bernasconi, P.A., Maeder, A.: 1996, *A&A* 307, 829.
- Bhattacharya, D., Van den Heuvel, E.P.J.: 1991, *Phys. Rev.* 203, 1.
- Bhattacharya, D., Wijers, R.A.M.J., Hartman, J.W., Verbunt, F.: 1992, *A&A* 254, 198.
- Biehle, G.T.: 1991, *Ap.J.* 380, 167.
- Blaauw, A.: 1961, *Bull. Astr. Inst. Netherlands* 15, 265.
- Bonnet-Bidaud, J.M., Chardin, G., 1988, *Physics Reports* 170, 325.
- Braun, H., Langer, N.: 1995, *A&A* 297, 483.
- Burrows, A.: 1987, in 'SN 1987A', ESO Workshop 26, ed. I.J. Danziger, ESO Garching, p. 315.
- Cannon, R., Eggleton, P.P., Zytokow, A.N., Podsiadlowski, Ph.: 1992, *Ap.J.* 386, 206.
- Cappellaro, E., Turatto, M., Benetti, S., Tsvetkov, D.Y., Bartunov, O.S., Makarova, L.N.: 1993, *A&A* 273, 383.
- Castor, J., Abbott, D.C., Klein, R.: 1975, *Ap.J.* 195, 157.
- Cervino, M., Mass-Hesse, J.M.: 1994, *A&A* 284, 749.
- Chandrasekhar, S.: 1957, 'An Introduction to the Study of Stellar Structure', Dover, New York

- Cherepaschuk, A.M.: 1975, *Sov. Astron. A.J.* 19, 47.
- Clayton, D.D.: 1968, 'Principles of Stellar Evolution and Nucleosynthesis', McGraw Hill, N.Y.
- Conti, P.S.: 1991, *Ap. J.* 377, 115.
- Conti, P.S.: 1994, in 'Evolution of Massive Stars: a Confrontation between Theory and Observation', eds. Vanbeveren, D., Van Rensbergen, W., De Loore, C., Kluwer: Dordrecht, p. 37.
- Counselman, C.C.: 1973, *Ap.J.* 180, 307.
- Cox, A.N., Stewart, J.N.: 1969, *Ap.J.Suppl.* 19, 243.
- Cox, A.N., Tabor, J.E.: 1976, *Ap.J. Suppl.* 31, 271.
- Cox, J.P., Giuli, R.T.: 1968, 'Principles of Stellar Structure I&II', Gordon & Breach.
- Crowther, P.A., Hillier, D.J., Smith, L.J.: 1995, *A&A* 293, 403.
- Dalton, W.W., Sarazin, C.L.: 1995a, *Ap.J.* 440, 280.
- Dalton, W.W., Sarazin, C.L.: 1995b, *Ap.J.* 448, 369.
- Darwin, G.H.: 1908, *Scientific Papers*, Vol. 2, Cambridge Univ. Press.
- Davidson, K., Ostriker, J.P.: 1973, *Ap.J.* 179, 585.
- De Donder, E., Vanbeveren, D., Van Bever, J.: 1997, *A&A* 318, 812.
- De Donder, E., Vanbeveren, D.: 1998a, *A&A* 333, 557.
- De Donder, E., Vanbeveren, D.: 1998b, *New Astronomy* (submitted).
- De Jager, C., Nieuwenhuyzen, H., Van der Hucht, K.A.: 1988, *A.A.Suppl.* 72, 259.
- De Kool, M., Van den Heuvel, E.P.J., Pylyser, E.: 1987, *A&A* 183, 47.
- De Loore, C., Doom, C.: 1992, 'Structure and Evolution of Single and Binary Stars', Kluwer Academic Publishers, Dordrecht, The Netherlands.
- De Loore, C., Vanbeveren, D.: 1992, *AA.* 260, 273.
- De Loore, C., Vanbeveren, D.: 1995, *A&A* 304, 220.
- Dewey, R.J., Cordes, J.M.: 1987, *Ap.J.* 321, 780.
- Dickey, J.M.: 1983, *Ap.J.* 273, L71.
- Drilling, J.S., Jeffery, C.S., Heber, U.: 1985; *IAU Circ. No.* 4086.
- Drissen, L., Lamontagne, R., Moffat, A.F.J., Bastei, P., Seguin, M.: 1986, *Ap. J.* 343, 426.
- Dudley, R.E., Jeffery, C.S.: 1990, *MNRAS* 247, 400.
- Eggleton, P.P.: 1983, *Ap.J.* 268, 368.
- Ergma, E., Yungelson, L.R.: 1998, *A&A* 333, 151.
- Filippenko, A.V., Matheson, T.H., Ho L.C.: 1995, *Ap.J.* 455, 614.
- Firmani, C., Koenigsberger, G., Bisiacchi, G.F., Moffat, A.F.J., Isserstedt, J.: 1980, *Ap.J.* 239, 607.
- Fryer, C., Burrows, A., Benz, W.: 1998, *Ap.J.* 496, 333.
- Fryxell, B.A., Arnett, W.D.: 1981, *Ap.J.* 243, 994.
- Gabler, R., Gabler, A., Kudritzki, R.P., Puls, J., Pauldrach, A.W.A.: 1989, *A&A* 226, 162.
- Garmany, C.D., Conti, P.S., Massey, P.: 1980, *Ap.J.* 242, 1063.
- Giacconi, R., Gorenstein, P., Gursky, H., Waters, J.R.: 1967, *Ap.J.* 148, L118.
- Gies, D.R., Bagnuolo, W.G., Ferrara, E.C. et al.: 1998, *Ap.J.* 493, 440.
- Gies, D.R., Bolton, C.T.: 1986, *Ap.J.* 304, 371.
- Gies, D.R.: 1987, *Ap.J. Suppl.* 64, 545.
- Habets, G.M.H.J.: 1985, Ph. D. thesis, University of Amsterdam.
- Habets, G.M.H.J.: 1986, *A&A* 187, 209.
- Halbwachs, J.L.: 1987, *A&A* 183, 234.
- Hamann, W.-R., Koesterke, L., Wessolowski, U.: 1995, *A&A* 299, 151.
- Hamann, W.-R., Koesterke, L.: 1998, *A&A* (in press).
- Harlaftis, E.T., Horne, K., Filippenko, A.V.: 1996, *PASP* 108, 762.
- Harries, H.T., Hilditch, R.W., Hill, G.: 1997, *MNRAS* 285, 277.
- Heger, A., Jeannin, L., Langer, N., Baraffe, I.: 1998, *A&A* (in press).
- Herbig, G.H., Preston, G.W., Smak, J., Paczynski, B.: 1965, *Ap.J.* 141, 617.
- Herrero, A., Kudritzki, R.P., Gabler, R., Vilchez, J.M., Gabler, A.: 1995, *A&A* 297, 556.
- Herrero, A., Kudritzki, R.P., Vilchez, J.M., Kunze, D., Butler, K., Haser, S.: 1992, *A&A* 261, 209.
- Hilditch, R.W.: 1974, *MNRAS* 169, 323.
- Hillier, D.J.: 1996, in 'Wolf-Rayet Stars in the Framework of Stellar Evolution', eds. J.M. Vreux, A. Detal, D. Fraipont-Caro, E. Gosset & G. Rauw, Université de Liège, p. 509.
- Hoffleit, D., Warren, Jr. W.H.: 1991, *The Bright Star Catalogue*, 5th Revised Ed., Yale University Observatory.
- Hogeveen, S.: 1991, Ph.D. Thesis, Univ. of Amsterdam.
- Hogeveen, S.: 1992, *Astrophys. Space Sci.* 196, 299.

- Howarth, I.D., Prinja, R.K.: 1989, *Ap.J. Supp* 69, 527.
- Humphreys, R.M.: 1978, *Ap. J. Suppl. Ser.* 38, 309.
- Humphreys, R.M., McElroy, D.B.: 1984, *Ap.J.* 284, 565.
- Humphreys, R.M., Davidson, K.: 1994, *PASP* 106, 1025.
- Hutchings, J.B.: 1975, *Ap.J.* 200, 122.
- Iben, I. Jr., Tutukov, A.V., Yungelson, L.R.: 1995a, *Ap.J. Suppl.* 100, 233.
- Iben, I. Jr., Tutukov, A.V., Yungelson, L.R.: 1995b, *Ap. J. Suppl.* 100, 217.
- Iben, I.J., Tutukov, A.V.: 1985, *Ap.J.S.* 58, 661.
- Iglesias, C.A., Rogers, F.J., Wilson, B.G.: 1992, *Ap.J.* 397, 717.
- Illarionov, A.F., Sunyaev, R.A.: 1975, *A&A* 39, 185.
- Jeffery, C.S., Drilling, J.S., Heber, U.: 1987, *MNRAS* 194, 429.
- Jorgensen, H., Lipunov, V.M., Panchenko, I.E., Postnov, K.A., Prokhorov, M.E.: 1997, *Ap.J.* 486, 110.
- Joss, P.C., Rappaport, S.: 1984, *Ann. Rev. Astron. Astrophys.* 22, 537, *A&A Suppl.* .
- Jura, M.: 1987, *Ap.J.* 313, 743.
- Kaper, L., Lamers; H.J., Ruymaekers, E., Van den Heuvel, E.P., Zuiderwijk, E.J.: 1995, *A&A* 300, 446.
- Kato, S.: 1966, *Publ. Astron. Soc. Japan* 18, 374.
- Khaliullin, Kh.F., Khaliullina, A.I., Cherepashchuk, A.M.: 1984, *Sov. Astron. (Letters)* 10, 250.
- King, A.: 1995, in 'X-ray Binaries', eds. W.H.G. Lewin, J. van Paradijs, E.P.J. van den Heuvel, Cambridge Astrophysics Series, p. 419.
- Kippenhahn, R., Ruschenplatt, G., Thomas, H.C.: 1980, *A&A* 91, 175.
- Kippenhahn, R., Weigert, A.: 1967, *Zeitschrift für Astrophysik* 66, 58.
- Kippenhahn, R., Weigert, A.: 1989, 'Stellar Structure and Evolution', Springer, Heidelberg.
- Koesterke, L., Hamann, W.-R., Wessolowski, U.: 1992, *A&A* 261, 535.
- Koesterke, L., Hamann, W.-W.: 1995, *A&A* 299, 503.
- Kopal, Z.: 1972, *Astrophys. Space Sci.* 16, 3.
- Langer, S.H., Rappaport, S.: 1982, *Ap. J.* 257, 733.
- Langer, N., Heger, A.: 1998, in 'Properties of Hot, Luminous Stars', ed. I. Howarth, ASP. Conf. Proceedings, Vol. 131, p. 76.
- Langer, N., Maeder, A.: 1995, *A&A* 295, 685.
- Langer, N., 1989, *A&A* , 210, 93.
- Lauterborn, D.: 1969, in 'Mass Loss from Stars', ed. M. Hack, D. Reidel. Publ. Com., Dordrecht, Holland, p. 262.
- Ledoux, P.: 1947, *Ap.J.* 105, 305.
- Leitherer, C., Heckman, T.M.: 1995, *Ap.J. Suppl.* 96, 9.
- Leitherer, C., Robert, C., Heckman, T.M.: 1995, *Ap. J. Suppl.* 99, 173.
- Leonard, P.J.T., Duncan, M.J.: 1988, *A.J.* 96, 222.
- Leonard, P.J.T., Duncan, M.J.: 1990, *A.J.* 99, 608.
- Lorimer, D.R., Bailes, M., Harrison, P.A.: 1997, *MNRAS* 289, 592.
- Lubow, S.H., Shu, F.H.: 1975, *Ap.J.* 198, 383.
- Lucy, L.B.: 1974, *A. J.* 79, 745.
- Maeder, A., Conti, P.: 1994, *Ann. Rev. Astron. Astrophys.* 32, 227.
- Maeder, A.: 1983, *A&A* 120, 113.
- Maeder, A.: 1992, *A&A* 264, 105.
- Maeder, A.: 1998, in 'Properties of Hot, Luminous Stars', ed. I. Howarth, ASP. Conf. Proceedings, Vol. 131, p. 85
- Marsh, T.R., Robinson, K., Wood, J.H.: 1994, *MNRAS* 226, 137.
- Marshall, F.E., Gotthelf, E.V., Zhang, W. et al.: 1998, *Ap.J.* 499, L179.
- Marston, A.P., Yocum, D.R., Garcia-Segura, G., Chu, Y.-H.: 1994, *Ap.J. Suppl.* 95, 151.
- Marston, A.P.: 1995, *A.J.* 109, 2257.
- Mason, B.D., Gies, D.G., Hartkopf, W.I. et al.: 1998, *Ap. J.* 115, 821.
- Mass-Hesse, J.M., Kunth, D.: 1991, *A&A Suppl.* 88, 399.
- Massey, P., Garmany, C.D., Silkey, M., Degioia-Eastwood, K.: 1989a, *Astron. J.* 97, 107.
- Massey, P., Parker, J.W., Garmany, C.D.: 1989b, *Astron. J.* 98, 1305.
- Massey, P., Johnson, O.: 1998, *Ap.J.* 505, 743.
- McErlean, N.D., Lennon, D.J., Dufton, P.L.: 1998, *A&A* 329, 613.
- Meurs, E.J., Van den Heuvel, E.P.J.: 1989, *A&A* 226, 88.
- Meyer, F., Meyer-Hofmeister, E.: 1979, *A&A* 78, 167.
- Meynet, G., Mermilliod, J.-C., Maeder, A.: 1993, *A&A Suppl.* 98, 477.

- Meynet, G., Maeder, A., Schaller, G., Schaerer, D., Charbonnel, C.: 1994, *A&A Suppl.* 103, 97.
- Meynet, G.: 1998, in 'Properties of Hot, Luminous Stars', ed. I. Howarth, ASP. Conf. Proceedings, Vol. 131, p. 96.
- Meynet, G.: 1995, *A&A* 298, 767.
- Mitra, 1996, *MNRAS* 280, 953.
- Moffat, A.F.J., Lamontagne, R., Seggewiss, W.: 1982, *A&A* 114, 135.
- Moffat, A.F.J., Seggewiss, W.: 1980, *A&A* 86, 87.
- Moffat, A.F.J.: 1996, in 'Wolf-Rayet Stars in the Framework of Stellar Evolution', eds. J.M. Vreux, A. Detal, D. Fraipont-Caro, E. Gosset & G. Rauw, Université de Liège, p. 199.
- Myers, P.C., Fuller, G.A.: 1992, *Ap. J.* 396, 631.
- Neo, S., Miyaji, S., Nomoto, K., Sugimoto, D.: 1977, *Publ. Astron. Soc. Japan* 29, 249.
- Niemela, V.S.: 1995, in 'WR stars: Binaries, Colliding Winds, Evolution', eds. K.A. Van der Hucht & P.M. Williams, Kluwer: Dordrecht, p. 223.
- Nota, A., Livio, M., Clampin, M., Schulte-Ladbeck, R.: 1995, *Ap.J.* 448, 788.
- Orosz, J.A., Baylin, Ch.D.: 1997, *Ap.J.* 477, 876.
- Pacini, F.: 1967, *Nature* 216, 567.
- Packet, W.: 1988, Ph. D. Thesis, Vrije Universiteit Brussels.
- Paczynski, B.: 1967, *Acta Astronomica* 17, 355.
- Parker, J.W., Garmany, C.D., Massey, P., Walborn, N.R.: 1992, *AJ* 103, 1205.
- Pauldrach, A.W., Kudritzki, R.P., Puls, J., Butler, K., Hunsinger, J.: 1994, *A&A* 283, 525.
- Penny, L.R.: 1996, *Ap.J.* 463, 737.
- Plavec, M.: 1986, in 'Hydrogen-Deficient Stars & Related Objects', IAU Coll. No. 87, eds. K. Hunger, D. Schönberner, N.K. Rao, Reidel, Dordrecht, p. 231.
- Podsiadlowski, P., Joss, P.C., Hsu, J.J.L.: 1992, *Ap. J.* 391, 246.
- Pols, O.R., Coté, J., Waters, L.B.F.M., Heise, J.: 1991, *A&A* 241, 419.
- Pols, O.R., Marinus, M.: 1994, *A&A* 288, 475.
- Pols, O.R.: 1994, *A&A* 290, 119.
- Popova, E.I., Tutukov, A.V., Yungelson, L.R.: 1982, *Astron. Space Sci.* 88, 55.
- Portegies Zwart, S.F., Verbunt, F.: 1996, *A&A* 300, 179.
- Portegies Zwart, S.F., Yungelson, L.R.: 1998, *A&A* 332, 173.
- Portegies Zwart, S.F.: 1995, *A&A* 296, 691.
- Portegies Zwart, S.F.: 1996, Ph. D. Thesis, University of Utrecht.
- Portegies Zwart, Verbunt, F., Ergma, E.: 1997, *A&A* 321, 207.
- Puls, J., Kudritzki, R.P., Herrero, A. et al.: 1996, *A&A* 305, 171.
- Rappaport, S., Joss, P.C.: 1983, in 'Accretion Driven Stellar X-ray Sources', eds. W.H.G. Lewin & E.P.J. Van den Heuvel, Cambridge Univ. Press: Cambridge.
- Reid, N., Tinney, C., Mould, J.: 1990, *Ap.J.* 348, 98.
- Remillard, R.A., McClintock, J.E., Bailyn, Ch. D.: 1992, *Ap.J.* 339, L145.
- Remillard, R.A., Orosz, J.A., McClintock, J.M., Bailyn, Ch. D.: 1996, *Ap. J.* 459, 226.
- Roxburgh, I.: 1978, *A&A* 65, 281.
- Roxburgh, I.: 1989, *A&A* 211, 361.
- Roxburgh, I.: 1992, *A&A* 266, 291.
- Sanwal, D. et al.: 1993, *Ap.J.* 460, 437.
- Sargent, W.L.W., Searle, L.: 1970, *Ap.J.Letters*, 162, 155.
- Sato, N., Nagase, F., Kawai, N. et al.: 1986, *Ap.J.* 304, 241.
- Schaerer, D., Maeder, A.: 1992, *A&A* 263, 129.
- Schaller, G., Schaerer, D., Meynet, G., Maeder, A.: 1992, *A&AS*, 96, 268.
- Schmutz, W.: 1996, in 'Wolf-Rayet Stars in the Framework of Stellar Evolution', eds. J.M. Vreux, A. Detal, D. Fraipont-Caro, E. Gosset & G. Rauw, Université de Liège, p. 553.
- Schmutz, W.: 1997, *A&A* 321, 268.
- Schmutz, W., Geballe, T., Schild, H.: 1996, *A&A* 311, L25.
- Schönberner, D., Drilling, J.S.: 1983, *Ap.J.* 268, 225.
- Schwarzschild, M.: 1958, 'Structure and Evolution of the Stars', Dover Publ., Inc., N.Y.
- Searle, L., Sargent, W.L.W., Bagnuolo, W.G.: 1973, *Ap.J.* 179, 427.
- Shapiro, S.L., Lightman, A.P.: 1976, *Ap. J.* 204, 555.
- Shu, F.H., Lubow, S.H.: 1981, *Ann. Rev. Astron. Astrophys.* 19, 277.
- Smith, K.C., Howarth, I.D., Siebert, K.W.: 1998, in 'Properties of Hot, Luminous Stars', ed. I. Howarth, ASP. Conf. Proceedings, Vol. 131, p. 153.

- Sparks, N.M., Stecher, T.P.: 1974, *Ap.J.* 188, 148.
- St.-Louis, N., Howarth, I.D., Willis, A.J.: 1993, *A&A* 267, 447.
- Stella, L., White, N.E., Rosner, R.: 1986, *Ap.J.* 308, 669.
- Stencel, R.E., Pesce, J.E., Bauer, W.H.: 1989, *A.J.* 97, 1120.
- Stevens, I.R., Willis, A.J., 1988, *MNRAS* 234, 783.
- Sutanty, W.: 1975, *A&A* 41, 47.
- Sutanty, W.: 1978, *Ap.&SS* 54, 479.
- Taam, R.E., Bodenheimer, P., Ostriker, J.P.: 1978, *Ap. J.* 222, 269.
- Talon, S., Zahn, J.P., Maeder, A., Meynet, G.: 1997, *A&A* 322, 209.
- Tauris, T.M., Takens, R.J.: 1998, *A&A* 330, 1047.
- Thorne, K.S., Zytkov, A.N.: 1977, *Ap.J.* 212, 832.
- Tutukov, A.V., Yungelson, L.R., Iben, I.: 1992, *Ap.J.* 386, 197.
- Underhill, A.B., Greve, G.R., Louth, H.: 1990, *PASP* 102, 749.
- Van Bever, J., Vanbeveren, D.: 1997, *A&A* 322, 116.
- Van Bever, J., Vanbeveren, D.: 1998, *A&A* 334, 21.
- Van den Heuvel, E.P.J., Heise, J.G.: 1972, *Nature Phys. Sci.* 239, 67.
- Van den Heuvel, E.P.J.: 1969, *A.J.* 74, 1095.
- Van den Heuvel, E.P.J.: 1993, in 'Interacting Binaries', Saas-Fee Advanced Course 22, eds. H. Nussbaumer & A. Orr, Springer-Verlag: p. 263.
- Van der Hucht, K.A., Schrijver, J., Stenholm, B. et al.: 1997, *New Astronomy*, Vol. 2, 245.
- Van Kerkwijk, A.H., Van Paradijs, J., et al.: 1995, *A&A* 303, 483.
- Van Kerkwijk, M.H., 1993, *A.A* 276, L8.
- Van Kerkwijk, M.H., Charles, P.A., Geballe, et al.: 1992, *Nature* 355, 703.
- Vanbeveren, D., De Donder, E., Van Bever, J., Van Rensbergen, W., De Loore, C.: 1998b, *New Astronomy* 3, 443.
- Vanbeveren, D., De Loore, C.: 1994, *A&A* 290, 129.
- Vanbeveren, D., Herrero, A., Kunze, D., Van Kerkwijk, M.: 1994, *Space Sci. Rev.* 66, 395.
- Vanbeveren, D., Packet, W.: 1979, *A&A* 80, 242.
- Vanbeveren, D., Van Bever, J., De Donder, E.: 1997, *A&A* 317, 487.
- Vanbeveren, D.: 1991, *A&A* 252, 159.
- Vanbeveren, D.: 1995, *A&A* 294, 107.
- Vanbeveren, D., Van Rensbergen, W., De Loore, C., 1982, *A&A* 115, 68.
- Vanbeveren, D., Van Rensbergen, W., De Loore, C.: 1998a, 'The Brightest Binaries', ed. Kluwer: Dordrecht.
- Verbunt, F., Wijers, R.A.M.J., Burn, H.: 1990, *A&A* 234, 195.
- Verbunt, F.: 1990, in 'Neutron Stars and Their Birth Events', ed. W. Kundt, Kluwer, Dordrecht, p. 179.
- Vereshchagin, S., Kraicheva, Z., Popova, E., Tutukov, A., Yungelson, L.: 1987, *Pis'ma v Astronom. Zhurnal* 13, 63.
- Vereshchagin, S., Tutukov, A., Yungelson, L., Kraicheva, Z., Popova, E.: 1988, *Astrophys. Space Sci.* 144, 245.
- Walborn, N.R.: 1971, *Ap.J.* 164, 267.
- Walborn, N.R.: 1976, *Ap.J.* 205, 419.
- Waters, L.B.F.M., Pols, O.R., Hogeveen, S.J., Coté, J., Van den Heuvel, E.P.J.: 1989, *A&A* 220, L1.
- Webbink, R.F.: 1984, *Ap.J.* 277, 355.
- Wijers, R.A.M.J., Van Paradijs, J., Van den Heuvel, E.P.J.: 1992, *A&A* 261, 145.
- Woosley, S.E., Langer, N., Weaver, T.A.: 1993, *Ap. J.* 411, 823.
- Woosley, S.E., Langer, N., Weaver, T.A.: 1995, *Ap. J.* 448, 315.
- Woosley, S.E., Weaver, T.A.: 1995, *Ap. J. Suppl.* 101, 181.
- Woosley, S.E.: 1986, in 'Nucleosynthesis and Chemical Evolution', 16th Saas-Fee Course, eds. B. Hauck et al., Geneva Observatory, p.1.
- Zahn, J.P.: 1983, in 'Astrophysical Processes in Upper MS Stars', 13th Saas-Fee Course, eds. B. Hauck & A. Maeder, p.253.
- Zahn, J.P.: 1994, *Space Science Rev.* 66, 285.